The *cis*-Effect of the N-donor Moiety on the Rate of Chloride Substitution in (N^N^N) and (N^C^N) Platinum(II) Complexes by Nitrogen Bio-relevant Nucleophiles

By

Musawenkosi Ngubane

Master of Science

School of Chemistry and Physics

Pietermaritzburg

The *cis*-Effect of the N-donor Moiety on the Rate of Chloride Substitution in (N^N^N) and (N^C^N) Platinum(II) Complexes by Nitrogen Bio-relevant Nucleophiles

Submitted in fulfilment of the academic requirements for the degree of

Master of Science

By

Musawenkosi Ngubane

BSc (HONS) University of KwaZulu-Natal

College of Agriculture, Engineering and Science

School of Chemistry and Physics

University of KwaZulu-Natal

Pietermaritzburg

November 2013

Declaration

I hereby declare that this thesis reports on original experimental results from the work conducted in the School of Chemistry and Physics, University of KwaZulu-Natal, Pietermaritzburg, and has not been submitted for the fulfilment of any degree at any University.

……

Musawenkosi Ngubane

I hereby certify that this is correct.

……

Prof. D. Jaganyi (supervisor)

College of Agriculture, Engineering and Science

School of Chemistry and Physics

University of KwaZulu-Natal

Pietermaritzburg

November 2013

Table of Contents

Abstract

In this study, a total of seven monofunctional platinum(II) complexes of the type $[Pt(N^N^N)Cl]^+$ and [Pt(N^C^N)Cl] were synthesized and characterized using NMR, Mass spectrometry and elemental analysis. In both, N^N^N and N^C^N chelating ligands, the structural variances are the *cis* groups, *viz*. pyridine, pyrazole, 8-quinoline and 7-azaindole, of the 1,3-substituted phenyl and 2,6-substituted pyridine respectively. The nucleophilic substitution reactions of these complexes with a series of bio-relevant azole nucleophiles *viz.* Pyrazole (**Pz**), 1,2,4-Triazole (**Tz**), Imidazole (**Im**), 1-methylimidazole (**MIm**) and 1,2-dimethylimidazole (**DMIm**) were studied in ethanolic solutions. The substitution reactions were investigated under *pseudo* first-order conditions as a function of nucleophile concentration and temperature using stopped flow and UV-Visible spectrophotometry.

[Pt(N^C^N)Cl] complexes containing a strong σ-donor phenyl group *trans* to the chloride leaving group reacted faster than their $[Pt(N^N^N)Cl]^+$ counterparts with pyridine at the *trans* position. The reactivity trends of the complexes are discussed in terms of the electronic and structural effects due to the different *cis*-heterocycles. The poor π-acceptor nature of the *cis*-pyrazolyl rings compared to pyridinyl rings in C_{2v} complexes is consistent with the decreased reactivity of pyrazole containing N^C^N and N^N^N Pt(II) complexes, due to the accumulation of the electron density at the metal centre leading to the metal centre's electrophilicity being decreased and thus retarding the incoming nucleophile. The twisting of the bulky *cis* groups in six membered chelates slows the reactivity of these complexes in two ways; (1) the electronic communication between the Pt(II) centre and the *cis* groups is reduced and (2) Steric clash between the *ipso*-hydrogens hinders the approach and the final coordination of the entering nucleophile. Results from **DFT** calculations support the experimentally observed trends.

The general reactivity trend of the azole nucleophiles studied is **MIm>Im>DMIm>Pz>Tz**. The enhanced reactivity of **MIm** is due to the inductive σ-donation of electrons by the methyl substituent in the β-position to the reactive nitrogen, making the nucleophilic nitrogen more reactive. In **DMIm**, steric hindrance due to the additional methyl group in the α-position to the reactive nitrogen dominates over the inductive effect leading to steric clash in the transition state and retarded reactivity of the nucleophile. The reactivity of **Im**, **Pz** and **Tz** largely depends upon the basicities of the reactive nitrogens and these nucleophiles follow a linear free energy relationship (LFER) of the type $k_2 = \alpha(pK_a) + b$, typical of non sterically hindered N-donor nucleophiles. The significantly low but positive $\Delta H^{\ddagger}$ values and significantly negative values for $\Delta S^{\ddagger}$ support an associative substitution mechanism.

Acknowledgements

I would like to thank my supervisor Prof. Jaganyi for his endless support over the last two years. I am also very grateful to Mr Isaac Wekesa for guidance in the laboratories and during the writing of this thesis.

I also gratefully acknowledge financial support from the University of KwaZulu Natal and the National Research Foundation (NRF, South Africa).

I would like to also acknowledge:

- The instrument technicians for analysing the samples in time.
- The chemistry department for constructing an office for us in seminar room 45a.
- My colleagues; Grace, Papo Rose, G, Mathias, Meshack, Nelson and everyone I forgot to mention.
- I would also like to thank my family including Slie, your prayers and support contributed a lot to the success of this work.
- Lastly, I highly appreciate the proofreading and constructive feedback given by Dr. Allen Mambanda.

Conference Attended

16th Biennual South Africa Chemical Institute (SACI 2013) Inorganic Chemistry Conference. Incorporating the Carman Physical Chemistry Symposium, Southen Sun-Elangeni, Durban, South Africa, 30th June – 4th July, 2013. Poster presented; M. Ngubane, I. M. Wekesa and D. Jaganyi, " Mechanistic Studies on the Reactions of N^C^N Platinum(II) Complexes With Nitrogen Biorelevant Nucleophiles: Experimental and Computational Approach."

List of Abbreviation

A	Absorbance
A	Arrhenius pre-exponential factor (as indicated)
A	Associative mechanism
Å	Angstrom (10^{-10} m)
$CDCl_3$	deuterated chloroform
C	Celsius
cisplatin	cis-diaminedichloroplatinum(II)
dien	diethylenetriamine
DIm	1,2-dimethylimidazole
D	dissociative
DFT	Density functional theory
d	doublet
dd	doublet of dobublet
DMSO	Dimethyl Sulfoxide
DNA	Deoxyribonucleic acid
Ea	Arrhenius activation energy
ΔE	Energy gap between the HOMO and LUMO
ε	Extinction coefficient
EtOH	Ethanol
G	Gibbs free energy
h	Planck's constant
$\Delta H^{\neq}$	Change in enthalpy of activation
His	histdine
HOMO	Highest occupied molecular orbital
I	Ionic strength
I	Interchange
I_a	Associatively activated interchange
I_d	Dissociatively activated interchange
Im	Imidazole
k_1, k_{-1}, k_2, k_{-2}	rate constants
K_b	Boltzmann constant (1.3807×10^{-23} JK^{-1})
K	Equilibrium constant
K	Kelvin

k_{obs}	observed pseudo first-order constant
l	pathlength
LFER	Linear free energy relationship
LUMO	Lowest Unoccupied Molecular Orbital
MeOH	Methanol
M	Molarity (mol dm^{-3}) or metal
MIm	1-methylimidazole
NBO	Natural bond orbital
$n°_{Pt}$	Nucleophilicity of the incoming group Pt
NER	Nucleotide excision repair
nm	nanometer
NMR	nuclear magnetic resonance
Nu	Nucleophile
ppm	Parts per million
py	pyridine
Pz	pyrazole
R	Gas constant (8.3145 JK^{-1} mol^{-1})
RNA	ribonucleic acid
s	nucleophillic discrimination factor
s	singlet or strong
$\Delta S^{\neq}$	change in Activation entropy
T	Temperature
T	Transmittance
UV	Ultraviolet
Vis	Visible
vs	very strong
vw	very weak
w	weak
ν	frequency

List of Figures

List of Tables

Chapter 1

Platinum in Chemotherapy

1. Platinum in Chemotherapy

1.1. Introduction

Medicinal inorganic chemistry is a field of increasing importance since metal-based compounds offer more potential as therapeutic agents that are not readily available to organic compounds.[1] Medicinal properties of metals have been explored by ancient cultures in treatment of wide range of chronic diseases as early as 2500 B.C. Metals centres, being positively charged, are ideal for binding to negatively charged biomolecules such as nucleic acids and proteins in mammalian bodies.[2] Thus, inorganic and medicinal chemists use their knowledge of accessible redox states, coordination numbers, geometries, kinetic and intrinsic properties of metal ions in the development of metal based drugs.[1-2] However, this is not an easy task since accumulation of metal ions in the body can lead to negative effects.[2] Thus the drug's biodistribution, pharmacological specificity and clearance are to be considered before a metal complex can be regarded as a drug.[2] Even though metals have long been used for medicinal purposes, the potential of metal based anticancer drugs has only been extensively explored after the discovery of the biological activity of platinum based organometallic compounds.[1-3]

1.2 The Antitumor activity of Platinum complexes

The anticancer activity of platinum based drugs was serendipitously discovered when Barnett Rosenberg and co-workers were investigating the effect of an electric field on *Escherichia coli* cell division and observed growth inhibition accompanied by a filamentous clustering of the cells around the platinum electrode.[3-5] Further investigation revealed that the major cause of such a result was due to the formation of electrolysis products from the reaction of the platinum electrodes and the components of the cell culture medium.[6] The isolation of the products gave a mixture of Pt(II) and Pt(IV) compounds; *viz. cis*-$[Pt(NH_3)_2Cl_2]$, (**1**), *trans*-$[Pt(NH_3)_2Cl_2]$,(**2**), *cis*-$[Pt(NH_3)_2Cl_4]$, (**3**) and *trans*-$[Pt(NH_3)_2Cl_4]$, **(4)** (Figure 1.1).[5] Further tests revealed that the active platinum complexes in the medium are the *cis*-complexes, (**1**) and (**3**).

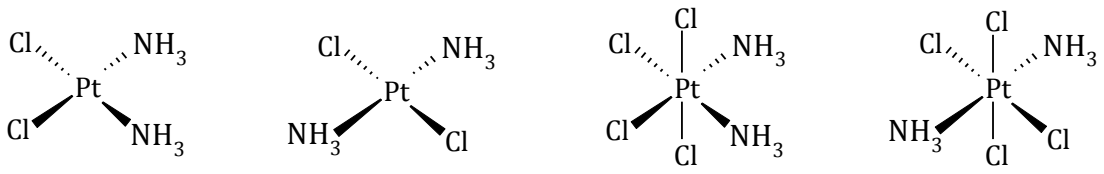

(1) **(2)** **(3)** **(4)**

Figure 1.1 Structures of platinum complexes initially studied for antitumor activity.[6]

After the discovery that *cis*-dichlorodiammineplatinum(II) or Cisplatin (**1**) was active in inhibiting the development of the solid Sarcoma – 180 tumor in mice, cisplatin was put on clinical trials in 1971 and approved by the Food and Drug Administration (FDA) in 1978.[5, 7] Now cisplatin is one of the most commonly used drugs due to its effectiveness against a wide spectrum of human malignancies, namely; testicular, ovarian, bladder, cervical, head and neck, small-cell and non-small-cell lung cancers.[8] The reactivity of cisplatin is highly dependent on the relative displacement of the labile chloride ligands and as a result, any chemical modification at these ligands will significantly influence the chemical reactivity of the complex.[3, 9] A number of observations suggest that the primary cellular target of Cisplatin is DNA.[3] Chemical and structural studies suggest that cisplatin coordination to DNA occurs mainly through the nucleophilic nitrogens (N7) of Adenine (**A**) and Guanine (**G**) bases, (Figure 1.2) which are exposed in the major groove of the DNA double helix and are not involved in base-pairing hydrogen bonding.[1-3, 9-10] Cisplatin exerts its antitumor effects by interacting and forming adducts with DNA which then leads to interference with transcription and replication leading to programmed cell death also known as apoptosis.[1-3, 9-11]

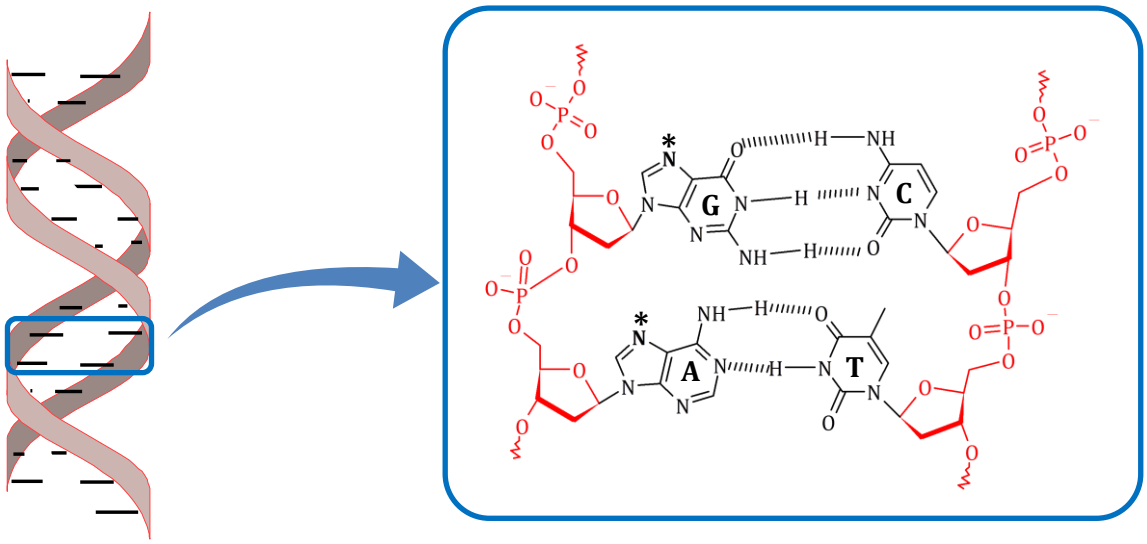

Figure 1.2 Schematic representation of DNA double helix showing the complementary base pairing of the bases, Adenine (**A**) with Thymine (**T**) and Guanine (**G**) with Cytosine (**C**) and the reactive nitrogens (*) of purines **A** and **G**.[12]

1.2.1 Mode of Action of Cisplatin

The usual introduction of cisplatin to the body is intravenously rather than orally and this is due to solubility problems.[2, 6] For cisplatin to work, it must first be aquated to form the more reactive species, *cis*-$[Pt(NH_3)_2Cl(OH_2)]^{2+}$, (Figure 1.3) and if aquation occurs in the bloodstream before diffusion, the aquated species will be more likely to react with nontarget species, leading

to toxicity of the drug.[6] Fortunately, the blood is approximately 100 mM in chloride ion, forcing the hydrolysis equilibrium to the chloro complex (**1**).[3, 13] Once in the bloodstream, passive and active diffusion across the cell membrane into the cytoplasm takes place and since the chloride concentration is in the range of 4-20 mM, aquation is now favoured.[3, 12] Under physiological conditions, cisplatin aquation appears to be half complete in two hours[12] and during this time, the Pt(II) centre is exposed to a variety of bio-molecules, including sulfur donors such as thiols and thioethers, which have a high affinity for Pt(II) complexes.[14] Competitive studies have shown that although Pt(II) binding to sulfur donors is kinetically favoured, the more thermodynamically stable binding involves nitrogen.[15-16] Therefore, it is possible that binding to sulfur donor sites forms a temporary reservoir of platinum with subsequent transfer to the N7 sites of purines leading to cell death.[12] Alternatively, this N7 substitution occurs in the aquated species, whereby the water ligand is substituted instead of the sulfur ligand.

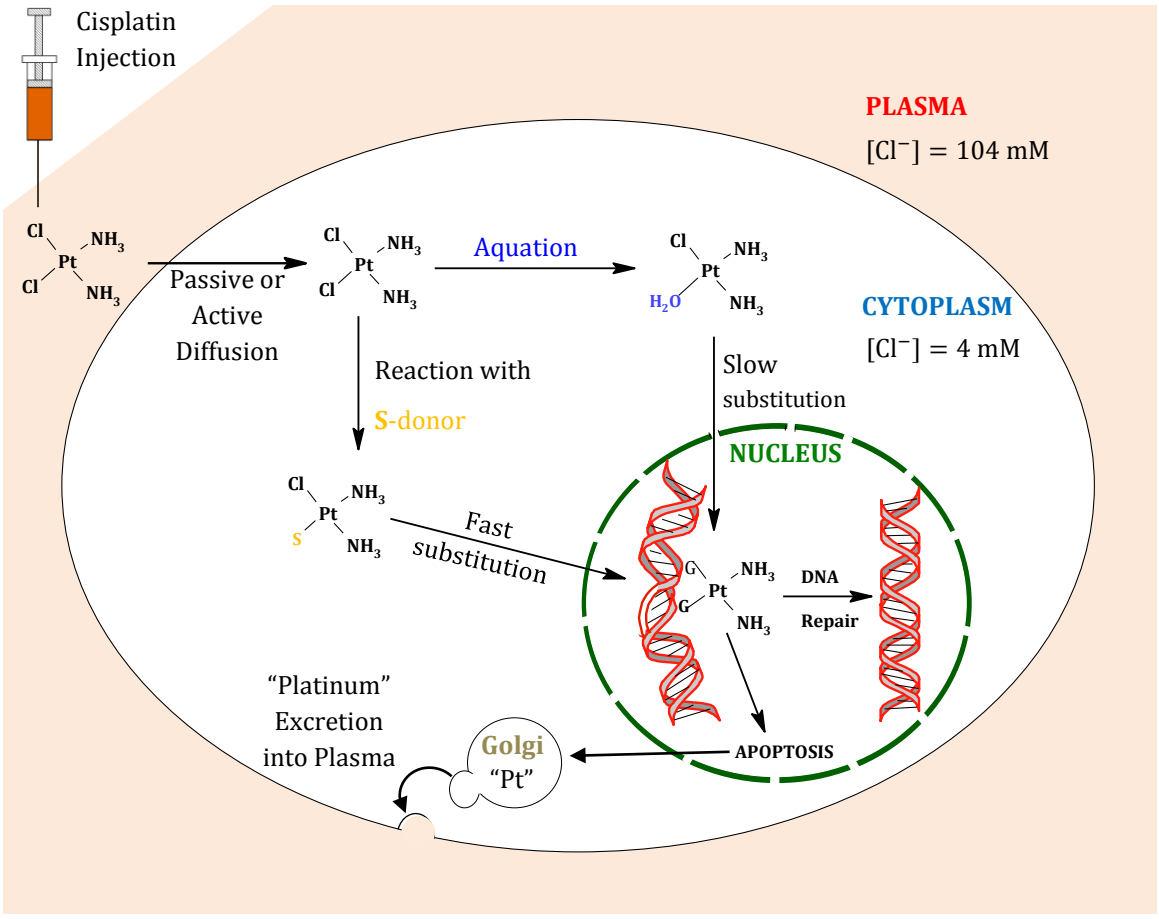

Figure 1.3 Administration and *in vivo* chemistry of cisplatin.[14]

In both cases, the covalent bonding of DNA to the sulfur/water containing Pt(II) intermediates, forms adducts (Figure 1.4) which then activates various signal transduction pathways such as DNA repair and programmed cell death (apoptosis).[1-3,8,12,17] The structures of some of these Pt(II)-DNA adducts have been elucidated by X-ray crystallography and nuclear magnetic resonance (NMR).[18] Such information has provided better understanding on the mode of action of cisplatin. The possible modes of binding of cisplatin to DNA leading to adducts include;

Unidentate Binding	This binding occurs through a single donor atom on DNA giving monofunctional adducts in the form of $[Pt(NH_3)_2Cl(DNA)]^+$.[3, 12, 18] This may later undergo ring closure to form bifunctional bindings in the form of chelates, interstrand or intrastrand cross-links and DNA-protein cross-links. (Figure 1.4)[12, 19-20]
Chelate formation	Here binding occurs through the two donor atoms of the same base as depicted in Figure 1.4. where a five-membered chelate ring is formed by binding of platinum to nitrogen and oxygen donor atoms of a guanosine base.[12]
Interstrand cross-links	This involves cross-linking of the two bases of different sugar-phosphate strands.[3,9,12,19-21]
Intrastrand cross-links	Platinum cross-link between two bases of the same sugar-phosphate strand. This is the most favoured form of binding; around 60-65% of the overall adducts are formed between adjacent guanines (GG) and 20-25% are formed between adjacent adenine and guanine (GA) bases. The rare binding of guanines separated by one nucleotide can also take place.[3,9,12,21]
DNA-Protein cross-link	The platinum ion may also cross-link DNA to other different donor molecules such as proteins or sulfur donors, which are present within the cell.[3,22]

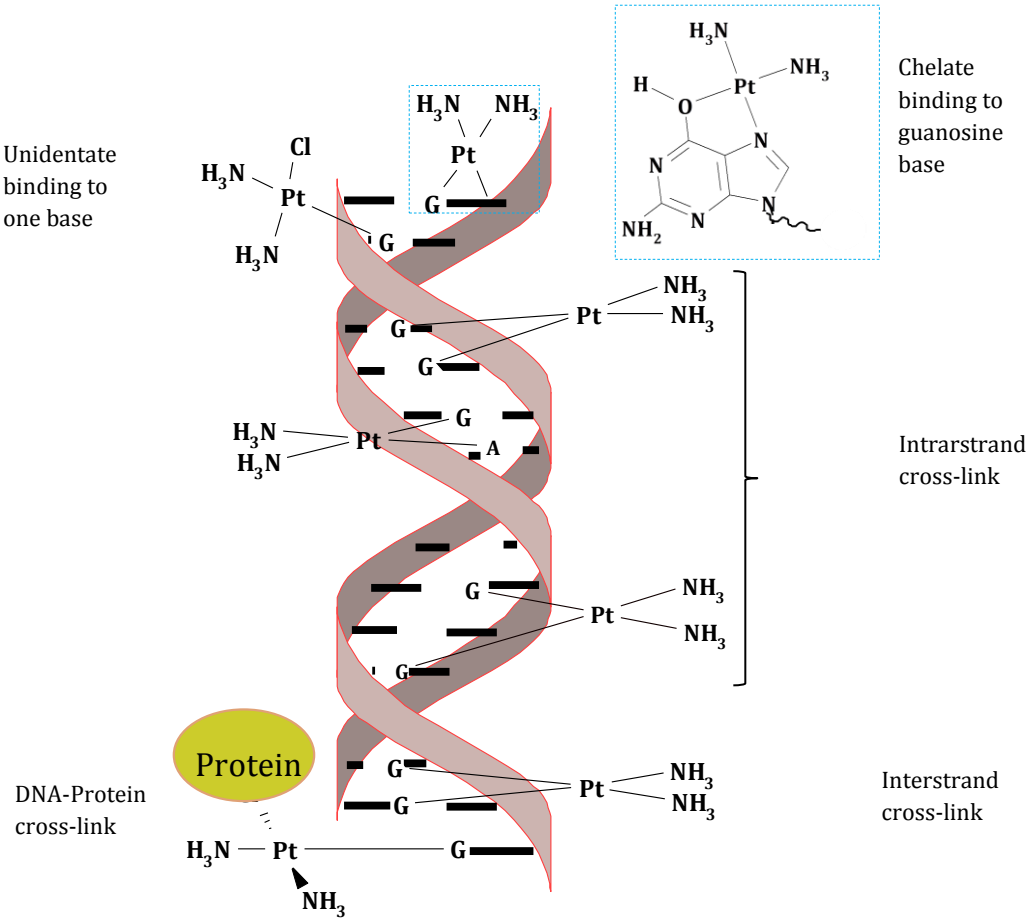

Figure 1.4 Various adducts produced by the interaction of cisplatin and DNA. Insert, Chelate binding of cisplatin to a guanosine base.[22]

There is still debate as to which adducts are of the most importance in mediating tumor cell killing.[19] Some studies support Intrastrand adducts,[23] whereas others indicate that Interstrand crosslinks may be of greater biological significance.[24] 1,2-intrastrand adducts are supported by the finding that the inactive *trans* isomer of cisplatin is sterically unable to form these adducts,[23,25] whereas other studies have shown that even though interstrand adducts are present in a small portion (~2%) of the overall adducts, there is a direct relationship between cell killing and the number of formed Interstrand adducts.[24]

Bifunctional Pt-DNA cross-links are responsible for the distortion in DNA double helix leading to inhibition in DNA transcription and replication which triggers cell death pathways.[3, 12] The distorted, platinated DNA is also recognised by a variety of nuclear components.[26] These include DNA repair enzymes such as nucleotide excision repair (NER) which contain DNA repair machinery that removes cisplatin intrastrand cross-links leading to the recovery of the cell.[12] Alternatively, such distortions may be recognised by other proteins that meditate the antitumor

activity of the drug, such as high mobility group (HMG)-domain proteins.[3, 12, 17] These HMG-proteins play a vital role in DNA transcription during cell division. Therefore, when a cell is exposed to a lethal dose of cisplatin, forming about $10^4 - 10^5$ adducts, and the HMG-proteins bind with the similar affinity to these Pt-DNA adducts, the proteins could be titrated away from their gene regulation sites resulting in cell death.[3] In addition, these proteins also enhance the effectiveness of the drug by blocking the entry of the proteins responsible for DNA repair such as NERs by the process commonly known as repair shielding.[3, 12]

Cell death has also been found to be triggered by platination occurring in the telomeric regions of DNA which are located at the ends of the chromosomes.[27] These telomeric regions are guanosine rich with their main responsibility being the protection of the ends of the chromosomes from degradation and to transfer genetic information during cell division.[12, 27] During each successive cell division, part of the telomeric region is lost and when the telomeric region become significantly short, the cell stops dividing and eventually dies.[12] However, there is a ribonucleoprotein, telomerase, which is responsible for the addition of sections to the shortened telomeric regions leading to a prolonged cell life. Cisplatin binding to telomeric regions degrades the telomeric regions and inhibits telomerase activity, leading to cell death.[12]

Cisplatin cytotoxicity against various solid tumors is considered a major success in cancer chemotherapy.[21] However, the use of the drug has been limited by the negative effects including toxicity and resistance.[14, 16] These drawbacks of cisplatin have prompted a continuous search for improved platinum based anticancer drugs. [28]

1.2.2 Cisplatin Toxicity and Resistance

Cisplatin resistance is an important factor limiting the use of the drug. Some cells may be intrinsically resistant to cisplatin whereas others may acquire resistance during chemotherapy. [12] There are various effects that operate to produce cisplatin resistance and to date no single mechanism can account for the observed pattern of resistance. Firstly, resistance can be due to decreased intracellular accumulation of the drug if the rate of uptake of the drug is decreased significantly while the release rates remain constant.[12, 27] A second possibility involves enhanced production of complexing agents such as thiols which leads to the competition between thiols and DNA for binding to cisplatin.[14] A third possible cause of cisplatin resistance is due to enhanced stimulation of DNA repair activity by nucleotide excision repair (NER) in the lesions of platinated DNA region.[27] Cisplatin resistance and its side effects such as nephrotoxicity, myelotoxicity, ototoxicity, peripheral neuropathy, severe nausea and vomiting almost led to discontinuation of studies of cisplatin.[8,29] However, it prompted a parallel synthesis effort to less toxic and more effective platinum analogues.[30] The hypothesis was that, the use of less labile

leaving groups in modified cisplatin would alter toxicity and the search for the less toxic analogue began.

The search for novel Pt(II) anticancer agents was pursued at the Institute for Cancer Research and this led to the development of diamine[1,1-cyclobutanedicarboxylato(2-)]-*O,O'*-platinum(II) carboplatin (**5**) (structure shown in Figure 1.5).[3,31] The leaving group in carboplatin is a cyclobutanedicarboxylate ligand that is two orders of magnitude less labile compared to the chloride ligands in cisplatin.[12,21] In addition, carboplatin was found to have reduced side effects while its anticancer effects were retained.[32] However, since the amine inert ligands are the same in cisplatin and carboplatin, the DNA adducts they form are the same, which explains why the two compounds display a high degree of cross-resistance.[21]

The search for an analogue with a broader tumor spectrum and reduced resistance led to screening of hundreds of Pt(II) complexes in which different inert ligands were attached to the amine ligands.[3] Out of the tested complexes, oxaliplatin **(6)** became the only internationally recognised anticancer drug of this class.[3,12,31] In oxaliplatin **(6)**, the 1,2-diaminocyclohexane (DACH) replaces the original amine ligands whereas the chloride ligands are substituted by an oxalate group. After binding of oxaliplatin to DNA, the inert DACH chelate results in steric configuration of the Pt-DNA adduct and inhibit DNA repair mechanisms leading to cell death in some platinum resistant tumors.[21] A combination of oxaliplatin **(6)** and other compounds such as 5-fluorouracil and leucovorin has been found to be active in the treatment of colorectal cancers, which are resistant to cisplatin and carboplatin chemotherapy.[12,21,31] Reduced nephrotoxicity displayed by oxaliplatin due to the slower aquation of the complex has led to the continuous use of the drug.[12] However, this drug has been associated with sensory neuropathy, a common characteristic of DACH containing Pt(II) derivatives.[3]

Other Pt(II) drugs that are approved in selected countries include; nedaplatin **(7)**, Lobaplatin **(8)** and SK12053R **(9)**.[33] Nedaplatin **(7)** is currently registered in Japan and is used for head, neck, lung and oesophageal cancer.[3,12,21] Clinical trials of this drug revealed cross-resistance similar to cisplatin (**1**) due to the similarities of the adducts formed, but with reduced toxicity than cisplatin because of the less labile leaving group.[3] Lobaplatin **(8)** is currently used in China while SK12053R **(9)** is still under phase II clinical trials.[33]

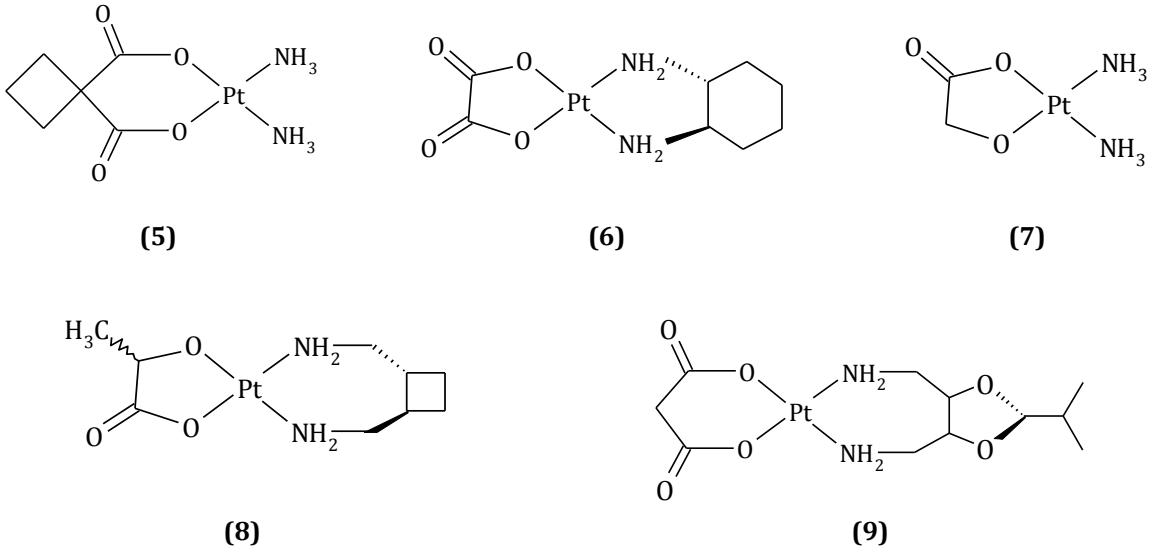

Figure 1.5 Platinum complexes which are currently in clinical use globally or in selected countries.[33]

1.3 Recent Development in Cancer Chemotherapy

The anticancer effectiveness of cisplatin and its analogues led to the introduction of numerous classical structure–activity relationships (SARs) which required that an active platinum antitumor complex should at least possess the following features; square-planar geometry, contain a pair of labile leaving groups in a *cis* conformation, have a neutral charge in order to facilitate passive diffusion across cell membranes, and contain inert amine ligands as non-leaving groups. [34] Since that time, however, many non-classical "rule-breakers", have been discovered which could therefore display a different spectrum of anticancer activity in efforts to overcome cisplatin toxicity and resistance.[35] These include compounds with *trans* stereochemistry [36] of the general formula $trans$-$[PtCl_2(NH_3)L]$, where L is a planar N-donor ligand, Pt(IV) complexes, multinuclear platinum compounds [37] which contain two or more linked Pt centres that are each capable of binding to DNA to form completely different DNA adducts compared to cisplatin and monofunctional Pt(II) complexes[38] with one leaving group (X) such as $[Pt(NH_3)_2(Am)Cl]^+$, where Am = pyridine, pyrimidine or purine.[39] However, focus here will be primarily on the monofunctional Pt(II) complexes.

1.4 Monofunctional Pt(II) complexes

Early studies performed on monofunctional Pt(II) complexes such as $[Pt(dien)Cl]^+$ **(10)**, where dien = diethylenetriamine and $[Pt(NH_3)_3Cl]^+$ **(11)** suggested that such complexes were inactive against cancer cells. [40-41] However, pyriplatin *cis*-$[Pt(NH_3)_2(Py)Cl]^+$ **(11)** and several of its analogues displayed significant antitumor activity with a different spectrum than the classical bifunctional crosslinking agents such as cisplatin.[42] These bind to DNA monofunctionally at the N7 of guanine residues with no significant distortion on DNA double helix. The resulting monofunctional adducts inhibit transcription while avoiding repair.[43] Such unique features of pyriplatin and its analogues prompted further studies of monofunctional Pt(II) complexes as anticancer candidates.

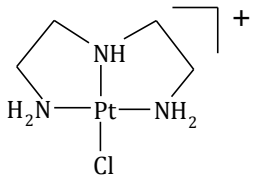

(10)

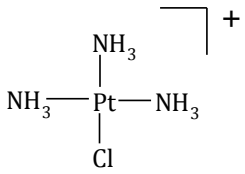

(11)

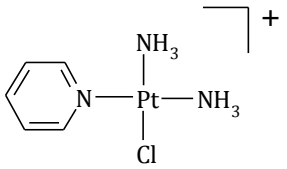

(12)

Another investigated class of monofunctional compounds are the cyclometallated Pt(II) complexes containing multidentate $\boldsymbol{\pi}$-conjugated organic ligands. [44] These have attracted much interest for the application of cytotoxic anticancer agents. The planar motifs of these Pt(II) complexes could insert between two adjacent DNA base pairs through non-covalent ligand-ligand $\boldsymbol{\pi - \pi}$ stacking interactions thus making them DNA metallointercalators.[45] Various research groups have reported platinum complexes containing DNA intercalators.[45-46] From these studies, it was noted that the binding mode of monofunctional complexes to DNA resulting in considerable antitumor activity is different from that of the currently used Pt(II) drugs, suggesting that the formation of DNA bifunctional adducts is not always essential for Pt(II) complexes to show significant cytotoxicity.

The use of π-conjugated, tridentate chelating ligands such as terpy in Pt(II) complexes (**13)** has been linked to desired cytotoxic against human ovarian carcinoma.[47] Therefore, more studies have been directed towards tuning the reactivity of the Pt(II) centre by slight alterations of the inert N^N^N ligand. Part of the protracted studies includes understanding of the kinetics of interaction of these compounds with nitrogen and sulfur donor biomolecules, which can help to gain more information on possible interactions of Pt(II) complexes with *in vivo* targets.[14] Kinetic and thermodynamic data affirms that the lability of the leaving group in monofunctional Pt(II) complexes with tridentate chelating ligands is influenced by the steric hindrance as well as σ

and π-effects of the ancillary groups. Planar complexes which form rigid five membered chelate rings as in $[Pt(terpy)Cl]^+$ (**13**) are usually more reactive than complexes with flexible six membered chelates such as $[Pt(tpdm)Cl]^+$ (**14**) where tpdm = tripyridinedimethane due to decreased ring strain and increased steric hindrance in the six membered chelated complexes.[48]

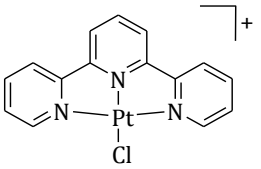

(13)

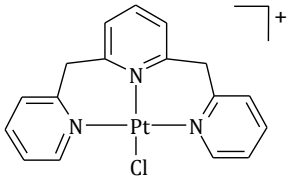

(14)

To gain full understanding of possible factors controlling reactivity of Pt(II) complexes, requires a systematic study in which the feature of interest is varied while all the other structural features are kept constant.

1.4.1 Objectives of This Study

The aim of this work is to investigate the electronic and steric effects of selected *N*-heterocyclic *cis*-moieties in chelated monofunctional Pt(II) complexes on the rate of chloride substitution by five membered nitrogen donor ligands, viz. pyrazole (**Pz**), 1,2,4-triazole (**Tz**), imidazole (**Im**), 1-methylimidazole (**MIm**) and 1,2-dimethylimidazole (**DMIm**). This was achieved by systematically varying the ligands *cis* to the chloride leaving group while keeping the *trans* phenyl/pyridine moiety constant. The electronic effects were investigated by changing the *cis* pyridinyl groups to electron deficient pyrazolyl *cis*-groups. In addition, the effect of simultaneously increasing the π-conjugation and chelate ring sizes was investigated. This was achieved by employing fused ring *cis* groups, namely; 7-azaindole and 8-quinoline respectively. DFT computations were performed to account for the reactivity difference of the studied complexes. The kinetic and mechanistic studies performed in this project are briefly introduced below and discussed in **Chapters 4** and **5** of this dissertation.

Chapter 4

The *cis*-Effect of The N-donor Moiety on the Rate of Chloride Substitution in Monofunctional N^N^N Pt(II) Complexes: *A Kinetic and Computational Approach*. In this section, the N^N^N tridentate chelate framework was maintained with a pendant pyridine ring while the *cis* aromatics were modified with pyridine (**Pt1**), pyrazole (**Pt2**), quinoline (**Pt3**) and azaindole (**Pt4**).

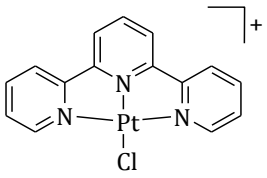

Pt1

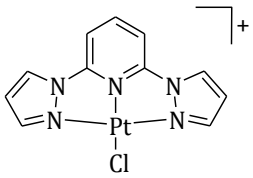

Pt2

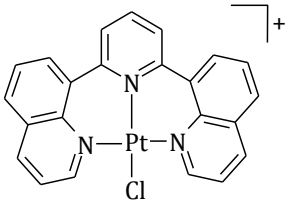

Pt3

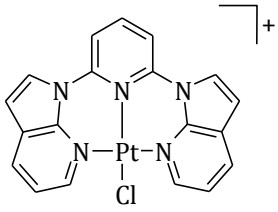

Pt4

Chapter 5

Mechanistic Studies on the Reactions of N^C^N Platinum(II) Complexes With Nitrogen Bio-relevant Nucleophiles: *Experimental and Computational Approach*. This chapter is about the investigation of the kinetics and mechanisms of chloride substitution in chelated, neutral N^C^N Pt(II) complexes, where C represents a common 1,3-substituted phenyl ring *trans* to the leaving chloride group and N represents the varying *N*-heterocyclic cis-moieties, *viz*. pyridine (**PtL1**), pyrazole (**PtL2**), quinoline (**PtL3**) and azaindole (**PtL4**).

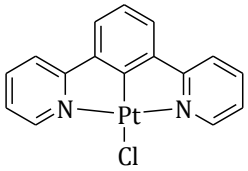

PtL1

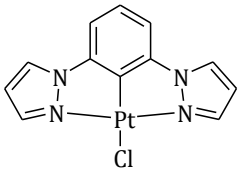

PtL2

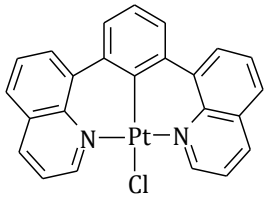

PtL3

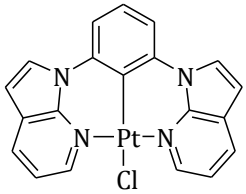

PtL4

The N-donor azole nucleophiles used differ in the position and the number of N-atoms, basicity and steric hindrance due to methyl groups. These were chosen because of their biological relevance in biomolecules such as histidine and DNA. It is therefore expected that the output of this study will be valuable in the search for a lead Pt(II) drug of improved efficacy.

1.5 References

1. P. C. A. Bruinincx and P. J. Sadler, *Current Opinion in Chemical Biology* **2008,** *12*, 197 – 206.
2. I. Kostova, *Recent Patents on Anti-Cancer Drug Discovery,* **2006***, 1*, 1 – 22
3. B. Lippert in *Cisplatin. The Chemistry and Biochemistry of a Leading Anticancer Drug*, *Vol.* Willey - VCH, Weinheim, **1999**, 3 - 100, 184 – 190.
4. B. Rosenburg, L. VanCamp, T. Krigas, *Nature*, **1965**, 205, 698 - 699.
5. B. Rosenberg, L. Van Camp, J. E. Trosko and V. H. Mansour, *Nature*, **1969**, *222*, 385.

6. F. Arnesano and G. Natile, *Coordination Chemistry Reviews* **2009**, *253*, 2070 - 2081.
7. B. Rosenburg, L. Van Camp, J. E. Trosko and V. H. Mansour, *Nature* **1969**, *222*, 385.
8. B. Rosenburg in *Platinum Complexes For the Treatment of Cancer: Why the Search Goes On. Lippert B, editor. Chemistry and Biochemistry of a Leading Anticancer Drug*, *Vol.* Willey - VCH, New York, pp. 1 - 27.
9. J. Kozelka, *Inorganica Chimica Acta* **2009**, *362*, 651 – 668.
10. N. J. Wheate and J. G. Collins, *Coord. Chem. Rev.*, **2003,** *241*, 133 – 145.
11. V. Milacic and Q.P. Dou, *Coord. Chem. Rev.*, **2009**, *253*, 1 – 12.
12. C. Jones, J. Thornback, Medicinal Applications of Coordination Chemistry, RSC Publishing, **2007**, pp. 63 - 65, 220-257.
13. J. E. Huheey, E. A. Keiter and R. L. Keiter in *Inorganic Chemistry*, *Vol.* Harper Collins College Publishers, New York, **1993**, p. 957
14. Ž. D. Burgarčić, J. Bogojeski, B. Petrović, S. Hochreuther, R. van Eldik, *Dalton. Trans.*, **2012**, *41*, 12329 - 12345.
15. T. Soldatovic, Ž. D. Bugarčić, *J. Inorg. Biochem*, 2005, *99*, 1472 - 1479.
16. J. Redijk, Eur. *J. Inorg. Chem*., **2009**, 1303 - 1312.
17. L. Kelland, *Nature. Reviews*., **2007**, *7*, 573 - 584
18. M. P. Takahana, A. C. Rosenzweig, C.A. Frederick, S.J. Lippard, *Nature*, **1995**, *377*, 649 - 652.
19. L. R. Kelland, *Drugs*, **2000**, 59 Suppl4, 1 - 8.
20. H. Huang, B. R Zhu L, *Science*, **1995**; *270*, 1842-1845.
21. J. Fischer, C. R. Ganellin, *Analogue Based Drug Discovery*, Wiley-VCH, **2006**, pp. 385 - 393.
22. P. A. Andrews, S. B. Howell, *Cancer Cells*, **1990**, *2*, 35 - 43.
23. L. A. Zwelling, T.A. Anderson, K. W. Kohn, *Cancer. Res*, **1979**, *39*, 365-369.
24. A. Eastman, M. A. Barry, *Biochemistry*, **1987**, *26*, 3303-3307.
25. D. E. Szymkowski, K. Yarema, J. M. Essigmann, *Proc. Natl. Acad. Science*. USA, **1992**, *89*, 10772 - 10776.
26. D. Wang, S. J. Lippard, *Nature Reviews*, **2005**, *4*, 307 - 320.
27. E. R. Jamieson and S. J. Lippard, *Chem. Rev.*, **1999**, *99*, 2467 – 2498.
28. L. Ronconi, P. J. Sadler, *Coord. Chem. Rev*., **2007**, *251*, 1633 - 1648.
29. P.J. Loehrer and L.H. Einhorn, *Annals of Internal Medicine*, **1984**, *100*, 704
30. T. A. Connors, M. Jones, W. C. Ross, P. D. Braddock, A. R. Khokhar and M. L. Tobe, *Chem. Biol. Inter*, **1972**, *5*, 415.

31. M. Gieleng and E. R. T. Tiekink, *Metallotheraputic Drugs and Metal-Based Diagnostic Agents: The Use of Metals in Medicine*, John Wiley and Sons Ltd, Canada, **2005**, pp. 489 - 501.
32. K. R. Harrap, *Cancer. Tret. Rev*., **1985**, *12*, 2 1 - 33.
33. E. Wong, C. M. Giandomenico, *Chem. Rev.,* **1999**, *99*, 2451 - 2466.
34. N. J. Wheate, , S. Walker, G. E. Craig, R . Oun, *Dalton Trans*., 2010, *39*, 8113 – 8127.
35. R. C. Todd, S. J. Lippard, *Metallomics*, **2009**, *1*, 280 – 291.
36. S. M. Aris and N. P. Farrell, *Eur. J. Inorg. Chem*., **2009**, 1293 – 1302.
37. N. Farrel, *Comments. Inorg. Chem.,* **1995**, *16*, 373 - 389.
38. L. S. Hollis, A. R. Amundsen and E. W. Stern, *J. Med. Chem*.,**1989**, *32*, 128 – 136.
39. N. J. Wheate and J. G. Collins, C*oord. Chem. Rev*., **2003**, *241*, 133 – 145
40. M. J. Cleare, J. D. Hoeschele, *Bioinorg. Chem*., **1973**, *2*, 187 – 210.
41. V. Brabec, V. Boudny, *Met.-Based Drugs*, **1994**, *1*, 195−200.
42. G. Y. Park, J. J. Wilson, Y. Song, S. J. Lippard, *PNAS*, **2012**, *109*, 11987 - 11992.
43. K.S. Lovejoy, *Proc Natl Acad Sci USA*, **2008**, *105*, 8902 – 8907.
44. P. Haake, P. A. Cronin, *Inorg. Chem*, **1963**, *2*, 879 - 880.
45. N. Cutillas, G. S. Yellol, C. de Haro, C. Vicente, V. Rodríguez, J. Ruiz, *Coord. Chem. Rev*., **2013**, *257*, 2784 – 2797.
46. K. W. Jennette, S. J. Lippard, G. A. Vassiliades, W. R. Bauer, *Proc. Natl. Acad. Sci. U. S. A,* **1974**, *71*, 3839.
47. G. Lowe, A. S. Droz, G. W. Weaver, J. J. Park, J. M. Pratt, L. Tweedale, L. R. J. Kelland*, J. Med. Chem.*, **1999**, *42*, 3167 - 3174.
48. Petrović, B., Burgarčić, Ž. D., Dees, A., Ivanović-Burmazović, I., Heinemann, F. W., Puchta, R., Steinmann, S. N., Corminboeuf, C., van Eldik, R., *Inorg. Chem.,* **2012**, *51*, 1516 - 1521.

Chapter 2

Substitution Reactions

2. Substitution Reactions

2.1. Introduction

In general, a substitution reaction is a process in which a ligand in the coordination shell is replaced by another in the reaction medium.[1] A simple substitution reaction on the other hand is referred to as the substitution reaction with no change in the oxidation state of the reaction centre.[2] However, since simple substitution reactions involve bond making and bond breaking, a temporary change in the coordination number in the transition state is observed.[2]

Work by Ingold and Hughes[3] made it possible to classify substitution reactions at carbon centres according to the mode of bond breaking between the reaction centre and the leaving group.[3] A chemical bond, represented by a shared pair of electrons, can be broken homolytically or heterolytically.[3-4] In the former, both fragments hold one electron each, whereas in the latter, a pair of electrons either remains with the reaction centre (electrophilic heterolysis) or departs with the leaving group (nucleophilic heterolysis).[4] Reactions (2.1), (2.2) and (2.3) represent these reactions, where M and X represents the reactive centre and the leaving group respectively.[2]

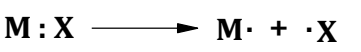

Homolysis (2.1)

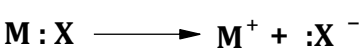

Nucleophilic heterolysis (2.2)

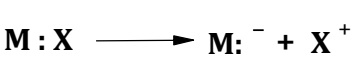

Electrophilic heterolysis (2.3)

Heterolytic processes are basically Lewis acid-base reactions, the reaction centre acts as a Lewis acid during nucleophilic processes and as a Lewis base during electrophilic processes.[2] In nucleophilic processes, the change in number of attached ligands does not affect the oxidation state, this is thus categorised as simple substitution reaction. Attachment of an electrophile, however, leads to bonding of the two previously non-bonding electrons also known as a two-electron oxidation.[2] If a ligand leaves as a Lewis acid, the electrophilic substitution takes place, and the attachment of the ligand from the medium leads to the stabilization of the higher oxidation state intermediate. In electrophilic processes, a dissociative two electron reduction takes place leading to a bonding pair of electrons to become non-bonding. The gain of an electron pair acceptor completes the substitution by restoring the oxidation state, while the loss of a Lewis base leads to reductive elimination. The nucleophilic and electrophilic processes are summarised in Figure 2.1

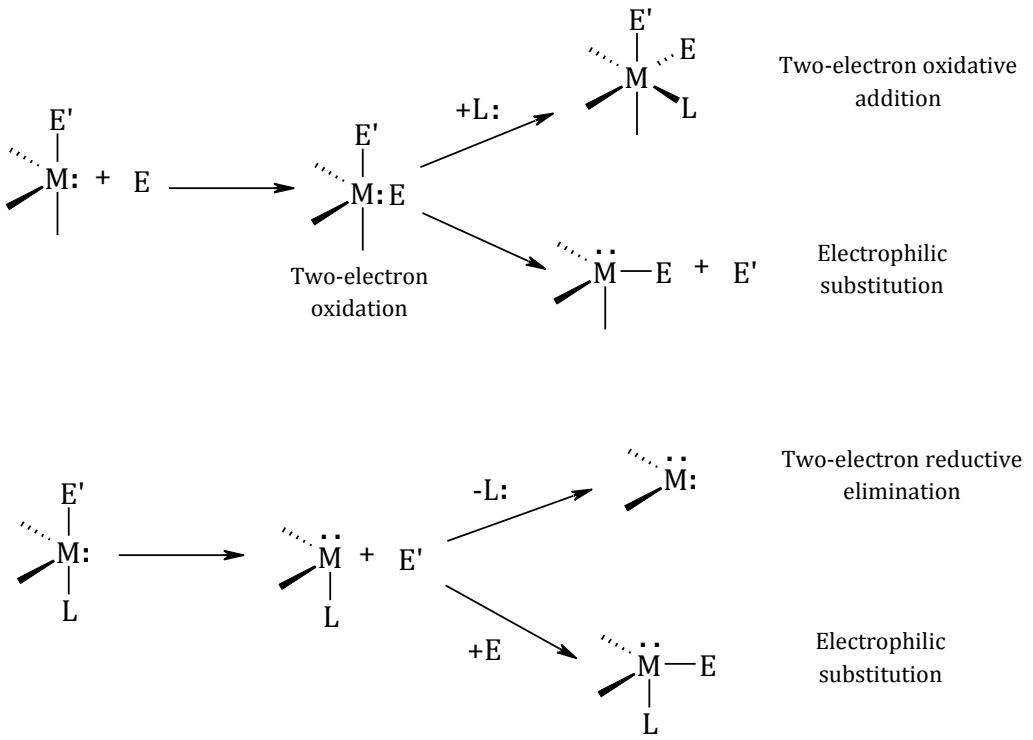

Figure 2.1 Heterolytic bond breaking and bond making processes.[2]

2.2. Substitution Reaction Mechanisms

In an attempt to classify inorganic substitution reactions, Langford and Gray[5] defined the mechanisms by bringing the concept of stoichiometric mechanism and intimate mechanism. The stoichiometric mechanism can be further classified into three groups depending on the nature of the intermediate species.[2,5]

a) Dissociative (*D*) – Is a process whereby the departing ligand leaves and a detectable intermediate of lower coordination number is formed.[1-2,4,6,7,8] A bond breaking step is the rate determining step, therefore, the rate of the substitution reaction considerably depends upon the nature of the leaving group.[1-2,4-8]

b) Associative (*A*) – In this process, the incoming ligand adds to the complex with the leaving ligand still intact, forming an identifiable intermediate with a higher coordination number. [1-2, 4-8] Since bond forming is the rate determining step, the rate of the reaction depends on the nature of the incoming group.[1-2,4-8]

c) Interchange (I) – Here, the intermediate is not detectable, since the act of bond making and bond breaking are either simultaneous or occur within a pre-formed aggregate. [1-2,4,6,8]

Interchange mechanisms are believed to be assisted by the incoming nucleophile, and the degree of assistance determines the class of intimate mechanism it falls under.[8]

i. Dissociative Interchange (I_d) – The degree of assistance by the incoming nucleophile is small since in the rate determining transition state there is minimal interaction between the reaction centre and the entering group.[1-2,4,6,8] Therefore, in the transition state, there is a large degree of bond breaking of the leaving group and a small amount of bond making to the entering group, thus the reaction rate is more sensitive to the nature of the leaving group.[1-2,4,6,8]

ii. Associative Interchange (I_a) – This mechanism is primarily associative in nature, implying that the incoming group bonds to the reaction centre before the leaving ligand bond is weakened in the transition state. The reaction rate is more sensitive to the nature of the incoming ligand. [1-2,4,6,8]

To clearly distinguish between these groups of substitution mechanisms, dependence of the rate of substitution on the nature of the entering group is used. If the rate depends on the entering ligand (nature and concentration), then it is either A or I_a and if there is no such dependence, then the mechanism is either D or I_d. The latter can be separated depending on whether an intermediate of reduced coordination number exists. This is however not easy since the primary difference is the depth of the energy well (minimum).[4, 7] The energy profiles representing dissociatively activated and associatively activated stoichiometric and intimate reaction mechanisms are given in Figure 2.2, where Y represents the entering ligand.

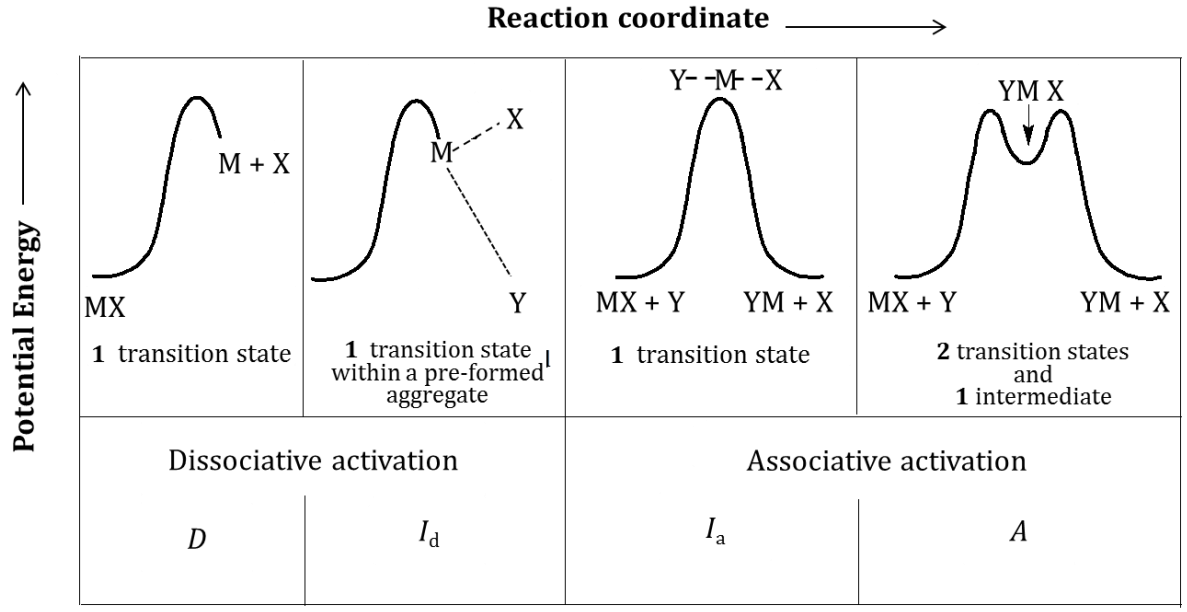

Figure 2.2 The relationship between the mechanism of substitution and its energy profile.[2,7]

Competitive studies are useful to test the selectivity towards entering ligands.[4, 7] A similar approach is also useful in differentiating between *A* or I_a.[4]

The central atom and the surrounding ligands in the ground state can be determined from a combination of steric and electronic factors. Therefore the favoured changes going to the transition state are also determined by the resulting number of factors.[2] The reaction pathway in which the tetrahedral *sp* block elements undergo is generally nucleophilic: S_N1 and S_N2, with the balance changing as one moves down the periodic table. When moving across the first row *d*-block M^{2+} and M^{3+} reactive centres, the reactivity changes from I_a to I_d. The *f*-block elements generally react variously by associative and dissociative due to the small energy difference between numerous seven and eight coordinate species. Of all the mentioned areas, the substitution reactivity of square-planar *d*-block complexes is of substantial consistency with the majority of complexes following an associative substitution pathway and a few exceptions to this general trend.[2]

2.3. Substitution at Square-Planar Complexes

Originally, the term square-planar was only used to refer to complexes whose all four ligands are the same as in the case of $[PtCl_4]^{4+}$.[2-4] The term is now used generally to refer to most complexes formed by metal ions having 8 electrons in their *d*-orbitals, such as Pt(II), Au(III), Pd(II), Ni(II), Rh(I) and Ir(I).[1-2,4,6,8] Such square-planar complexes display a diamagnetic character.[7] Since the 18-electron valence shell dominates the stability of inorganic complexes,

the four coordinate d^8 metal complexes only consist of a 16-electron valence shell and are therefore regarded as coordinatively unsaturated. [1-2,4,6,8]

Divalent d^8 metal complexes of Ni(II), Pd(II) and Pt (II) are the most characteristic square-planar complexes.[2] Ni(II) complexes consist of a wide range of spin multiplicities, coordination numbers and geometries. Square-planar Ni(II) and Pd(II) complexes react *via* a common mechanism to Pt(II) complexes, but at reactivity rates that are increased by at least five orders of magnitude more than Pt(II) complexes, as a result Ni(II) and Pd(II) substitution reactions are less attractive for study.[2] Platinum(II) complexes, on the other hand are by far the most stable and most intensively studied square-planar complexes.[6] Systematic kinetic studies of Pt(II) began in the 1950s,[9] and due to the similarity of the reaction mechanisms of Pt(II) complexes with the other square-planar complexes, the obtained information can thus be applicable to the other square-planar complexes.[2, 9]

2.3.1. Mechanism of Substitution reaction

Substitution reactions of square-planar platinum(II) complexes are often represented by a direct displacement of a unidentate leaving group (X) by another ligand (Y), which can be represented as follows:

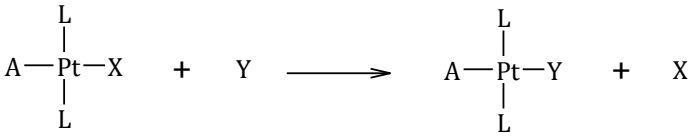

(2.4)

The rate law for this substitution reaction consists of two terms; one is first order with respect to the complex (PtL_2AX) and the other one is first order in both the metal complex (PtL_2AX) and the entering ligand (Y)

$$\text{Rate} = -\frac{d[\text{PtL}_2\text{AX}]}{dt} = k_1[\text{PtL}_2\text{AX}] + k_2[\text{PtL}_2\text{AX}][\text{Y}] = (k_2 + k_2[\text{Y}])[\text{PtL}_2\text{AX}] \quad (2.5)$$

Under *pseudo* first-order conditions, where the concentration of the entering nucleophile (Y) is large enough, the experimental *pseudo* first-order rate constant (k_{obs}) is related to the individual rate constants as follows:

$$\text{Rate} = k_{\text{obs}}[\text{PtL}_2\text{AX}] \quad (2.6)$$

$$k_{\text{obs}} = k_1 + k_2[\text{Y}] \quad (2.7)$$

Therefore a plot of k_{obs} vs [Y] will have an intercept of k_1 and a slope of k_2. The value of k_1 is independent of the entering ligand while k_2 depends on the reactivity of the entering nucleophile. A typical plot for the substitution reactions of *trans*-[$Pt(Py)_2Cl_2$] by different nucleophiles is represented by Figure 2.3.[10]

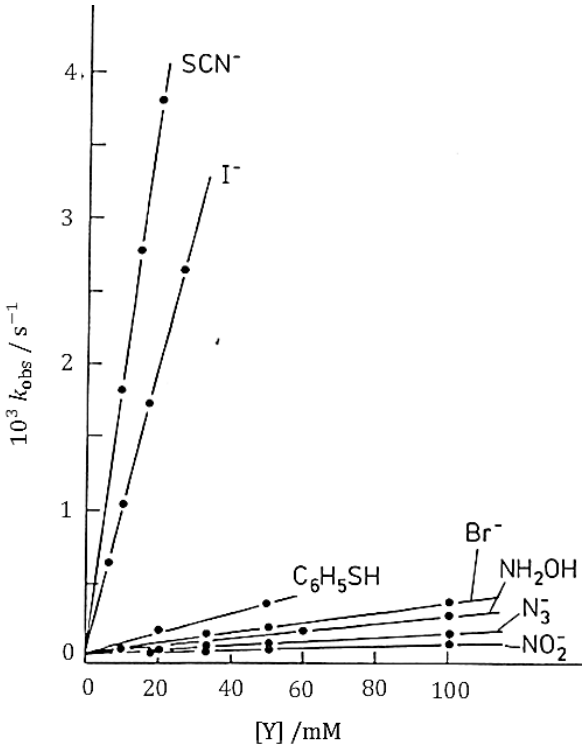

Figure 2.3 Rates of reaction of *trans*-[$Pt(Py)_2Cl_2$] as a function of the concentrations of different nucleophiles in methanol at 30 °C.[7, 10]

Since most of the substitution reactions are carried out in coordinating solvents such as water and methanol, the k_1 term can be attributed to the associative solvolysis pathway, which is a slow displacement of the leaving group (X) by the solvent (S) followed by the rapid replacement of (S) by the entering ligand (Y) as shown by Figure 2.4. However, this is not always the case as positive k_1 values can also be representative of the reverse reaction.[9]

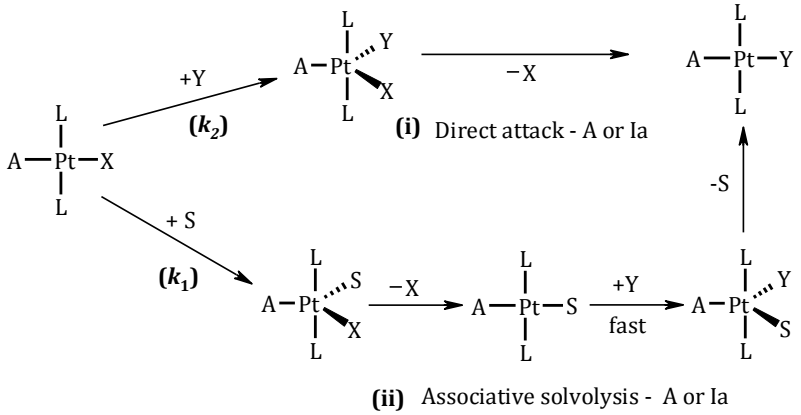

Figure 2.4 Schematic representation of a proposed two-path associative mechanism for the substitution reaction of a square-planar complex, $\mathbf{PtL_2AX}$ by Y to yield $\mathbf{PtL_2AY}$.[2, 9]

The acceptable reaction pathway for Pt(II) complexes is associative (*A*), however, the dissociative (*D*) mechanism has been reported in rare cases.[2] This is reasonable since the formed transition state in associative reactions consist of a five-coordinate 18-electron valence shell which is more energetically favoured compared to a three-coordinate 14-electron valence shell intermediate in dissociatively activated substitution reaction mechanisms. In addition, Pt(II) complexes have a p_z orbital of low energy which can accommodate the pair of electrons from the entering ligand and stabilize the five-coordinate transition state.[14] Synthesis and isolation of five coordinate trigonal bipyramidal salts such as $Pt(SnCl_3)_5^{3-}$ supports the stability of five-coordinate 18-electron Pt(II) complexes.[2, 14] Further evidence to support an associative reaction comes from the fact that the *cis* and *trans* configurations of the starting materials are retained in the products as shown by Figure 2.5. This is unlikely for a dissociative reaction pathway, because after forming a three-coordinate intermediate, the entering ligand has two possible sites of entry, and thus the product can either be *cis* or *trans.*

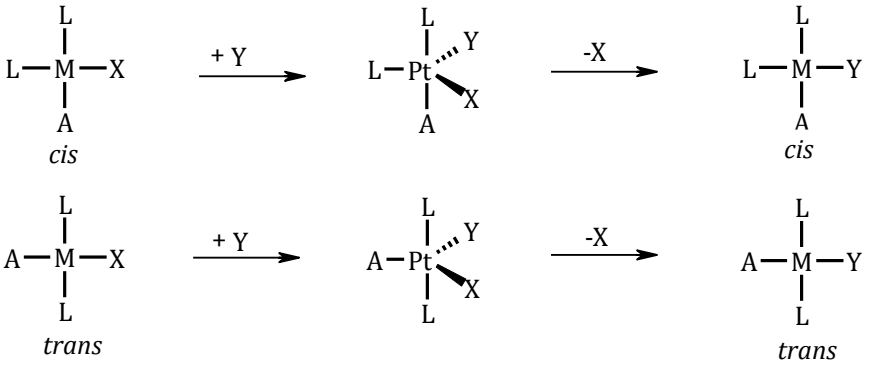

Figure 2.5 Retention of configuration in *cis* and *trans* square-planar Pt(II) complexes during an associative substitution reaction.[14]

2.3.2. Geometries of the Intermediates

There are two open positions for the attack of the incoming ligand in square-planar complexes during an associative substitution pathway, therefore, the approach of the incoming ligand can take place from either side.[4, 6] Substitution reactions of square-planar complexes involve the formation of an intermediate with an increased coordination number of five. General considerations of the shape and the available orbitals support only the formation of a trigonal bipyramidal geometry. However, it has been found that during the course of substitution, both square pyramidal and trigonal bipyramidal geometries are formed.[4] The potential energy profile of the associative reaction is shown in Figure 2.6

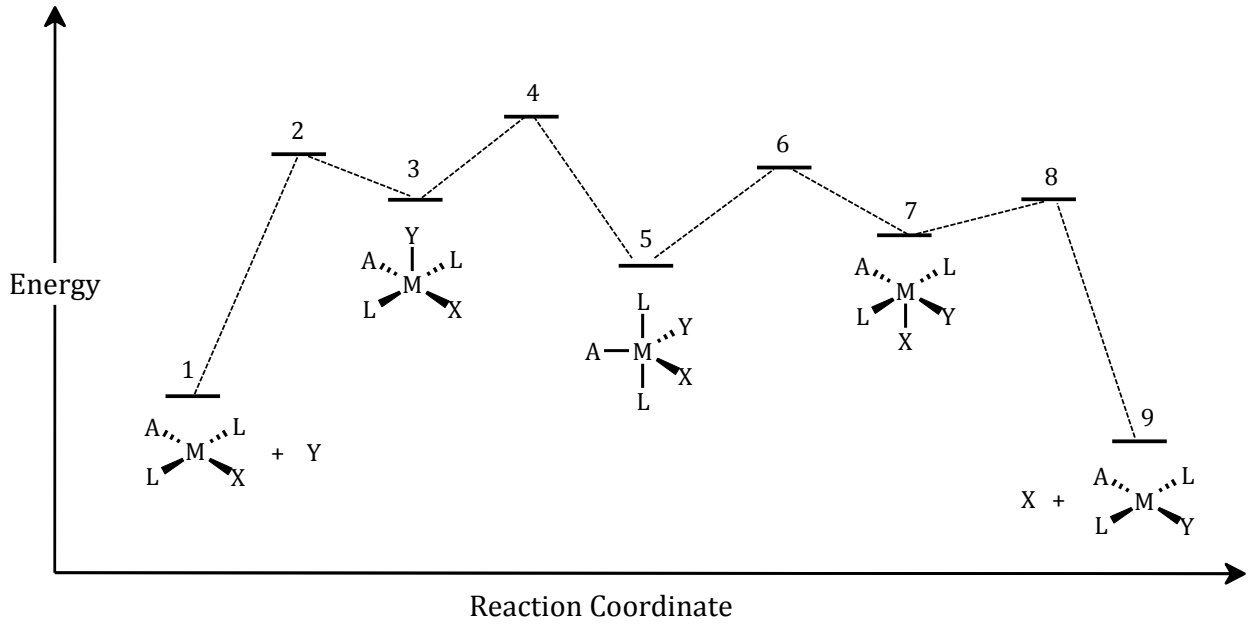

Figure 2.6 Schematic energy profile and possible steric changes during a square-planar substitution reaction of ligand X by Y: Energy maxima at **2**, **4**, **6** and **8** represent the transition states and the intermediates have energies at **3**, **5** and **7**.[4]

Figure 2.6 shows that the main intermediate is the trigonal bipyramidal and the high energy intermediates are square pyramidal. In addition, complexes at **1** and **9** show that the substitution takes place with a complete retention of configuration as previously depicted for associative substitution pathway, typical of d^8 Pt(II) complexes.[14]

2.4. Factors Controlling the Reactivity of Square-Planar Complexes

The reactivity of monofunctional square-planar complexes, where one of the four ligands is labile (X) and the remaining ligands are inert, is affected by various factors.

2.4.1. The *trans*-Effect

One of the important factors is the effect of the coordinated ligand (A) on the rate of substitution of the *trans*-ligand (X).[1-2, 4, 6, 7-8] This was first noticed by Werner[11] and later understood and utilized in Russia in 1926, when Chernyaev and co-workers[12] introduced the concept of *trans-effect* to correlate many reactions of Pt(II) complexes. The *trans-effect* is the effect of the coordinated ligand on the rate of substitution of the ligand *trans* to it.[1-2, 4, 6, 7-8, 10] By comparing a wide range of ligand substitution reactions, an empirically established and generally accepted order of the *trans-effect* is:

$$CO,\ CN^-,\ C_2H_4 > PR_3\ , H^- > CH_3^-,\ SC(NH_2)_2 > C_6H_5^-,\ NO_2^-,\ I^-, SCN^- > Br^-,\ Cl^- > Py,\ NH_3, OH^-,\ H_2O$$

This order follows that, inert ligands with the high *trans-effect* will lead to elevated substitution reactions of up to six orders of magnitude compared to ligands with low *trans effect*.[13-15] In addition, this order is very useful in rationalizing the synthetic procedures of square-planar complexes.[14] A classic example of the application of this empirically established trend is the synthesis of the *cis* and *trans* isomers of $PtCl_2(NH_3)_2$.[14]

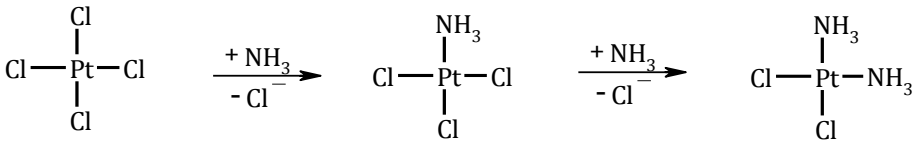

(2.8)

Charges omitted

The *cis* isomer is prepared by treating $[PtCl_4]^{2-}$ with ammonia (NH_3) as depicted by Equation ((2.**8**)). After the displacement of the first chloride ion in Equation (2.**8**), the *trans-effect* takes control of the reaction, and since the *trans* labilizing effect of Cl^- is greater than that of NH_3 , displacement of the second chloride ion by NH_3 takes place in the position *trans* to one of the coordinated chloride ions, to yield *cis*-$PtCl_2(NH_3)_2$. Preparation of the *trans*-isomer involves the treatment of $[Pt(NH_3)_4]^{2-}$ with chloride ions (Equation (2.9)). The first chloride group replaces any of the NH_3ligands, and this newly coordinated chloride ion directs the second incoming chloride ion into the position *trans* to it.

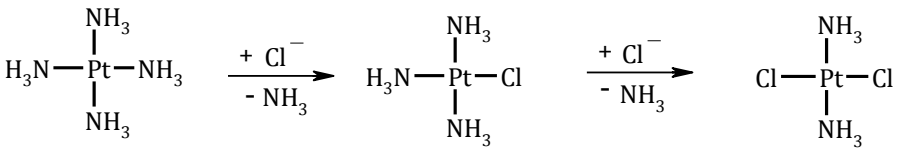

(2.9)

Charges omitted

When considering the *trans-effect* in substitution reactions of Pt(II) complexes, it should be noted that, ligands with the highest *trans-effect* form either unusually strong σ-bonds, such as

H^-, CH_3^-, and $SnCl_3^-$ or unusually strong π-bonds, such as C_2H_4, CO and CN^-. Therfore, in order to rationalize the order of the ligands in the *trans-effect* series, it is essential to understand both their σ and π bonding properties.[1, 14]

2.4.1.1. The σ-Bonding Theory

The high *trans-effect* of the strong σ-donor ligands can be explained in terms of the weakening of the *trans* $M-X$ bonds, observable by X-ray crystallography (increased $M-X$ bond lengths) or by spectroscopic measures such as NMR chemical shifts and IR spectrum stretching frequencies $\upsilon_{(M-X)}$.[4,14,16-17] This weakening of the $M-X$ bond is expected since strong σ-donor ligands in the *trans* position contribute more electron density to the shared p_x orbital and weakens the bond to the leaving group as shown in Figure 2.7.[7]

(a) (b)

Figure 2.7 Ground state representation of σ-bonding of $\mathbf{A-Pt-X}$. (a) σ-bond strengths are almost equal in the presence of a weak σ-donor. (b) The strong σ-donor ligand (A) weakens the bond to the *trans*-ligand (X).[7]

Such a change in the ground state thermodynamic properties of the complex is termed the *trans influence.*[18] This influence is a thermodynamic effect, separate from the *trans-effect*, but contributing to the overall kinetic result. [1, 4, 8, 17] The effect of $M-X$ bond lengthening is however minute in the trigonal bipyramidal intermediate since the strong σ-donor ligand A, does not directly share the same p orbital with X.[4] The order of the *trans-effect* due to σ-donation is as follows:[7]

$$H^- > PR_3 > SCN^- > I^- \; CH_3^-, CO, CN^- > Br^- > Cl^- > NH_3, > OH^-$$

From this order, it can be noticed that only the ligands; CO and CN^- are showing major deviations from the order of the *trans effect.*[4, 7] The behaviour of such ligands is thus attributed to their π-bonding capabilities. [4, 7]

2.4.1.2. The π-Bonding Theory

This theory suggests that π-bonding ligands are higher in the *trans-effect* series because of their ability to stabilize the transition state during the course of substitution.[7] This is because, the transition state involves the attack of the nucleophile, leading to a net increase in electron density, thus, a ligand with π-acceptor properties can remove this increased electron density from the metal centre leading to a stabilized five-coordinate transition state.[14]

Pauling[19] first introduced this theory to justify the Ni − C bond lengths in $Ni(CO)_4$ as well as the cyanide complexes of transition metals as compared to non-transition metals. Ligands such as CO, $CN^-$and phosphines of the formula (PR_3) are π-acceptors with empty orbitals that can accept the electron density from the filled metal d-orbitals.[8, 14] To account for the *trans-effect* due to π-bonding, Chatt *et al*[20] and Orgel[21] independently proposed π-bonding stabilization of the activated complex.[14] Chatt *et al* proposed that the removal of charge from Pt(II) by π-bonding of *trans*-ligand A will enhance the addition of Y allowing a more rapid associative reaction. Orgel suggested that, the stability of the transition state is increased due to π-bonding because of the reduction of electron density on the Pt(II) along the Pt − X and Pt − Y bonds. An example representing the formation of both the σ and π-bond between the Pt(II) centre and the *trans*-ligand A is depicted in Figure 2.8 where the σ-bond is formed by the two electron donation from ligand A to platinum and the π-bond is formed by the overlap between a filled *d*-orbital of platinum and an empty *d* or π^* orbital of the *trans* ligand A. [1, 4, 14]

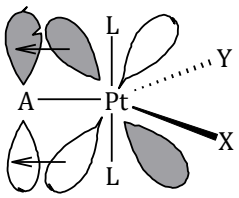

Figure 2.8 Activated complex for the associative substitution of reaction of *trans*-$\mathbf{PtL_2AX}$ by incoming nucleophile Y.

It should be noted that, since the π-bonding theory requires a 5-coordinate 18-electron activated complex, therefore it is applicable in associatively activated mechanisms (A or I_a) discussed earlier in this chapter.[2, 14]

2.4.1.3. The σ and π-*trans-effect*

The σ and π-*trans-effect* can be explained in terms of the molecular orbital (M.O.) theory as this gives the best explanation of the bonding in square-planar Pt(II) systems.[14] A simplified M.O. diagram for $[PtCl_4]^{2-}$ is shown in Figure 2.9. From this diagram, it is clear that the most stable σ-bonding orbitals and the second most stable π-bonding molecular orbitals are positioned mainly on the chloride ligands.[14] These are followed by the anti-bonding $\sigma^* and\, \pi^*$ M.O.'s derived from the Pt(II) 5d atomic orbitals. The order of stability of these anti-bonding M.O.'s is; ${\pi_{xz}}^*, {\pi_{yz}}^* > {\sigma_{z^2}}^* > {\pi_{xy}}^* > {\sigma_{x^2-y^2}}^*$. The highest energy orbitals are ${\sigma_s}^*$, ${\sigma_x}^*$ and ${\sigma_y}^*$ which are derived from the $p_z$valence orbital with no σ-bonding properties.

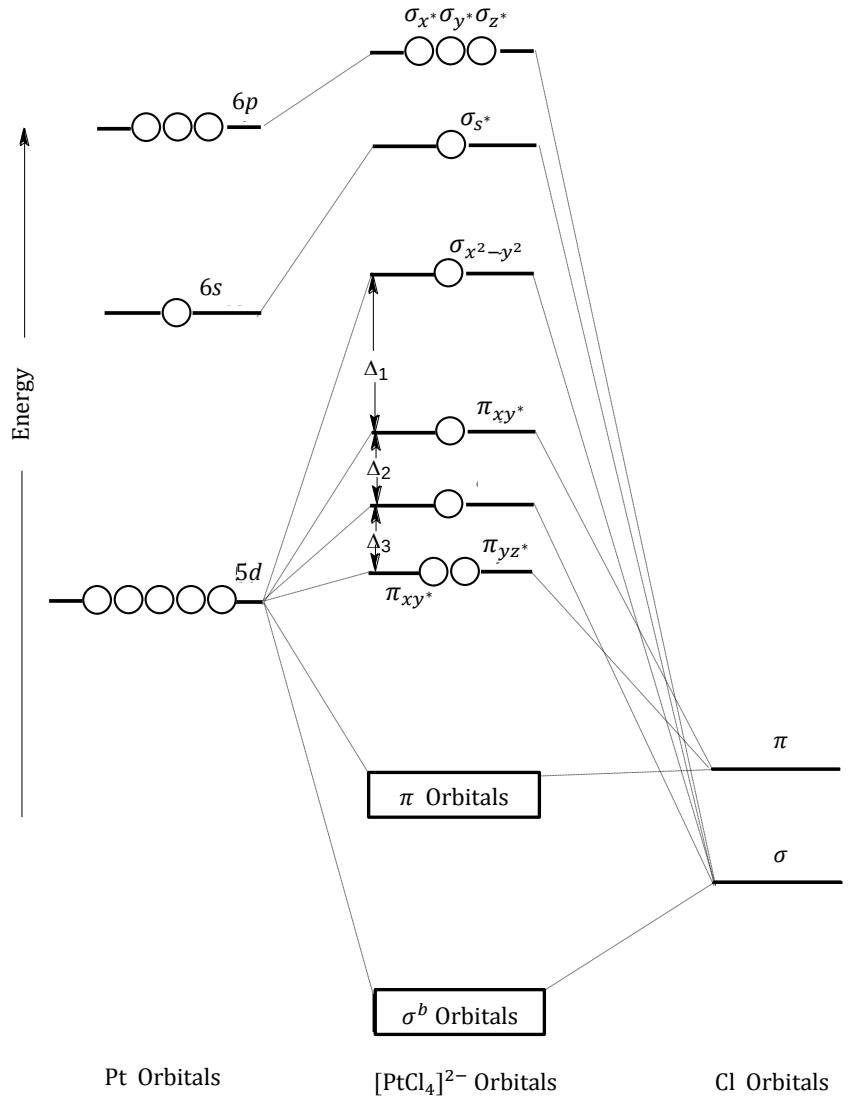

Figure 2.9 Molecular Orbital diagram of $[\mathbf{PtCl_4}]^{\mathbf{2-}}$.[14, 15]

In square-planar complexes, there are four metal valence orbitals used in σ-bonding ($d_{x^2-y^2}{}^*$, s, p_x and p_y.[14] Out of the four, only p-orbitals are effective *trans* directors, meaning that A and X in $trans-[PtL_2AX]$ share the same σ_x orbital in the overall M.O.[4, 7, 14] The strong σ-donor *trans*-ligand A takes a larger share of the σ_x bonding M.O. than the leaving group X.[14] This leads to the ground state Pt − X bond weakening which enhances the substitution reaction of X by Y (Figure 2.7). An additional explanation of the rate enhancement due to σ-donation was provided by Langford and Gray.[22] This suggests that strong σ-donors such as $CH_3{}^-$ and H^- stabilize the trigonal bipyramid by the process called the σ-*trans* effect.[22] The driving force of this stabilization is the fact that there are more orbitals for σ-bonding in the five coordinate intermediate than in the ground state square-planar complex. During the associative substitution reaction, X moves out of the x-axis after the addition of the entering nucleophile Y resulting in a trigonal plane containing Pt, A, X and Y (Figure 2.10). This newly formed

intermediate has two orbitals for three bonding ligands which is better than one orbital shared by two ligands in the ground state.[14] Therefore, the high *trans-effect* of the good *σ*-donor ligands due to this extra *p* character is referred to as the *σ-trans effect*.[22]

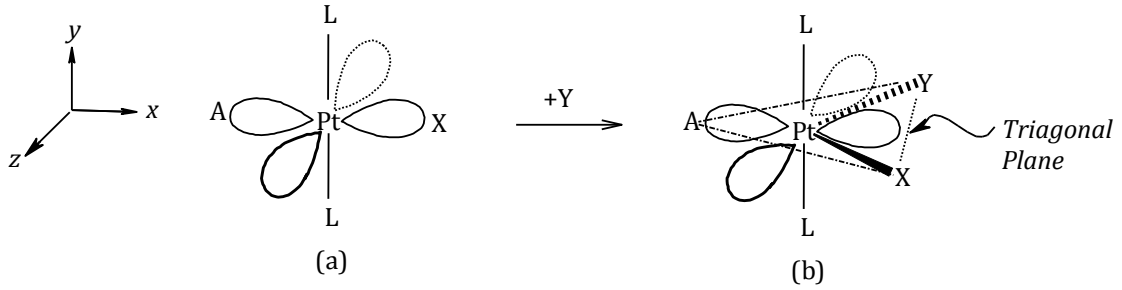

Figure 2.10 The σ-*trans-effect* due to the stabilization of the trigonal bipyramidal intermediate. (a) Only the $\boldsymbol{p_x}$ orbital is available for $\boldsymbol{\sigma}$-bonding of ligands A and X (b) $\boldsymbol{p_x}$ and the $\boldsymbol{p_z}$ orbitals are available for $\boldsymbol{\sigma}$-bonding of ligands A, X and Y in a trigonal plane.

In the case of strong π-acceptor ligands, the π-bonding theory discussed earlier can be explained in terms of the M.O. theory and refer to it as the π-*trans* effect.[22] Square-planar complexes consist of three M.O.'s with proper symmetry for π-bonding; $\pi_{xz}{}^*$, $\pi_{yz}{}^*$ and $\pi_{xy}{}^*$.[14] However, addition of the entering nucleophile to form a trigonal bipyramid leads to the additional M.O. ($\pi_{x^2-y^2}{}^*$) with a proper symmetry for π-bonding.[14] Therefore, all the three ligands in the trigonal plane share these four M.O.'s, which is responsible for the stabilization of the transition state if *trans* ligand A is a good π-acceptor ligand. Thus, the net effect of a good π-acceptor ligand A is to stabilize the transition state by lowering the activation energy of the reaction (**Error! Reference source not found.**).[7, 14]

2.4.2. The *cis*-Effect

The effect of the *cis* ligand (L) on the reactivity of Pt(II) complexes is generally accepted to be relatively much smaller than the *trans*-effect, except in the presence of steric hindrance.[2, 7] To account for the importance of steric hindrance of the *cis* ligands, the stability of the five coordinate intermediate formed during an associatively activated reaction mechanism has to be taken into consideration. In the trigonal bipyramidal intermediate, the *trans* ligand (A) shares the equatorial trigonal plane and is 120° away from the entering and leaving group. On the other hand, the *cis* ligand (L) is 90° away from the equatorial groups.

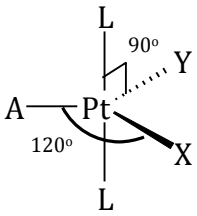

Figure 2.11 Transition state bond angles in the substitution reaction of ***trans***-[$\mathbf{PtL_2AX}$] by the nucleophile Y.

Therefore, increase in the size of ligands in the *cis* position will lead to more steric crowding between the *cis* ligand (L) and ligands X and Y in the equatorial plane leading to destabilization of the trigonal bipyramid and decreased substitution rate. Experimental evidence obtained for the substitution reaction of *cis*-$Pt(PEt_3)_2LCl$ by pyridine (Py) have shown that changing from L = phenyl to L = 1,3,5-trimethylbenzene leads to a reactivity rate decrease of about five orders of magnitude, whereas in the *trans* isomers of $Pt(PEt_3)_2LCl$, changing the *trans* ligands (L) from L = phenyl to L = 1,3,5-trimethylbenzene groups leads to a decrease by a factor of about 30.[4, 23] From this result and related studies, it is now accepted that the steric *cis* effect reduces the reactivity more than the corresponding steric *trans-effect*.[2, 24]

Table 2.1 Steric effects on the rates of substitution of *cis*- and *trans*-$\mathbf{Pt(PEt_3)_2LCl}$ by pyridine at 25 ℃.

Complex	Ligand, L	$k_{obs}\ /s^{-1}$
$\boldsymbol{cis-Pt(PEt_3)_2LCl}$	Phenyl (0°C)	8.0×10^{-2}
	o-tolyl (0°C)	2.0×10^{-4}
	1,3,5-trimethylbenzene	1.0×10^{-6}
$\boldsymbol{trans-Pt(PEt_3)_2LCl}$	Phenyl	1.2×10^{-4}
	o-tolyl	1.7×10^{-5}
	1,3,5-trimethylbenzene	3.4×10^{-6}

In the absence of steric hindrance, replacement of a weak *cis* *σ*-donor nitrogen by a strong *σ*-donor carbon leads to slower reactions, whereas, addition of strong *π*-acceptors leads to enhanced reactivity of the complex.[24] In addition, changing the Pt-C bond from the *trans* position of (1,3- bis(pyridyl)benzeneplatinum(II) chloride) to the *cis* position (6-pheny-l2,2′-bipyridineplatinum(II) chloride), drastically decrease the reactivity of the complex with thioureas and azole nucleophiles, suggesting that the phenyl group activates the metal centre differently in the *cis* and *trans* position.[25-27] Further kinetic investigatins of the *cis* effect have shown that the *cis* effect can sometimes be greater than the *trans-effect* in the absence of steric hindrance.[27-28] A study by Hofmann *et al*[27] revealed that monofunctional $[Pt(N-(pyridyl-2-methyl)-1,2-diaminoethane)OH_2]^{2+}$(**aap**) containing a strong π-acceptor *cis*-pyridinyl group reacts faster than $[Pt(2,6-bis-aminoethylpyridine)OH_2]^{2+}$ (**apa**) containing the same group in the *trans* position. This was found to be due to the ground state accumulation of the electron density in the **apa** complex leading to decreased electrophilicity of the metal centre in **apa** and slow substitution reactions.[28]

2.4.3. The Effect of the Chelating Ligand

In mononuclear Pt(II) complexes, binding ligands can be classified into two groups depending on their denticity. Ligands with one site of binding to the metal centre are referred to as unidentate such as NH_3.[8] The second group is called multidentate and consists of ligands with two or more points of attachment. The latter can also be termed chelating ligands, and the metal complexes they form are called chelates.[8] The importance of chelation on the reactivity rate of

Pt(II) complexes was realized when it was noticed that the introduction of aromaticity within a chelate ring leads to enhanced reactivity.

A study by Haake and Cronin[29] revealed that the rate of reaction of $Pt(en)Cl_2$ (en = ethylenediamine) is about two orders of magnitude less than that of $Pt(bipy)Cl_2$ (bipy = 2,2'-bipyridine) when dithiooxamide is an incoming nucleophile. In addition, the rate of reaction of $Pt(dien)Cl^+$ (dien = diethylenetriamine) has been found to be 10^5-10^6 times slower than that of the unsaturated system $Pt(terpy)Cl^+$ (terpy = 2,2':6',2"-terpyridine) when thiourea (**tu**) is an incoming nucleophile.[30-31] This high reactivity of unsaturated chelates has been attributed to the strong *π-trans-effect* due to the aromaticity in the platinum-α-diimine five membered chelate ring formed.[29] The $Pt-N$ π-bonding responsible for aromaticity of the chelate ring can be rationalized on the M.O. theory basis. The filled $2p_z$ orbitals on N overlaps with the empty *d*-orbitals on the platinum metal to produce an aromatic five-membered chelate ring with eight electrons, leading to a low electron density on the chloride side of the complex and a large *trans*-effect.[14, 29]

Introduction of multidentate ligands that form six membered chelate rings reduces the ring strain within the complex leading to the formation of twisted Pt(II) complexes.[32] Such twisting in six-membered chelates has been found to retard the reactivity of the complexes in at least one of two ways. (1) The π-back bonding ability of the ligand is significantly decreased since there is reduced overlap between the filled *d*-orbital of platinum and the empty *d* or π^* orbital in six membered chelates.[33] This can be confirmed using DFT calculations. (2) The approach of the entering nucleophile can be sterically hindered during an associatively activated mechanism leading to reduced reactivity of these complexes.[33]

Chelation has also been found to play a major role in oncotherapy, during the development of efficient second and third generation platinum drugs. Replacement of the two chloride groups in the cisplatin molecule by the more stable bidentate chelating ligands, 1,1-cyclobutanedicarboxylate in carboplatin and oxalate in oxaliplatin, was found to reduce the toxicity effects while retaining the antitumor potency of these formed Pt(II) complexes.[34] The observed pharmacokinetic difference is primarily attributed to the slower rate of conversion of carboplatin to the reactive species. Furthermore, the 1,2-diaminocyclohexane bidentate carrier ligand in oxaliplatin increases the specificity of the drug. Therefore, altering the nature (aromaticity, size and denticity) of the chelating ligand, can be useful in the ongoing research of finding novel platinum cancer drugs.

2.4.4. The Effect of the Entering Nucleophile (Y)

As mentioned before, the rate of reaction in associative reactions largely depends on the nature of the entering nucleophile. The nucleophilicity of the entering nucleophile (Y) has been found to be influenced by a number of factors such as; basicity, polarizability, oxidizability, solvation energy and the nature of the metal centre.[4] The existing kinetic data for Pt(II) complexes suggested that the order of reactivity of the nucleophiles is different than the order of their basicities, whereas the polarizability of the nucleophile plays an important role.[7] The nucleophilic reactivity order is as follows:[6,14]

$$PR_3 > tu > I^-, SCN^-, N_3^- > NO_2^- > Br^- > Py > NH_3, Cl^- > H_2O > OH^-$$

Polarizability of the nucleophiles can be explained using the theory of "hard" and "soft" acids and bases (HSAB), that was first proposed by Pearson in 1963.[35-36] This theory suggested that soft (polarizable) nucleophiles prefer soft substrates and hard (nonpolarizable) nucleophiles prefer hard substrates. Hard metal ions (acids) are highly charged with a valence shell that cannot be easily distorted whereas soft metal ions are large, bearing a low charge and have a valence shell that can be easily distorted and removed.[7] Therefore, the high tendency of larger donors to be effective nucleophiles towards Pt(II) complexes indicates that Pt(II) is a soft centre. In efforts to gain more understanding on the reactivity of various nucleophiles with Pt(II) centres, a detailed study on the displacement of chloride from *trans*-$Pt(py)_2Cl_2$ was conducted in methanol at 30 °C (Equation ((2.**10**)))

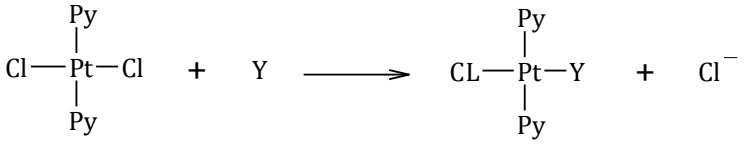

(2.10)

From this study, the nucleophilic reactivity constant, n_{Pt}^o, for each nucleophile was determined from Equation ((2.**11**))

$$n_{Pt}^o = log\frac{k_Y}{k_S} \quad (2.11)$$

$k_Y = rate\ constant\ for\ the\ entering\ nucleophile$

$k_s = rate\ constant\ for\ the\ attack\ by\ solvent$ (MeOH)

This constant measures the reactivity of the entering nucleophile towards the Pt(II) centre.[7] The n_{Pt}^o values given in (table 2.2) for the reactions of $Pt(py)_2Cl_2$ are also useful in linking the kinetic data for other Pt(II) complexes.[6]

Table 2.2 The nucleophilic reactivity constants for the reactions of $\mathbf{Pt(py)_2Cl_2}$ with various nucleophiles.

Nucleophile (Y)	$k \times 10^3/\mathrm{M^{-1}s^{-1}}$	n^o_{Pt}
$\mathbf{Cl^-}$	0.45	3.04
$\mathbf{NH_3}$	0.47	3.07
$\mathbf{NO_2^-}$	0.68	3.22
$\mathbf{N_3^-}$	1.55	3.58
$\mathbf{Br^-}$	3.70	4.18
$\mathbf{I^-}$	107	5.46
$\mathbf{SCN^-}$	180	6.65
tu	6000	7.17
$\mathbf{PPh_3}$	249000	8.93

Plots of $\log k_Y$ against n^o_{Pt} for other Pt(II) complexes were found to be linear (Figure 2.12), signifying a linear free energy relationship (L.F.E.R.) of the form:[6-7, 14]

$$\log k_Y = \mathrm{s}\, n^o_{Pt} + \log k_S \qquad (2.12)$$

$s = nuclephilic\ discrimination\ factor$

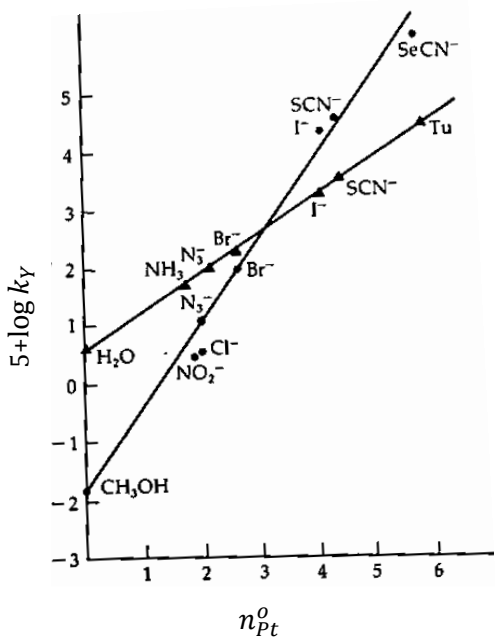

Figure 2.12 Correlation of the rate of substitution reactions of Pt(II) complexes with the standard complex $trans-Pt(py)_2Cl_2$ for different nucleophiles: ● = $trans-Pt(PEt_3)_2Cl_2$ in methanol at 30°C, ▲ = $Pt(en)Cl_2$ in water at 35 °C.

The constant *s* measures the sensitivity of the metal centre to the nucleophilicity of the entering ligand.[7] The value of *s* for the standard complex *trans*- $Pt(py)_2Cl_2$ is 1. A large value of *s* implies a high sensitivity of the reaction rate to changes in nucleophilic character.[7] Therefore an increase in the *s* value suggests an increase in the discriminating ability of the complex, leading to an inverse proportion between the reactivity of the complex and its *s* value. The discrimination factor *s*, also has an inverse correlation with the rate constant k_S, of the poorest nucleophile whose effect can be measured in a solvent S.[6-7] If k_S is small, this implies that the tendency for the complex to react is small and its reactivity will rely more on the changes in the nucleophile. Complexes with the high values of *s,* such as those of phosphine and arsine, have ligands that are capable of π-bonding in the transition state, which may enhance the addition of the entering nucleophile.[6,14] Therefore, the rate of substitution of such systems is highly sensitive to the nature of the entering nucleophile.

2.4.5. The Effect of the Leaving Ligand (X)

The entering group (Y) and the leaving group (X) effects are closely related since these groups occupy equivalent positions in the transition state during an associative reaction.[7] The magnitude depends on the relative amounts of bond formation and bond weakening in the transition state.[2] The large dependence of the reactivity of Pt(II) complexes on the nature of the leaving group dominates in dissociative reactions since the rate determining step is the $Pt - X$ bond breaking.[1-2, 4, 6-7, 14] For associative reactions, the effect of the leaving group has also been found to have an influence on the rate of substitution.[2] This effect is the most difficult to systematize since it is not only related to the nature of the entering nucleophile, but it is also closely related to the nature of the reaction centre, the nature of the *trans* ligand and the solvent polarity.[2] The use of inert tridentate ligands such as dien leads to the formation of more stable complexes and makes it easy to understand the effect of the single labile ligand. Substitution reactions of $[Pt(dien)X]^+$ by the pyridine (py) nucleophile in aqueous solution have been studied in detail to get more understanding of the leaving group effects (Equation ((2.**13**))).

$$[Pt(dien)X]^+ + Py \rightarrow [Pt(dien)Py]^{2+} + X^- \qquad (2.13)$$

From the results obtained, it has been found that the rate of substitution of the leaving group *X* decrease in the order:

$$NO_3^- > H_2O > Cl^- > Br^- > I^- > N_3^- > SCN^- > NO_2^- > CN^-$$

The fact that the members of the series differ in the rate constants by as much as six orders of magnitude, suggests that there is a substantial amount of bond breaking in the transition state, even in a primarily associative reaction.[7]

2.4.6. The Role of the Solvent

The solvent plays at least two important roles in substitution reactions of square-planar complexes. It can act as a nucleophile in the solvolysis (k_1) path of the reaction as mentioned earlier in this chapter and also as a reaction medium. Depending on the nucleophilicity of the solvent and the entering ligand, the observed rate law may be dependent or independent of the entering nucleophile.[7]

It is difficult to obtain the nucleophilicity sequence using the k_1 path since substitution reactions are mainly controlled by the k_2 path and therefore, the k_1 rate constant is either negligible or seriously affected by the experimental error.[14] Experimental data suggests that the k_1 path is independent of the entering nucleophile (Y), but changes with the nature of the solvent by a few orders of magnitude.[6-7, 14] Such a small change is expected since most solvents are considered to be relatively poor nucleophiles.[6] However, for solvents that are capable of coordinating strongly to the Pt(II) centre, a large value of k_1 relative to k_2 is observed with the general order of: $(CH_3)_2SO > CH_3NO_2,\ H_2O >$ ROH.[6]

Data for the studies of the effect of the solvent on the chloride exchange reactions (Equation ((2.**14**))) is presented in Table 2.3.

$$trans\text{-}Pt(py)_2Cl_2 + {}^{36}Cl^- \rightarrow trans - Pt(py)_2Cl({}^{36}Cl) + Cl^- \qquad (2.14)$$

This data suggests that there is a direct proportion between the reaction rate and the nucleophilicity of the solvent in the case of coordinating solvents. For solvents that poorly coordinate to Pt(II) substrates, the k_2 path dominates and the differences in rate constants on changing the solvents is due to the polarity of the solvent. The use of nonpolar solvents, leads to enhanced reaction rates because the chloride is not solvated and thus highly reactive.

Table 2.3 Solvent effect on the chloride substitution reaction.[37]

Coordinating ability	**Solvent**	$\boldsymbol{k\ /10^{-5}s^{-1}}$
Strong	$(CH_3)_2SO$	380
	H_2O	3.5
	EtOH	1.4
	$n-$PrOH	0.4
Coordinating ability	**Solvent**	$\boldsymbol{k\ /M^{-1}s^{-1}}$
Weak	CCl_4	10^4
	C_6H_6	10^2
	$i-$BuOH	10^{-1}
	$(CH_3)_2C(O)$	10^{-2}
	$(CH_3)_2NC(O)H$	10^{-3}

In the presence of ligands of low coordination ability, there are several indications that the planar complexes tend to be solvated by the weak coordination of the reaction medium (solvent molecules) at axial positions in the ground state.[8] This axial solvation is lost during the formation of the intermediate in associative reaction. The nucleophilic discrimination factor *s* has been found to be approximately the same on changing the solvents in the presence of complexes containing good $\sigma-$donor and $\pi-$acceptor ligands, meaning that the metal-solvent interactions are kinetically insignificant.[8] Furthermore, there is no change in the nucleophilicity order on changing the solvent and the kinetics follows the LFER.[4-6]

2.4.7. Steric Effect

There have been several studies on the effects of the use of sterically hindered substrates and reagents. Out of these studies, at least two types of effects have been found. The presence of steric hindrance in the substrate or reagent molecule only causes a decrease in the rate of bimolecular substitution reaction.[2, 4, 6-7] The substrate can be so crowded that the common bimolecular attack of the incoming nucleophile cannot occur anymore, leading to a dissociative reaction mechanism.[2]

In the case of bimolecular (*A* or I_a), the usual consequence of steric hindrance is retardation in the reaction rate which can be due to shielding of the two "open" positions for attack of the incoming nucleophile in the ground state. In addition, destabilization of the five coordinate transition state compared to the ground state can also be responsible for this retardation due to steric hindrance.[14]

The use of sterically hindered ligands in square-planar complexes is helpful in changing the mechanism of substitution from associative to dissociative.[2] This is because the intermediate in associative reactions is more crowded than that of the dissociative mechanism. Therefore, the use of bulky ligands in the ground state allows the formation of the less crowded intermediate and speeds up the dissociative reaction to relieve the steric strain.

2.5. References

1. R. B. Jordan, *Reaction Mechanisms of Inorganic and Organometallic Systems*, Oxford University Press, New York, **1991**, p. 29 - 40
2. M. L. Tobe and J. Burgess, *Inorganic Reaction Mechanisms*, Addision Wesley, London, **1999**, p. 30 - 39
3. C. K. Ingold, *Structure and Mechanism in Organic Chemistry*, *2*nd Ed., Cornell University Press, Ithaca, New York, **1969**, p. 241.
4. S. Ašperger, *Chemical Kinetics and Inorganic Reaction Mechanisms*, *2nd* Ed., Kluwer Academic/Plenum Publisher, New York, **2003**, p. 38 - 40,105 - 106.
5. C. H. Langford and H. B. Gray, *Ligand Substitution Processes*, Benjamin, New York, **1966**, p. 7 - 10.
6. R. G. Wilkins, *Kinetics and Mechanisms of Reactions of Transition Metal Complexes*, *2nd* Ed., VCH, Weinheim, **1991**, p. 199 - 201.
7. J. D. Atwood, *Inorganic and Organic Reaction Mechanisms*, 2nd Ed., Wiley-VCH Inc., New York, **1997**, p. 32 - 34, 43 – 61.
8. G. L. Miessler and D. A. Tarr, *Inorganic Chemistry*, Prentice Hall Internatioal Inc, New Jersey, **1991**, p. 372 - 375.
9. F. Basolo, *Adv. Chem. Ser*. **1965**, *49*, 81.
10. U. Belluco, L. Cattalini, F. Basolo, R. G. Pearson and A. Turco, *J. Am. Chem. Soc.,* **1965**, 87, 241 - 246.
11. Z. Werner, *Anorg. Chem*. **1893**, *3*, 267.
12. I. I. Chernaev, *Ann. Inst. Platine USSR*., **1962**, *4*, 216
13. A. Yamamoto, *Organotransition Metal Chemistry*, John Wiley & Sons, New York, **1986**, 180 - 201.
14. F. Basolo and R. G. Pearson, *Mechanisms of Inorganic Reactions: A Study of Metal Complexes, 2nd* Ed., John Wilet & Sons, New York, **1967**, p.351 - 406.

15. Moeller, T., *Inorganic Chemistry: A modern Introduction*, John Wiley & Sons, New York, **1982**, p.714 - 719.
16. B. A. Coyle and J. A. Ibers *Inorg. Chem.* **1972**, 1105 - 1109.
17. T. G. Appleton, H. C. Clark and L. E. Manzer, Coord. Chem. Rev. **1973**, 10, 335.
18. A. Pidcock, R. E. Richards and L. M. Venanzi. *J. Chem. Soc.* **1966**, 1707 - 1710.
19. L. Pauling, *The Nature of the Chemical Bond,* Cornell University Press, Ithaca, New York, *3rd* Ed, **1960**, p.332
20. J. Chatt, L. A. Duncanson, and L. M. Venanzi, *J. Chem. Soc.*, **1955**, 4461 - 4469.
21. L. E. Orgel., *Inorg. Nucl. Chem.,* **1956**, *2*, 137.
22. C. Langford and H. B. Gray, *ligand Substitution Processes*, W. A. Benjamin, New York, **1966**, 18 – 45.
23. F. Basolo, J. Chatt, H. B. Gray, R. G. Pearson and L. B. Shaw*, J. Chem. Soc*., **1961**, 2207 - 2215.
24. Hofmann, L. Dahlenburg, R. van Eldik., *Inorg. Chem.,* 2003, 42, 6528 - 6538
25. Jaganyi, D.; Reddy, D.; Gertenbach, J. A.; Hofmann, A.; van Eldik, R., *Dalton Trans.,* **2004**, 299 - 304.
26. D. Reddy, K. J. Akerman, M. P. Akerman, D. Jaganyi, *Transition. Met. Chem*., **2011**, *36*, 593 - 602.
27. A. Hofman, L. Dalhenburg, R. van Eldik, *Inorg. Chem*. **2003**, 42, 6528 - 6538.
28. A.Hofman, D.Jaganyi, O. Q. Munro, G. Liehr, R. van Eldik, *Inorg. Chem*. **2003**, 42, 1688 - 1700.
29. P. Haake and P. A. Cronin, *Inorg. Chem,* **1963**, 2, 879 - 880.
30. Pitteri, B., Marangoni, G., Cattalini, L., Bobbo, T., *J. Chem. Soc. Dalton. Trans.* **1995**, 3853 - 3859.
31. Romeo, R., Plutino, M. R., Scolaro, J. M., Stoccoro, S.,Minghetti, G. *Inorg. Chem.* **2000**, 39, 4749 - 4755.
32. T. G. Appleton and R. J. Hall*, Inorg. Chem*., **1970***, 9*, 1800 - 1806.
33. Petrović, B., Burgarčić, Ž. D., Dees, A., Ivanović-Burmazović, I., Heinemann, F. W., Puchta, R., Steinmann, S. N., Corminboeuf, C., van Eldik, R., *Inorg. Chem.,* **2012**, *51*, 1516 - 1521.
34. Kostova, I. *Recent Patents on Anti-Cancer Drug Discovery*. **2006**, *1*, 1 - 22
35. R. G. Pearson, *J. Am. Chem. Soc.* **1963**, *85*, 3533 - 3543.
36. R. G. Pearson*, J. Am. Chem. Educ.* **1968**, *45*, 643 - 648
37. R. G. Pearson, H. B. Gray, F. Basolo, *J. Am. Chem. Soc*. *82*, **1960**, 787 - 792.

Chapter 3

Chemical Kinetics

3. Chemical Kinetics

3.1. Introduction

Quantitative studies of chemical reactions fall into two groups.[1] The first group deals with the actual occurrence of the reaction regardless of its rapidity.[1-2] This is known as chemical thermodynamics and measures quantities such as the standard enthalpy change and standard Gibbs energy change of a reaction.[2] The second group is known as chemical kinetics and deals with the rapidity of the reaction over time and allows for the determination of the reaction rate under hypothetical conditions.[2-3]

The main prerequisite for studying chemical kinetics is for the structure of the reactants and products to be known.[1] Kinetic studies are often done to develop an understanding of the reaction mechanism, which deals with all the individual collisional and other elementary processes involving molecules that take place simultaneously or consecutively in producing the overall reaction.[4] Thus, the reaction mechanism basically describes all the pathways by which a reactant is converted into products. It shows whether a given chemical reaction occurs in a single molecular process or in several elementary steps.[5] There are two key questions when defining the mechanism. Is the mechanism consistent with all the known facts about the system? If not, then there is a high possibility for the mechanism to be incorrect.[5] Are there any new predictions from the mechanism? such as the stereochemical consequence of the reaction.[5]

The rate of a reaction is influenced by a number of factors, the major ones being; concentration, solvent, intensity of absorbed radiation and physical conditions.[3]

Concentration	Increasing the concentration of the reactants leads to enhanced reaction rates.
Solvent	Reaction rates differ with the solvent's property such as; polarity, viscosity, donor number, added electrolyte and buffer components.

Intensity of absorbed radiation	In the case of studies other than the photochemical effects, light from external sources such as sunlight and laboratory lights may alter the rate of the chemical reaction.
Physical conditions	Physical conditions such as pressure and temperature affect the rates; as a consequence, these are normally kept constant in a given study.

It is therefore important to control these factors in order to obtain meaningful kinetic data. Of all these variables, concentration is the most considered factor in quantitative analysis of the rapidity of the reaction.[3]

In this chapter, some important aspects of chemical kinetics will be considered, including; simple rate laws and some of the techniques used for obtaining kinetic and mechanistic data.

3.2. Rate Laws

The most important tool in mechanistic studies is the determination of the experimental rate law.[5] This gives the number and types of molecules involved in the formation of the transition state.[5] In addition, it gives comparable reaction speeds.[5-6] The interpretation of a rate law is reasonably straight forward. Considering the hypothetical reaction;

$$A_i \rightarrow B \tag{3.1}$$

taking place in a closed system, the rate of this reaction is given by the rate of decrease of the concentration of the reactants (A_i) or by the rate of increase of the concentration of the product(s), B over time, t.[1-3,7]

$$Rate = \frac{-d[A_i]}{dt} = \frac{d[B]}{dt} \tag{3.2}$$

However, it should be noted that it is unusual for the reaction rate to be influenced by the concentration of the products.[2] Therefore, the rate law in Equation (3.1) may be simply expressed in terms of the reactants and all the species such as catalysts, which may affect the reaction rate:[7]

$$Rate = -k_n \prod_i [A_i]^{\alpha}{}_i [X_j]^{\beta}{}_j \tag{3.3}$$

Where A_i represent the chemical symbols for reactants i, k_n is the n^{th} order rate constant, and X_j are other species such as catalysts, that may affect the rate. α and β are reaction orders with respect to A_i and X_j respectively. The reaction order is defined as:

$$Reaction\ order\ (n) = \sum_i \alpha_i \tag{3.4}$$

The units of the rate of the reaction are M s^{-1} and depending on the order (n) of the reaction, the units of the rate constant (k_n) may vary. For a first-order reaction, where the reaction order $=$ 1, the rate constant has the units per second (s^{-1}), whereas for the second-order reaction, where the reaction order is 2, the units are $M^{-1}s^{-1}$. [7-8]

3.3. Integrated Rate Equations

3.3.1. First-order reactions

3.3.1.1. Irreversible first-order reactions

Often the rate of the reaction is first-order with respect to one reactant or performed under conditions that approximate first-order kinetics.[7-8] For simplicity, consider the first-order conversion of reactant A to form product B,

$$\boldsymbol{A} \xrightarrow{\boldsymbol{k_1}} \boldsymbol{B} \tag{3.5}$$

that proceeds to completion according to the rate law

$$rate = -\frac{d[A]}{dt} = k_1[A] \tag{3.6}$$

Rearranging the equation to separate the variables, $[A]$ and t, yields:

$$-\frac{d[A]}{[A]} = k_1 dt \tag{3.7}$$

which upon integration between the limits ($\boldsymbol{t = 0}$, $[\boldsymbol{A}]_{\boldsymbol{0}}$) and ($\boldsymbol{t = t}$, $[\boldsymbol{A}]_{\boldsymbol{t}}$) gives

$$-\int_{[\boldsymbol{A}]_0}^{[\boldsymbol{A}]_t} \frac{1}{[A]} d[A] = \int_0^t k_1 dt \tag{3.8}$$

$$ln\frac{[A]_t}{[A]_0} = -k_1 t \tag{3.9}$$

$$ln[A]_t = ln[A]_0 - k_1 t \tag{3.10}$$

Equation (3.10) shows that a $\boldsymbol{ln[A]_t}$ will be a linear function of *t*, implying that the logarithm of the reactant concentration decrease linearly with time. From this, the slope can be used to determine the rate constant, $\boldsymbol{k_1}$. Taking antilogarithms of each side of Equation (3.10), affords equation,

$$\boldsymbol{[A]_t = [A]_0\, e^{-k_1 t}} \tag{3.11}$$

which indicates the exponential decrease of the reactant concentration over time. [2-3, 7-8]

For a reaction that is first-order with respect to one reactant A, any factor that is proportional to the concentration such as absorbance, pressure, conductivity or volume can be used to directly follow the kinetics of the reaction.[3,8]

3.3.1.2. Reversible first-order reactions.

Some reactions such as isotopic exchange and unimolecular isomerism are reversible under reaction conditions, such that the starting material A attains dynamic equilibrium with the product, B.[2-3,8] In principle, the rates of the forward and the reverse reactions are equal.[2] Considering the elementary reaction:

$$\boldsymbol{A} \underset{\boldsymbol{k\text{-}_1}}{\overset{\boldsymbol{k_1}}{\rightleftharpoons}} \boldsymbol{B} \tag{3.12}$$

The rate law for this reaction according to the disappearance of A is given by

$$-\frac{d[A]}{dt} = k_1[A]_t - k_{-1}[B]_t \tag{3.13}$$

At the start of the reaction, $t = 0$, $[B]_0 = 0$ and $[A]_0 = [B]_t$; whereas at any time ($t = t$),

$$[B]_t = [A]_0 - [A]_t \tag{3.14}$$

Substituting Equation (3.14) into Equation (3.13), gives

$$-\frac{d[A]}{dt} = k_1[A]_t - k_{-1}([A]_0 - [A]_t) \tag{3.15}$$

At equilibrium,

$$-\frac{d[A]}{dt} = 0 \tag{3.16}$$

and Equation ((3.**15**) becomes

$$k_1[A]_{eq} = k_{-1}[B]_{eq} = k_{-1}([A]_0 - [A]_{eq}) \tag{3.17}$$

Which can also be rearranged to give an expression in which [A] is the only concentration variable:

$$[A]_0 = \frac{k_1 + k_{-1}}{k_{-1}}[A]_{eq} \tag{3.18}$$

Substitution of Equation ((3.**18**) to Equation ((3.**15**) leads to the following;

$$\ln\left(\frac{[A]_0 - [A]_{eq}}{[A]_t - [A]_{eq}}\right) = (k_1 + k_{-1})t \tag{3.19}$$

which upon rearrangement leads to

$$\boldsymbol{ln}([\boldsymbol{A}]_{\boldsymbol{t}} - [\boldsymbol{A}]_{\boldsymbol{eq}}) = \boldsymbol{ln}([\boldsymbol{A}]_{\boldsymbol{0}} - [\boldsymbol{A}]_{\boldsymbol{eq}}) - (\boldsymbol{k_1} + \boldsymbol{k_{-1}})\boldsymbol{t} \tag{3.20}$$

According to Equation (3.20), a plot of $\mathbf{ln}([\boldsymbol{A}]_{\boldsymbol{t}} - [\boldsymbol{A}]_{\boldsymbol{eq}})$ versus time, t will give a straight line with the slope of $-(\boldsymbol{k_1} + \boldsymbol{k_{-1}}) = -\boldsymbol{k_{obs}}$ and an intercept of $\boldsymbol{ln}([\boldsymbol{A}]_{\boldsymbol{0}} - [\boldsymbol{A}]_{\boldsymbol{eq}})$. In order to individually obtain $\boldsymbol{k_1}$ ***and*** $\boldsymbol{k_{-1}}$, the equilibrium rate constant, $\boldsymbol{K_{eq}}$ must be evaluated from Equation (3.21)

$$K_{eq} = \frac{[B]_{eq}}{[A]_{eq}} = \frac{k_1}{k_{-1}} \tag{3.21}$$

However, it is not easy to accurately measure $[\boldsymbol{A}]_{\boldsymbol{eq}}$ from the reversible first-order reactions.

3.3.2. Second-Order Reactions

In second-order reactions, the rate may be proportional to the square of the concentration of one reagent.[3] This is commonly encountered in situations such as the decay of short-lived transients and rare in stable substances since those that decompose by reacting with themselves are difficult to concentrate in pure form.[3] The most encountered type of second-order reactions are those that are first-order in two reagents, and these will be considered in this chapter.

3.3.2.1. Irreversible Second-Order Reactions

For the second-order reaction,

$$A \quad + \quad B \xrightarrow{k_2} C \tag{3.22}$$

The rate law for this reaction is

$$rate = \frac{d[C]}{dt} = -\frac{d[A]}{dt} = -\frac{d[B]}{dt} = k_2[A][B] \tag{3.23}$$

If the initial concentrations of A and B are $[A]_0$ and $[B]_0$ respectively, let x be the decrease in the concentrations of A and B over time t. At time t, when the concentration of A and B are $([A]_0 - x)\ and\ ([B]_0 - x)$, the rate law becomes

$$rate = -\frac{d[A]}{dt} = k_2([A]_0 - x)([B]_0 - x) \tag{3.24}$$

And since $x = [A]_0 - [A]_t$ Equation (3.24)can be rewritten as

$$rate = -\frac{dx}{dt} = k_2([A]_0 - x)([B]_0 - x) \tag{3.25}$$

or

$$\frac{dx}{([A]_0 - x)([B]_0 - x)} k_2 dt \tag{3.26}$$

Integrating between the limits $(x = 0,\ t = 0)$ and $(x = x,\ t = t)$

$$\int_0^x \frac{dx}{([A]_0 - x)([B]_0 - x)} \int_0^t k_2 dt \tag{3.27}$$

gives

$$\frac{1}{([A]_0 + [B]_0)} \left(\ln \frac{([A]_0 - x)}{[A]_0} - \ln \frac{([B]_0 - x)}{[B]_0} \right) = k_2 t \tag{3.28}$$

This can be simplified by combining the two logarithms and noting that $[A]_t = [A]_0 - x$ and $[B]_t = [B]_0 - x$ to give

$$\frac{1}{([A]_0 + [B]_0)} \ln \frac{[B]_0}{[A]_0} \frac{[A]_t}{[B]_t} = k_2 t \tag{3.29}$$

The second-order rate constant, k_2 may be determined from a plot of $\ln [A]_t/[B]_t$ versus t, which should be linear with a slope equal to $([A]_0 + [B]_0)\, k_2$. However, finding all the necessary variables used in Equation (3.29); $[A]_0, [B]_0, [A]_t$ and $[B]_t$ may be time consuming and complicated.[7] To overcome this, the reactions can be studied under *pseudo*-first-order conditions where the concentration of one of the reactants is in large excess ($[B]_0 \gg [A]_0$).[1] Thus the concentration of reagent B will not significantly change during the course of the reaction and the rate law in Equation (3.23) simplifies to a first-order rate law.

$$rate = k_2 [B]_t [A]_t = (k_2 [B]_0)[A]_t = k_{obs} [A]_t$$

Where $k_{obs} = k_2 [B]_0$ (3.30)

$\boldsymbol{k_{obs}}$ is the observed rate constant in s^{-1} and may be obtained by plotting the graph of $\ln[A]_t$ versus t, which gives the observed rate constant k_{obs} (s^{-1}) as the slope. To obtain the second-order rate constant, $\boldsymbol{k_2}$, a series of $\boldsymbol{k_{obs}}$ values can be determined by varying the initial concentrations of B, $[\boldsymbol{B}]_\mathbf{0}$ and plotting $\boldsymbol{k_{obs}}$ versus $[\boldsymbol{B}]_\mathbf{0}$ which gives $\boldsymbol{k_2}$ as a slope in $M^{-1}\, s^{-1}$.[7]

3.3.2.2. Reversible Second-Order Reactions

Some second-order reactions such as complexation reactions do not go to completion; instead, they proceed towards equilibrium where the measurable concentration of reactants remains.[1] Considering the second-order reversible reaction,

$$A + B \underset{k_{-2}}{\overset{k_2}{\rightleftharpoons}} C \tag{3.31}$$

with mixed-order behaviour, second-order with respect to the forward reaction and first-order with respect to the reverse reaction. Selecting *pseudo* first-order conditions for the forward reaction simplifies the quantitative analysis of such reactions. Therefore under *pseudo* first-order conditions ($[B]_0 \gg [A]_0$), the rate law is

$$-\frac{d[A]}{dt} = -\frac{d[B]}{dt} = \frac{d[C]}{dt} = k_2[A]_t[B]_t - k_{-2}[C]_t \tag{3.32}$$

Assuming that the reaction has a stoichiometric ratio of (1: 1: 1) and at the start of the reaction, $t = 0$ and $[C]_o = 0$, the mass balances at time $t = t$ are

$$[A]_t = [A]_0 - [C]_t$$

$$[B]_t = [B]_0 - [C]_t \tag{3.33}$$

And at equilibrium, the mass balances are

$$[A]_{eq} = [A]_{eq} - [C]_t$$

$$[B]_{eq} = [B]_{eq} - [C]_t \tag{3.34}$$

Noting that at equilibrium, the rate of forward and reverse reactions are the same, gives

$$-\frac{d[A]}{dt} = k_2[A]_{eq}[B]_{eq} - k_{-2}[C]_{eq} = 0 \tag{3.35}$$

or

$$k_2[A]_{eq}[B]_{eq} = k_{-2}[C]_{eq} \tag{3.36}$$

Substituting Equations (3.34) and Equation (3.35) into Equation (3.36), gives an expression in terms of the concentrations of reagents A and B.

$$k_2[A]_{eq}[B]_{eq} = k_{-2}([A]_0 - [A]_{eq})$$

$$k_{-2}[A]_0 = k_2[A]_{eq}[B]_{eq} + k_{-2}[A]_{eq} \tag{3.37}$$

Rearranging Equation ((3.**33**)): $[C]_t = [A]_0 - [A]_t$ and substituting it into Equation ((3.**32**) gives

$$-\frac{d[A]}{dt} = k_2[A]_t[B]_t - k_{-2}([A]_0 - [A]_t)$$

$$= k_2[A]_t[B]_t - k_{-2}[A]_0 - k_{-2}[A]_t \tag{3.38}$$

Substituting Equation ((3.**37**) into Equation ((3.**38**) yields:

$$-\frac{d[A]}{dt} = k_2[A]_t[B]_t - k_2[A]_{eq}[B]_{eq} - k_{-2}[A]_{eq} - k_{-2}[A]_t \tag{3. 39}$$

Under pseudo first-order conditions, Equation ((3. **39**) can be written as

$$-\frac{d[A]}{dt} = k_2[A]_t[B]_0 - k_2[A]_{eq}[B]_0 - k_{-2}[A]_{eq} - k_{-2}[A]_t$$

$$= (k_2[B]_0 + k_{-2})([A]_t - [A]_{eq}) \tag{3.40}$$

Rearranging Equation (3.38) and integrating between the limits $(x = 0,\ t = 0)$ and $(x = x,\ t = t)$

$$\int_{[A]_0}^{[A]_t} \frac{d[A]}{[A]_t - [A]_{eq}} = -(k_2[B]_0 + k_{-2}) \int_0^t dt \tag{3.41}$$

gives

$$\ln\left(\frac{[A]_t - [A]_{eq}}{[A]_0 - [A]_{eq}}\right) = -(k_2[B]_0 + k_{-2})t$$

$$= -k_{obs}\, t$$

Where $$k_{obs} = k_2[B]_0 + k_{-2} \tag{3.42}$$

According to Equation ((3.**42**), a plot of k_{obs} versus $[B]_0$ is linear with a slope of k_2 and an intercept of k_{-2}. The equilibrium constant K_{eq}, can be determined as a ratio of k_2/k_{-2}

3.4. Effect of Temperature on Reaction Rates

The rate laws discussed above are essential in determining a reaction mechanism and the rate constant. Temperature dependence studies are also very useful in determination of the activation parameters from the variation of the rate constant with temperature.[2]

Quantitative experimental rate measurements based on temperature dependence studies were first proposed by Arrhenius in 1889.[9] From this research, it was pointed out that the effect of temperature can be expressed with considerable accuracy by the Arrhenius Equation:

$$k = Ae^{-(E_a/RT)} \tag{3.43}$$

Where A is the Arrhenius pre-exponential factor measured in $M^{-1}\,s^{-1}$, E_a is the Arrhenius activation energy in $J\,mol^{-1}$, R is the Gas constant = 8.314 $J\,K^{-1}\,mol^{-1}$ and T represents the temperature in Kelvin. Taking logarithms affords Equation ((3.**44**)), which suggests that a plot of $\ln k$ versus $(1/T)$should be a straight line with the slope of E_a/R and intercept of $\ln A$

$$\ln k = \ln A - \frac{E_a}{R}\left(\frac{1}{T}\right) \tag{3.44}$$

In addition to the Arrhenius Equation, another equation derived from the transition state theory (TST) may be useful in expressing the temperature dependence of the rate constant.[3] This theory is based on the application of statistical mechanics to reactants and the activated complex. The fundamental assumption of the transition state theory is that there is an equilibrium between the reactants and the transition state complex, $[A \cdots B]^*$, as depicted by Equation (3.45):[1-2]

$$\mathrm{A{-}B} \quad \underset{}{\overset{K^{\neq}}{\rightleftharpoons}} \quad \left[\,\mathrm{A{-}\,-\,-B}\,\right]^* \xrightarrow{k_2} \quad \mathrm{A} \quad + \quad \mathrm{B} \tag{3.45}$$

It should be noted that since the concentration of the transition state complex is negligible in relation to the starting material, the equilibrium does not require any significant depletion of the concentration of the starting material.[2] The rate of the reaction based on the transition state complex is as follows,

$$\frac{d[A]}{dt} = k_2[A \cdots B]^* = \frac{k_b T}{h}[A \cdots B]^* \tag{3.46}$$

Where k_b is Boltzmann's constant ($1.38 \times 10^{-23}\, J\, K^{-1}$) and h is Planck's constant ($6.626 \times 10^{-34}\, Js^{-1}$).

The equilibrium constant ($K^{\neq}$) for the first part of Equation (3.45) can be expressed as

$$K^{\neq} = \frac{[A \cdots B]^*}{A - B} \tag{3.47}$$

which rearranges to give:

$$[A \cdots B]^* = K^{\neq}[A - B] \tag{3.48}$$

Substituting Equation (**(3.48)**) into Equation (**(3.46)**) in order to get the rate law in terms of the concentration of the reactants gives

$$\begin{aligned} \frac{d[A]}{dt} &= k_2 K^{\neq}[A - B] \\ &= \frac{k_b T}{h} K^{\neq}[A - B] \end{aligned} \tag{3.49}$$

The experimental rate constant for the reaction (k_{expt}) can be related to the rate constant by:

$$\frac{k_b T}{h} K^{\neq} = k_{expt} \tag{3.50}$$

Thus, the rate law in Equation (3.**49**) can be simplified to

$$\frac{d[A]}{dt} = k_{expt}\,[A - B] \tag{3.51}$$

The equilibrium constant, $\boldsymbol{K^{\neq}}$ may also be expressed in terms of the corresponding Gibbs free energy of activation, $\Delta \boldsymbol{G^{\neq}}$ as follows

$$\Delta G^{\neq} = -RT \ln K^{\neq} = \Delta H^{\neq} - T\Delta S^{\neq} \tag{3.52}$$

Upon substitution of Equation (3.52) into Equation (3.50), the experimental rate constant, k_{expt} becomes:

$$k_{expt} = \frac{k_b T}{h} e^{\left(\frac{\Delta S^{\neq}}{R} - \frac{\Delta H^{\neq}}{RT}\right)} \tag{3.53}$$

After taking the logarithms, Equation (3.53) becomes,

$$\ln\left(\frac{k_{expt}}{T}\right) = -\frac{\Delta H^{\neq}}{RT} + \ln\left(\frac{k_b}{h}\right) + \frac{\Delta S^{\neq}}{R} \tag{3.54}$$

Substituting the constants, k_b and h, Equation(3.54) simplifies to,

$$\ln\left(\frac{k_{expt}}{T}\right) = -\left(\frac{\Delta H^{\neq}}{R}\right)\frac{1}{T} + \left(23.8 + \frac{\Delta S^{\neq}}{R}\right) \tag{3. 55}$$

A plot of $\ln(k_{expt}/T)$ will be a linear function of $1/T$, with the slope giving the standard activation enthalpy, $\Delta H^{\neq}$ and the intercept providing the standard activation entropy, $\Delta S^{\neq}$. This type of plot is referred to as an Eyring plot.[10]

3.5. Practical Measurement of Reaction Rates

The rate of the reactions can be practically measured using either chemical or physical methods.[1] Chemical methods involve sampling, quenching of the reaction and direct measurement of the concentration. Even though this method gives an absolute measure of the sample concentration, however it is not easily automated and does not work well with most fast reactions. Physical methods are relative and deal with any property which can be used to measure the reaction rate, such as conductance for ionic reagents, absorption of ultraviolet or visible light, rotation of polarised light in chiral molecules, etc. A common and significant feature in physical measurements of the reaction rate is the continuous, rapid-response measurement, without the need for sampling.[1]

In this study, the physical methods employed are based on the absorption of ultraviolet-visible light, *viz*. Ultraviolet-Visible spectrophotometry and stopped-flow spectrophotometry.

3.5.1. Ultraviolet-Visible Spectrophotometry

The ultraviolet-visible or UV-Vis method is the most frequently used of all spectroscopic methods in chemical kinetics.[11] It is used to measure the transmittance/ absorbance of a sample as a function of the wavelength of electromagnetic radiation.[12] The key components of a UV-Vis spectrophotometer include:

Radiation source	The light source used in this instrument covers the ultraviolet-visible region; 190 nm to 1100 nm.[11-12] The frequently used light source consist of two radiation sources with appropriate wavelengths (λ), *viz*. UV light ($\lambda = 190\ to\ 370nm$) and Vis light ($\lambda = 320\ to\ 1100nm$), which are derived from a deuterium arc lamp and a tungsten lamp respectively.[12] Alternatively a xenon lamp whivh covers both the UV and the Vis range can be used.[11-12] However, the level of noise from the latter is worse than that of deuterium and tungsten lamps.[12]
Monochromator	This is used for the isolation of the desired wavelength and consists of an entrance slit, a dispersion device, and an exit slit.[12-13] There are two types of dispersion devices to date *viz.* prism and dispersion gratings. Most modern spectrophotometers use dispersion gratings instead of prims due to additional advantages in the former, such as temperature insensitivity and linear angular dispersion.[12]
Sample compartment	Sample cells or cuvettes that are transparent in the spectral region of interest and are made using quartz or fused silica.[11]
Detector	The primary function of a detector is to converts a light signal into an electrical signal.[12] Spectrophotometers normally consist of either a photomultiplier tube detector or a photodiode detector. The photomultiplier is the commonly used means of detection and quantification of data in UV/Visible spectrophotometry.[11-13]

Since the measurement of absorption of ultraviolet-visible radiation is relative in nature, this means that there should be a continous comparison between the absorption of the sample and that of an analytical reference or blank in order to ensure the reliability of the measurement.[11] This was initially achieved by the employment of a *single-beam* instrument, whereby there is

only one optical path from the light source to the detector.[14] This means that after each reading, the sample has to be manually removed from the optical path and replaced by a reference after each reading. Drift in source intensity, electronic instability and any other changes in the optical system result in significant errors over time.[11]

Alternatively, the sample and the reference may be compared using a *double-beam* instrument, where there is simultaneous comparison between the sample and the reference.[11-13] Figure 3.1 shows a typical *double-beam* ultraviolet-visible spectrophotometer. When the light of different wavelengths enters the monochromator through the entrance slit, S_1, it is reflected to a diffraction grating, G where the wavelength of interest is selected, thus it exits through the exit slit, S_2 as monochromatic radiation. Since the sample and the reference are in different compartments, the radiation into the sample and reference cuvettes is then split using a rotating mirror or chopper 1(see Figure 3.1).[11] After passing through the cuvettes, the beams are recombined by another mirror, chopper2, wich transmits the reference beam and reflects the sample beam to allow both beams be detected very rapidly by a single detector.[11, 14]

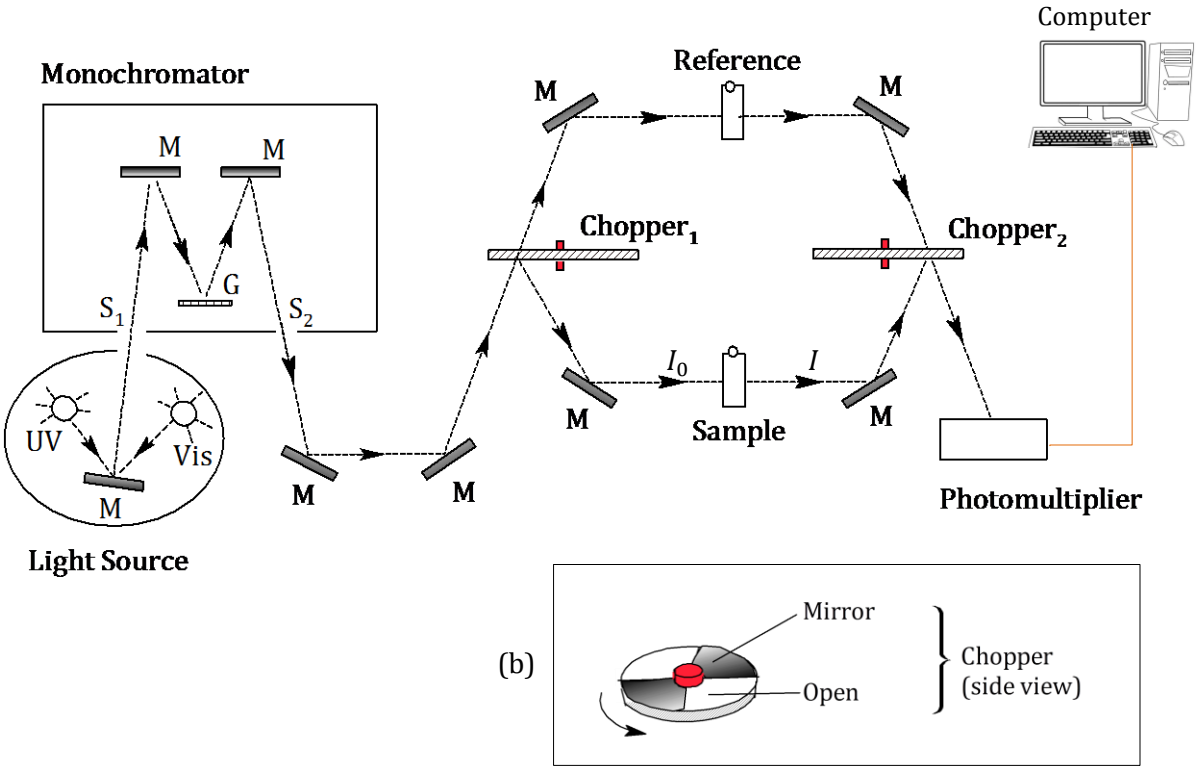

Figure 3.1 Schematic diagram of a *double-beam* Ultraviolet-Visible spectrophotometer, Insert (b): 3 dimensional view of the chopper.[11-12]

In principle, when a beam of radiation is passed through an absorbing substance, the intensity of incident radiation I_0 is greater than that of the emerging radiation I.[12-14] The quantities I_0 and I may be represented by transmittance, T,

$$T = \frac{I}{I_0} \tag{3.56}$$

which is a fraction of incident light that passes through a sample at a specific wavelength, λ.[14] This can also be related to the absorbance, *Abs* as follows:

$$Abs = -\log T \tag{3.57}$$

According to Beer's law, the absorbance, *Abs*, is directly proportional to the concentration of the absorbing species, *c*, and the path length of the absorbing medium, *l*, as shown by Equation (3.58):[12, 14]

$$Abs = \varepsilon cl \tag{3.58}$$

where ε is the molar absorptivity of the sample with the units $L\ mol^{-1}cm^{-1}$ if c is in $mol\ L^{-1}$ and *l* is in *cm*.[14]

For a first-order reaction,

$$\boldsymbol{A} \xrightarrow{\boldsymbol{k_1}} \boldsymbol{B} \tag{3.5}$$

the absorption at any time, t, is given by

$$Abs_t = \varepsilon_{\boldsymbol{A}}[A]_t + \varepsilon_B[B]_t \tag{3.59}$$

Where Abs_t = absorbance at time, t,

$\varepsilon_{\boldsymbol{A}}$ and $\varepsilon_{\boldsymbol{B}}$ = molar absorptivities of reagent **A** and product **B** respectively.

Upon completion of the reaction, the absorbance is represented by

$$Abs_\infty = \varepsilon_{\boldsymbol{A}}[A]_0 + \varepsilon_B[Y]_0 \tag{3.60}$$

Where Abs_∞ = absorbance at infinity

For kinetic studies, the absorbance of the sample can be related to time, *t* as follows:

$$\ln\frac{[A]_0}{[A]_t} = \ln\left(\frac{Abs_0 - Abs_\infty}{Abs_t - Abs_\infty}\right) = k_1 t \tag{3.61}$$

Which rearranges to give

$$(Abs_t - Abs_\infty) = (Abs_0 - Abs_\infty)e^{-k_1 t} \tag{3.62}$$

or

$$Abs_t = Abs_\infty + (Abs_0 - Abs_\infty)e^{-k_1 t} \tag{3.63}$$

A plot of $(Abs_t - Abs_\infty)$ versus time, t or a non-linear least squares fit,[7] Equation (3.63) of the experimental data, where absorbance (Abs_t) is plotted against time yields the experimental first-order rate constant. For concentration dependance studies, this is repeated at different concentrations of the reagent, keeping the wavelength and temperature constant, whereas for temperature dependence studies, the concentration and the wavelength are kept constant while the temperature is varied.

3.5.2. Stopped-Flow Technique

In the case of reactions with rate constants of up to about $5 \times 10^2\ s^{-1}(i.e., t_{1/2} \geq 1\ ms)$, more rapid mixing and detection of reagents without interfering with the rate of the reaction is required.[3] The most widely used technique in following such fast reactions in solution is the stopped-flow mixing.[1,11,15] This involves rapid mixing (within $1\ millisecond$) of two reagents which then drives a piston which is brought up against an external stop. Figure 3.1 shows a schematic diagram of the apparatus.

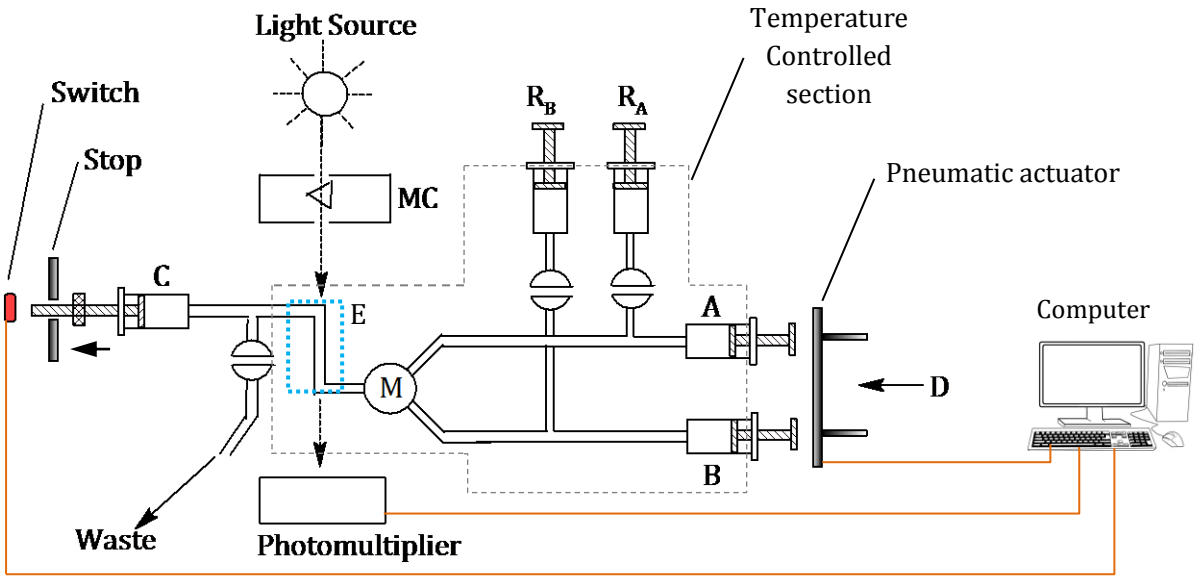

Figure 3.2 Schematic diagram of a *stopped-flow* spectrophotometer.[15]

Syringes A and B are filled with equal amounts of individual reactants from the reservoirs, R_A and R_B respectively. The motion, D from the pneumatic actuator drives the syringes, A and B, which forces the individual solutions into the mixing chamber, M and the mixed solution flows into the stopping syringe C, whose piston comes to rest against the fixed stop. The plunger in stop syringe C actuates the switch which allows for the rapid collection of the kinetic data spectrophotometrically from this stationary solution in the observation cell, E.

During spectrophotometric measurements, the light from the source enters the monochromator, MC and leaves as monochromatic radiation. After passing through the observation cell, E containing the mixed solution, it then goes to the photomultiplier where light signals are converted to electric signals, and the computer software is used to determine the change in absorbance and the observed rate constant (k_{obs}).[15] At the end of the measurement, the stop syringe is manually purged, making the instrument ready for the next experiment.[11] Once a high percentage of both reagents in the drive syringes has been consumed, drive syringes are refilled with reagents from the respective reservoirs. This is done at different times in order to avoid the possibility of cross contamination of the respective reagents.

3.6. References

1. B. G. Cox, *Modern Liquid Phase Kinetics*, Oxford University Press, New York, **1994**, p. 6 - 12, 23 - 30, 44, 59.
2. S. R. Logan, *Fundamentals of Chemical Kinetics*, Adison Wesley Longman, Harlow, **1996**, p 1 - 9, 17, 20, 33 - 34, 55, 70 - 71.
3. J. H. Espenson, *Chemical Kinetic and Reaction Mechanisms*, *2*nd Ed., McGraw-Hill, New York, **1995**, p. 1 - 40, 46, 253 - 255.
4. F. Basolo and R. G. Pearson, *Mechanisms of Inorganic Reactions: A Study of Metal Compleces*, *2*nd Ed., John Wilet & Sons, New York, **1967**, p.351 - 406.
5. R. A. Henderson, The Mechanisms of Reactions at Transition Metal Sites, Oxford University Press, New York, ***1993***, p1 - 6.
6. W. C. Gardiner, *Rates and Mechanisms of Chemical Reactions*, W.A. Benjamin Inc., Amsterdam, **1969**, p 25 - 28, 34 - 36.
7. J. D. Atwood, *Inorganic and Organic Reaction Mechanisms*, 2nd Ed., Wiley- VCH Inc., New York, **1997**, p. 1 - 31.
8. S. Ašperger, *Chemical Kinetics and Inorganic Reaction Mechanisms*, *2*nd Ed., Plenum Publisher, New York, **2003**, p. 1 - 23.
9. K. J. Laidler, J. H. Meiser, B. C. Sanctuary, *Physical Chemistry*, *4*th Ed., Houghton Mifflin Company, New York, **2003**, p. 374 - 379, 390 - 393.
10. Eyring, H. *J. Chem. Phys.,* **1935**. *3*, 107 - 115
11. G.D. Christian, J. E. O'Reilly, *Instrumental Analysis*, *2*nd Ed., Allyn and Bacon, Boston, **1986**, p. 184, 192 - 198.
12. T. Owen, *Fundamentals of UV-Visible Spectroscopy*, Hewlett-Packard, **1996**, p. 24 - 50.

13. D. C. Harris, *Quantitative Chemical Analysis*, 4th Ed., W. H. Freeman and Company, New York, **1995**, p. 480.
14. D. A. Skoog, A. M. West, F. J. Holler, S. R. Crouch, *Fundamentals of Analytical Chemistry*, 8th Ed., Thomson Brooks/Cole, Canada, **2002**, p. 374 - 379, 720, 769 - 775.
15. D.N. Hague, *Fast Reactions*, Wiley, London, **1971**, 16 - 17.

Chapter 4

The cis-Effect of the N-donor Moiety on the Rate of Chloride Substitution in Monofunctional N^N^N Pt(II) Complexes: A Kinetic and Computational Approach.

The *cis*-Effect of the N-donor Moiety on the Rate of Chloride Substitution From Monofunctional N^N^N Pt(II) Complexes: *A Kinetic and Computational Approach.*

Abstract

Three platinum(II) complexes of the type $[Pt(N^N^N)Cl]^+$ where N^N^N = 2,6-bis(N-pyrazolyl)pyridine, 2,6-bis(quinolin-8-yl)pyridine and 2,6-bis(7-azaindolyl)pyridine were synthesised for mechanistic studies in ethanolic media. The rate of substitution of the chloro ligand by Pyrazole (**Pz**), 1,2,4-Triazole (**Tz**), Imidazole (**Im**), 1-methylimidazole (**MIm**) and 1,2-dimethylimidazole (**DMIm**) was investigated under pseudo-first order conditions as a function of nucleophile concentration and temperature using stopped flow and UV-visible spectrophotometric techniques. The small but positive activation enthalpies and large negative activation entropies support an associative mechanism of ligand substitution. The data obtained suggests that structural modifications on the N^N^N chelating ligand have a strong influence on the second order rate constant. Changing from a strong π-acceptor pyridine *cis* group to a weaker π-acceptor pyrazole in five-membered chelates, results in deceleration of the substitution rate. The twisting of the bulky *cis* groups in six-membered chelates (**Pt3** and **Pt4**) slows the reactivity in two ways; (1) the electronic communication between the Pt(II) centre and the *cis* groups is reduced and (2) Steric clash between the *ipso*-hydrogens hinders the approach and the final coordination of the entering nucleophile. The reactivity of the complexes was also found to be dependent on the basicities and steric hindrance of the entering N-donor azole nucleophiles. DFT calculations support the kinetic results.

4.1. Introduction

Studies of interactions between square-planar d^8 Pt(II) complexes and bio-relevant nitrogen and sulfur donor nucleophiles have received considerable attention in the recent past, given that the mechanism behind anticancer activity of platinum drugs is primarily the interactions with N-donor nucleobases of genetic DNA.[1-2] However, the interaction of these drugs with S-donor biomolecules has been associated with the occurrence of toxic side effects.[1,3-4] These side effects and the narrow spectrum of cancer cell lines of the Pt(II) drugs under clinical use, has led to a continous search for new and more effective anticancer drugs.[5]

Most of the platinum compounds which entered into clinical trials in the early years of platinum anticancer drug discovery obeyed the traditional structure-activity relationships (SARs), which

required the complexes to at least possess the following characteristics; a neutral charge, have a square-planar coordination geometry, possess of a pair of *cis*-inert ligands in the coordination sphere, and a pair of labile ligands in the remaining two sites.[6] This ruled out the possibility for monofunctional Pt(II) complexes to be of clinical significance as supported by the early studies performed on complexes such as $[Pt(dien)Cl]^+$ and $[Pt(NH_3)_3Cl]^+$.[7-8] However, this generalization was later re-evaluated since certain members of this class of compounds were found to display significant antitumor activity, both *in vivo* and *in vitro*.[9] The cationic charge and the planarity of these complexes are responsible for the high affinity for DNA intercalation which gives rise to the observed anticancer activity.[10] The use of π-conjugated chelating ligands such as terpy in Pt(II) has been linked to desired cytotoxicity against human ovarian carcinoma,[11] and more studies have been conducted on tuning the reactivity of the platinum centre by slight modifications on the inert conjugated ligand.[12-18] Part of these protracted studies include understanding of the kinetics of interaction of these compounds with N- and S-donor biomolecules.

An extensively studied cationic complex, $[Pt(terpy)Cl]^+$ and its tridentate, monofunctional analogues have been found to be useful models for studying the ligand substitution reactions of Pt(II) complexes since only the fourth chloride ligand is substituted[4] and the presence of the π-conjugated ligand leads to greater stability of the tridentate ligand. Kinetic and thermodynamic data on substitution reactions of Pt(II) complexes suggests that the complexes undergo an associative mechanism with a few exceptions.[19-20] The driving force of the formation of a five coordinate $18e^-$ intermediate in $[Pt(terpy)Cl]^+$ is the ability of the π-acceptor polypyridine terpy ligand to accept the excess metal *d*-electrons through π-backbonding.[21-22] The π-back bonding is also responsible for the enhanced reactivity of $[Pt(terpy)Cl]^+$ compared to its non-conjugated monofunctional derivative $[Pt(dien)Cl]^+$.[21-22]

The reactivity of chelated monofunctional Pt(II) complexes has been found to be significantly affected by the *cis*-π effects. A recent study within our group has demonstrated that the increase in π-conjugation in one of the *cis* groups of the terpyridyl inert ligand, slightly decreases the reactivity of the complex with N-donor nucleophiles.[12] It has also been found that increasing the chelate ring size by employing a saturated methyl linker between the π-acceptor *cis* and *trans* groups retards the reactivity of the complex due to electronic and steric effects.

To gain more understanding on the effect of the *cis* groups on the reactivity of monofunctional Pt(II) complexes with selected N-donor azole nucleophiles, we explored the effect of changing the *cis* pyridinyl groups of terpy to electron deficient pyrazolyl *cis* groups. In addition, the effect of simultaneously increasing the π-conjugation and chelate ring sizes was investigated. This was

achieved by employing fused-ring *cis* groups, namely; 7-azaindole and 8-quinoline respectively. The four monofunctional Pt(II) complexes are of the type $[Pt(N\hat{}N\hat{}N)Cl]^+$, where N^N^N = *terpy*, 2,6-bis(N-pyrazolyl)pyridine, 2,6-bis(quinolin-8-yl)pyridine and 2,6-bis(7-azaindolyl)pyridine and were substituted from the metal centre by N-donor azole nucleophiles; Pyrazole (**Pz**), 1,2,4-Triazole (**Tz**), Imidazole (**Im**), 1-methylimidazole (**MIm**) and 1,2-dimethylimidazole (**DMIm**). DFT computations were performed in an effort to account for the reactivity difference of the studied complexes. The structures of the investigated complexes are summarised in Figure 4.1**.**

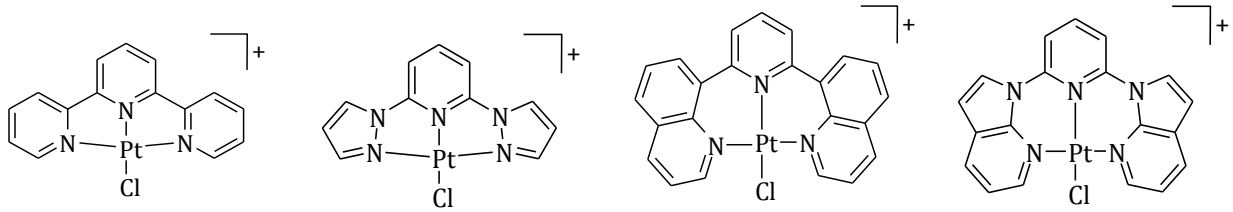

Figure 4.1 Structural representation of the investigated monofunctional Pt(II) complexes.

4.2. Experimental

4.2.1. Chemicals and General Procedures

The metal salt, potassium tetrachloroplatinate (K_2PtCl_4, 99.99%) was purchased from STREM and stored in a desiccator at room temperature. The $[Pt(COD)Cl_2]$ precursor was synthesised following the literature method.[23] The ligand terpy (**L1**), was purchased from Aldrich whereas ligands; 2,6-bis(N-pyrazolyl)pyridine (**L2**), 2,6-bis(quinolin-8-yl)pyridine (**L3**) and 2,6-bis(7-azaindolyl)pyridine (**L4**) were synthesized according to published procedures[24-26] with slight modifications. All solvents were dried and distilled prior to use. Other chemicals were purchased from Aldrich and used as received. The Pt(II) complexes were synthesized according to literature methods.[26-27]

4.2.2. Ligand Synthesis

2,6-Bis(*N*-pyrazolyl)pyridine, L2. A solution of of pyrazole (4.49g, 66 mmol) in 80 ml anhydrous diglyme was stirred with (2.4 g, 61.3 mmol) of potassium at 70 ℃ until the metal is dissolved. To this solution was added (3.0 g, 20 mmol)of 2,6-dichloropyridine in one portion. The resulting mixture was stirred at 110 ℃ for 5 days. The solvent was reduced in vacuo on a rotary evaporator. Final traces of solvent were removed by adding water to the resulting oil and

reducing the volume under vacuum. Water was added, and the resulting suspension was filtered to give white solid (72%, 3.22 g) ^{1}H NMR(400 MHz $CDCl_3$**)** δ 6.50 (dd, 2H) 7.76 (dd, 2H) 7.78-7.95 (m, 3 H), 8.60 (dd, 2 H) ^{13}C NMR(400 MHz $CDC1_3$) δ 108.08, 109.51, 127.0, 141.45, 142.5, 150.2. $^{+}$Anal. Calc. for $C_{11}H_9N_5$: C, 64.15; H, 5.17; N, 30.67 *Found:* C, 64.21 H, 4.93;N, 31.15. TOF MS-ES^{+}, m/z: 234.0756 $(M + Na)^{+}$

2,6-Bis(quinolin-8-yl)pyridine, L3. The ligand was prepared using the procedure developed by Buchwald and Co-workers. An oven-dried flask was filled with 2,6-dibromopyridine (210.2 mg, 0.887 mmol), quinoline-8-boronic acid (507.2 mg, 2.93 mmol), bis(dibenzylideneacetone)palladium(0) (18 mg, 0.032 mmol), 2-dicyclohexylphosphino- 2',6'-dimethoxybiphenyl (24 mg, 0.058 mmol) and ground K_3PO_4 (2240 mg, 10.54 mmol). The flask was evacuated and back filled with N_2. Toluene (20 mL) was added via a syringe and the resulting suspension was stirred at 100 ℃ for 18 hrs. After cooling to room temperature, the crude product was diluted with CH_2Cl_2 (40 mL) and filtered, the solvent was then reduced *in vacuo*. The solid was further purified by column chromatography using silica gel and 2.5% MeOH/CH_2Cl_2. The solid was recrystallized from a dichloromethane/hexane (50:50 %) solution to give off-white crystals (135 mg, 45.7%) *Anal. Calc*. for $C_{23}H_{15}N_3$: C 82.88, H 4.50, N 12.63, *Found*: C 82.44, H 4.55, N 12.73. $^{+1}$H NMR (400 MHz, $CDCl_3$): δ = 9.01 (dd, 2H,), 8.30 (dd, 2H), 8.25 (dd, 2H), 8.16 (d, 2H), 7.96 (t, 1H), 7.90 (dd, 2H) 7.68 (dd, 2H), 7.46 (dd, 2H) ^{13}C NMR (400 MHz, $CDCl_3$) δ = 156.64, 150.23, 145.97, 139.06, 136.49, 135.16, 131.59, 128.68, 128.60, 126.64, 125.50, 121.00. TOF MS-ES+, m/z: 334.1348 $(M + H)^{+}$

2,6-Bis(7-azaindolyl)pyridine, L4. A mixture of 2,6-dibromopyridine (406 mg, 1.6 mmol), 7-azaindole (609 mg, 5.06 mmol), K_2CO_3 (1.402 g, 10 mmol), *trans*-1,2-diaminocyclohexane(29 mg, 0.25 mmol), and CuI (8 mg, 0.042 mmol) in dry dioxane (6 mL) was degassed by three freeze-pump-thawcycles. The mixture was then heated at reflux under a nitrogen atmosphere for 72 hrs. The solvent was evaporated to yield a brown residue, which was extracted into CH_2Cl_2 and washed with water. The organic layer was dried over $MgSO_4$, and the solvent evaporated under reduced pressure. The resulting solid was washed with acetonitrile to yield the product as off-white solid (300 mg, 59%).^{1}H NMR400 MHz($CDCl_3$, ppm, 303K): δ = 8.83 (2H, d), 8.46 (2H,d), 8.43 (2H,dd), 8.05 (1H,t), 7.97 (2H,dd), 7.19 (2H,dd), 6.67 (2H,d). ^{13}C NMR 500 MHz($CDCl_3$, ppm,303K):δ = 149.12 149.2, 147.6, 143.3, 140.8, 129.1, 126.3, 123.4, 117.3, 111.6, 102.7 NMR ($CDCl_3$)δ = 149.12 (TOF MS-ES^{+}), m/z: 312.1248 $(M + H)^{+}$

4.2.3. Synthesis of Complexes

***Cis*-Pt(DMSO)$_2$Cl$_2$ precursor.** Prepared by adding 3 mmol of the DMSO to an aqueous solution of 1 mmol of K_2PtCl_4 in 10 mL of water and allowing the solution to stand at room temperature until yellow crystals precipitated. The complex was filtered, washed with water, ethanol and diethyl ether, and dried in vacuo. Yield (230 mg, 54.6 %) *Anal. Calc. for* $C_2H_6PtO_2SCl_2$: C, 11.37, H, 2.84, S, 15.16 *Found* C, 11.58, H 2.67, S 15.47

2,6-Bis(N-pyrazolyl)pyridine platinum(II) chloride, **Pt2.** K_2PtCl_4 (0.25 g, 0.605 mmol), **L2** (0.15 g, 0.71mmol) were refluxed in water (50 mL) for 4 days. The yellow-tan mixture was allowed to cool at room temperature, filtered, and the filtrate reduced to dryness *in* vacuo. The yellow solid was washed with ether and hexanes. The solid was purified by slow evaporation of methanol. Yield 51.4 % (161.2 mg), ^{1}H NMR (500 MHz, d_6-DMSO, 303K): δ = 8.93 (d, 2H), 8.14(t, 1H), 7.85(d, 2H), 7.81(dd, 2H), 6.62(d, 2H) TOF MS-ES$^+$, m/z: 441.0196 (M $^+$)

2,6-Bis(quinolin-8-lyl)pyridine platinum(II) chloride, Pt3. A mixture of 2,6-di(8-quinolyl)pyridine (100 mg, 0.3 mmol) and $PtCl_2(DMSO)_2$ (126 mg, 0.3 mmol) in a flask was evacuated and flushed three times with nitrogen gas, 10 mL of methanol was added via a cannula, the mixture was refluxed under a nitrogen atmosphere for 72 h. The precipitate which formed was collected by centrifugation and washed with water, methanol, ethanol, and diethyl ether, and dried under vacuum to give a grey solid. (30 mg, 17.8 %). *Anal Calc. for* $C_{23}H_{15}N_3PtCl_2.2H_2O$ C: 43.46, H: 2.36 N: 6.61 *Found*; C: 43.10, H: 2.55 N: 7.02. ^{1}H NMR (500 MHz, d_6-DMSO): δ = 9.23 (d, 2H), 8.98 (d, 2H), 8.89 (d, 2H), 8.50 (d, 2H), 8.45 (t, 1H), 8.30 (d, 2H), 8.06 (dd, 2H), 7.78 (dd, 2H). TOF MS-ES$^+$, m/z: 564.0676 (M + H)$^+$

2,6-Bis(7-azaindolyl)pyridine platinum(II) chloride, Pt4. A mixture of **L2**(80 mg, 0.26 mmol) and $Pt(DMSO)_2Cl_2$ (109 mg, 0.26 mmol) in 15 mL of methanol was degassed and back filled with nitrogen three times. The mixture was then refluxed for 72 hrs. The pale yellow precipitate was separated from the solution by centrifugation and washed with methanol, water, ethanol, diethyl ether, and dichloromethane(32 mg, 22.8%). ^{1}H NMR500 MHz (d_6-DMSO, ppm,303K)**:** δ = 8.72 (2H, d), 8.57 (2H,d), 8.50 (2H,d), 8.43 (1H, t), 7.88 (2H, d), 7.56 (dd, 2H), 7.31 (2H, d). *Anal Cald* % C; 39.50, H 2.30 N: 12.10 *Found* C: 39.3, H: 2.4; N: 11.7. TOF MS-ES$^+$, m/z: 542.0581 (M + H)$^+$

4.3. DFT Calculations

Geometry optimizations for the +1 cations: **Pt1**, **Pt2**, **Pt3** and **Pt4** were carried out in the gas phase using a density functional theory (DFT) method[28] at the level of B3LYP/LANL2DZ.[29-30] All of the computations were performed using the Gaussian 09 for Windows® software package.[31] The minimum energy optimised structures of the complexes are presented in Figure 4.2. The corresponding HOMO and LUMO DFT calculated structures with respective frountier molecular orbital energies are presented in Figure 4.2. Bond lengths, bond angles, NBO charges, energies of the frontier molecular orbitals and the chemical reactivity indices of the calculated structures are summarized in Table 4.1.

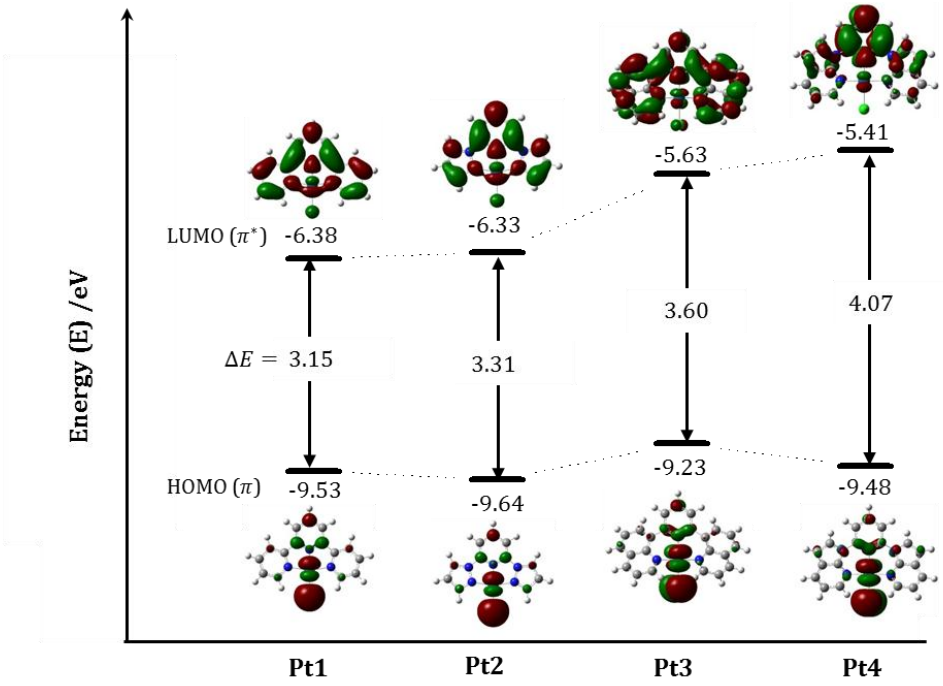

Figure 4.2 Frontier molecular orbitals with respective HOMO and LUMO energy levels of the studied complexes at B3LYP/LANL2DZ level of theory (Isovalue = 0.02).

Table 4.1 Selected DFT data for the investigated monofunctional Pt(II) complexes.

Property	 **Pt1**	 **Pt2**	 **Pt3**	 **Pt4**
Bond Length /Å				
trans N – Pt bond	1.963	1.979	2.030	2.093
Cl – Pt bond	2.392	2.378	2.412	2.400
Cl – $\boldsymbol{H_\alpha}$ contact	2.735	3.339	2.657	2.564
Bond angle / °				
Bite ($\boldsymbol{N_{cis} - Pt - N_{cis}}$)	162.34	160.72	178.39	177.50
Dihedral ($\boldsymbol{\theta}$)	0	0	32.15	22.56
NBO charges				
Pt	0.551	0.536	0.504	0.498
Energy (E) /eV				
LUMO energy	-6.384	-6.328	-5.626	-5.406
HOMO energy	-9.534	-9.637	-9.226	-9.480
$\Delta E_{LUMO-HOMO}$	3.15	3.31	3.60	4.07
Dipole moment ($\boldsymbol{D}$)	9.651	11.534	6.902	8.283
Chemical reactivity indices /eV				
Chemical hardness ($\boldsymbol{\eta}$)	1.58	1.66	1.80	2.04
Electrophilicity index ($\boldsymbol{\omega}$)	20.1	19.2	15.3	13.6
Symmetry	C_{2v}	C_{2v}	C_2	C_2
Planarity (side view)			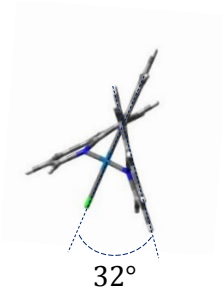 32°	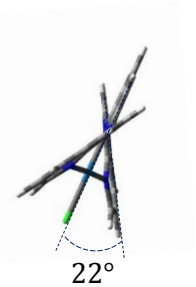 22°

4.4. Preparation of complex and nucleophile solutions

The solvent system used for preparing the complexes and nucleophiles for kinetic measurements was prepared by dissolving the required amount of $LiCF_3SO_3$ and LiCl in absolute ethanol to afford a solution of 0.10 M (0.09 M $LiCF_3SO_3$ + 0.01 M LiCl) ionic strength. The triflate ion ($CF_3SO_3^-$) was chosen because of its inability to coordinate to the Pt(II) centre.[32] Furthermore, LiCl was used to prevent any possibility of the occurrence of a spontaneous solvolysis reaction. Metal complex solutions were prepared by dissolving a required amount of metal complex in 250 mL of the solvent system. Stock solutions of the nucleophiles, *viz.* **Pz**, **Tz**, **Im**, **MIm** and **DMIm**, were prepared by dissolving a known amount of nucleophile in 25 mL of the ionic strength solution followed by subsequent dilutions of each stock solution to obtain a series of lower concentrations of the used nucleophile solutions.

4.5. Kinetic Analyses

All kinetic measurements were performed under *pseudo* first–order conditions using at least 10-fold excess of the nucleophile. The reactions were monitored by following the changes in absorbance as a function of time at suitable wavelengths using a Varian Cary 100 UV/Visible spectrophotometer with an online kinetics application and an attached Varian Peltier temperature control unit. Rapid reactions under sixteen minutes, with kinetics that cannot be followed using UV/Visible spectrophotometer, were studied using an Applied Photophysics SX.20MV (v2.2.5.6) stopped–flow system with an online Pro–Data ™ software for Windows®. All kinetic reactions were controlled to within 0.1 ℃. Graphical analyses were performed using the software package, Origin 7.5®.

The kinetic data at all the concentrations and temperatures were fitted to first-order exponential decay function to obtain the observed *pseudo* first-order rate constants (k_{obs}) using the online non-linear least squares fit, Equation (4.1):[33]

$$A_t = A_0 + (A_0 - A_\infty)\exp(-k_{obs}t) \qquad (4.1)$$

where A_0, A_t and A_∞ represent the absorbance of the reaction mixture initially, at the time, t and at the end of the reaction respectively. A typical UV/Visible absorbance spectrum with its respective kinetic trace obtained by mixing solutions of **Pt2** and **MIm** (1.10 mM) is shown in Figure 4.3.

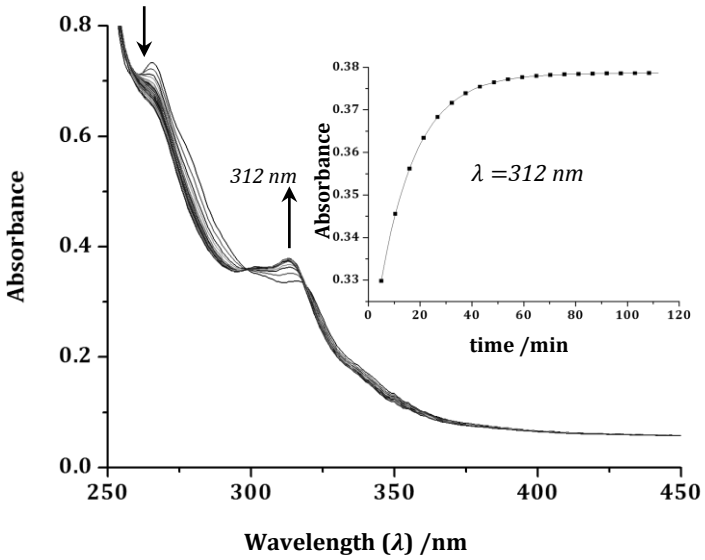

Figure 4.3 First-order exponential fit for the chloride substitution reaction from **Pt2** by **MIm** (1.10 mM) at $\boldsymbol{\lambda}$ =312 nm, T=298.15 K.

Kinetics of substitution of coordinated chloride (Scheme 1) from each of the Pt(II) complexes by five different nucleophiles (**Nu**), *viz.* Pyrazole (**Pz**), 1,2,4-Triazole (**Tz**), Imidazole (**Im**), n-Methylimidazole (**MIm**) and 1,2-Dimethylimidazole (**DMIm**), were investigated under pseudo-first order conditions.

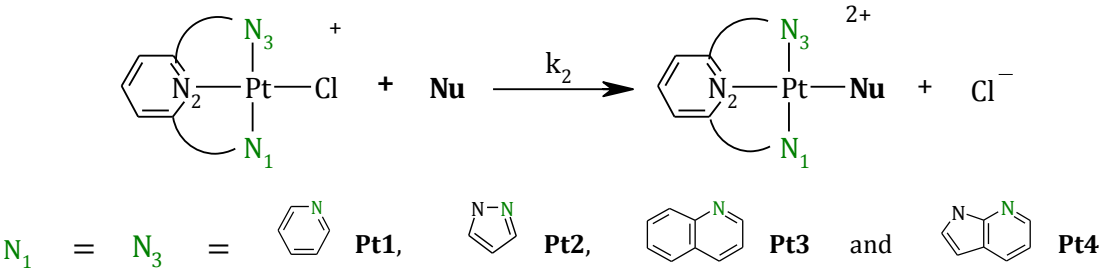

Scheme 1 (charges omitted for clarity)

The *pseudo* first-order rate constants k_{obs} were plotted against the concentration of the entering nucleophile to obtain the second-order rate constant, k_2 for the forward reaction from the slope as described by Equation (1).

$$k_{obs} = k_2[Nu] \quad (1)$$

Typical concentration dependence plots for **Pt2** with five azole nucleophiles at 25 °C are summarised in Figure 4.4 and the calculated values for the second-order rate constants, k_2 are summarised in Table 4.2. Literature values[12] for **Pt1** are also included for comparison.

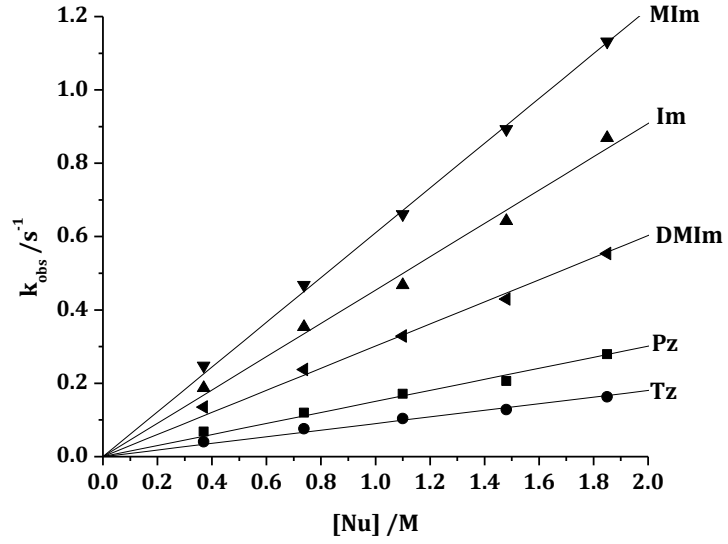

Figure 4.4 Dependance of the *pseudo* first-order rate constant ($\boldsymbol{k_{obs}}$) on the concentrations of the azole nucleophiles for **Pt2** substitution reactions in ethanolic solution at 298.15 K.

To confirm that the reactions follow an associative mechanism, typical of square-planar Pt(II) complexes, the temperature dependence studies of the second-order rate constants for all the complexes and nucleophiles was investigated in the temperature range of 15-35℃ at 5℃ intervals. Typical Eyring plots for the chloride substitution reactions of **Pt2** by the nucleophiles is presented in Figure 4.5. The calculated enthalpy ($\Delta H^{\neq}$) and entropy of activation ($\Delta S^{\neq}$) are summarised in Table 4.2.

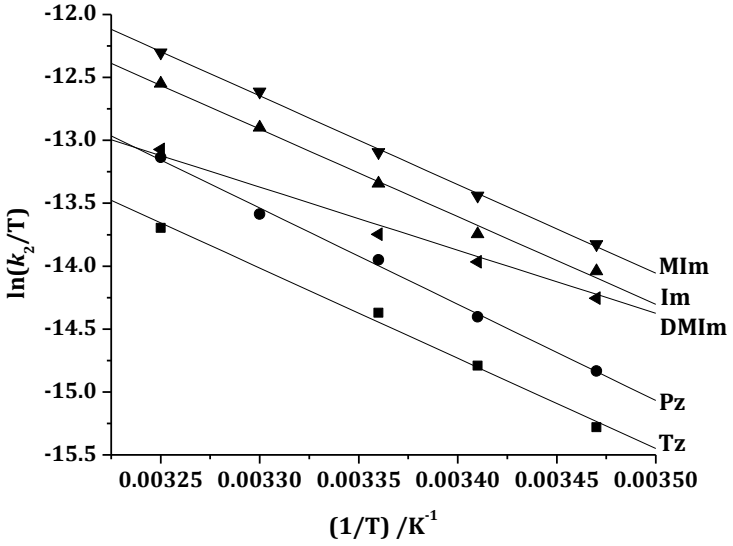

Figure 4.5 Typical Eyring plot used for temperature dependence studies of the chloride substitution reactions of **Pt2** by five azole nucleophiles.

Table 4.2 Summary of the second-order rate constants and the activation parameters for the substitution of the chloride from the platinum complexes by **Pz**, **Tz**, **Im**, **MIm** and **DMIm** in ethanol, (I = 0.10 M (0.09 M $LiCF_3SO_3$ + 0.01 M LiCl)) at 298.15 K.

Complex	Parameter	Nucleophile (Nu)				
		 Pz	 Tz	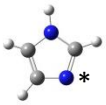 Im	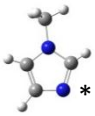 MIm	 DMIm
 Pt1[12]	k_2 /M^{-1} s^{-1}	1.26 ± 0.02	0.85 ± 0.02	3.70 ± 0.04	3.79 ± 0.07	1.49 ± 0.03
	$\Delta H^{\neq}$ /k J mol^{-1}	44 ± 1	40 ± 3	51 ± 1	46 ± 1	56 ± 8
	$\Delta S^{\neq}$ /J K^{-1} mol^{-1}	-96 ± 4	-114 ± 10	-67 ± 3	-84 ± 4	-53 ± 3
 Pt2	k_2 /M^{-1} s^{-1}	0.151 ± 0.006	0.091 ± 0.003	0.452 ± 0.01	0.610 ± 0.006	0.302 ± 0.01
	$\Delta H^{\neq}$ /kJ mol^{-1}	59 ± 4	64 ± 2	59 ± 3	59 ± 1	42 ± 2
	$\Delta S^{\neq}$ /J K^{-1} mol^{-1}	-118 ± 12	-101 ± 6	-114 ± 8	-109 ± 4	-171 ± 6
 Pt3	k_2 /M^{-1} s^{-1}	0.203 ± 0.001	0.069 ± 0.001	0.525 ± 0.008	0.679 ± 0.01	0.319 ± 0.004
	$\Delta H^{\neq}$ /kJ mol^{-1}	66 ± 2	60 ± 2	50 ± 2	53 ± 7	50 ± 2
	$\Delta S^{\neq}$ /J K^{-1} mol^{-1}	-80 ± 8	-107 ± 5	-126 ± 5	-114 ± 2	-128 ± 7
 Pt4	k_2 /M^{-1} s^{-1}	0.110 ± 0.004	0.049 ± 0.001	0.23 ± 0.01	0.373 ± 0.007	0.318 ± 0.006
	$\Delta H^{\neq}$ /kJ mol^{-1}	31 ± 2	55 ± 4	69 ± 4	54 ± 5	54 ± 2
	$\Delta S^{\neq}$ /J K^{-1} mol^{-1}	-173 ± 5	-125 ± 14	-68 ± 14	-118 ± 8	-117 ± 8

* Represents the reactive pyridinic nitrogen[12,15,36-39]

4.6. Discussion

Temperature dependence studies gave positive activation enthalpies and large negative activation entropies for all the studied complexes. These significantly negative values of the entropy of formation and the sensitivity of the second-order rate constant on the incoming nucleophile are consistent with the associative nature of d^8 square-planar Pt(II) complexes.[34]

The results in Table 4.2 demonstrate that the substitution of the chloride leaving group by the incoming azole nucleophiles follow the order **MIm** > **Im** > **DMIm** > **Pz** > **Tz**. Due to the strong dependence of the substitution reactions on the nature of the incoming nucleophile, this trend can be explained in terms of the nucleophilicities of the reactive pyridinic nitrogens (*****) obtained from the respective p*Ka* values.[12,15,35] In comparing the reactivities of the nucleophiles without methyl substituents attached, **Im** having the highest p*Ka* value (7.00) reacts significantly faster than **Pz** and **Tz** with the pKa values of 2.52 and 2.19 respectively. [36-38] Strikingly, however, upon the introduction of methyl substituent(s), **MIm** (p*Ka* = 7.30) reacts faster than **DMIm** (p*Ka* = 7.85).[39] The enhanced reactivity of **MIm** is due to the inductive σ-donation of electrons by the methyl substituent in the β-position to the reactive nitrogen, making the nucleophilic nitrogen more reactive.[12, 15] In **DMIm**, steric hindrance due to the additional methyl group in the α-position to the reactive nitrogen dominates over the inductive effect leading to steric clash in the *trans*ition state and retarded reactivity of the nucleophile.[35]

This reactivity trend is consistent with the previous studies where it was found that the reactivity of these five-membered N-donor nucleophiles depend linearly on their basicities according to a linear free energy relationship (LFER) of the type $k_2 = \alpha(pK_a) + b$ where α and b account for the electronic and steric effects.[35] In all cases, **DMIm** was found to deviate from linearity supporting the notion that LFER works well with nucleophiles that are not sterically hindered.

In addition, the data in Table 4.2 illustrates that the general reactivity trend obtained in this comparative study of the rates of chloride substitution from $[Pt(terpy)Cl]^+$and its analogues is; **Pt1** > **Pt3** > **Pt2** > **Pt4**. This trend is consistent for all the nucleophiles. The complexes under investigation have a common pendant Pyridine and the variances are the *cis*-aromatic heterocyclic moieties of different ring sizes and type. Optimized DFT structures of **Pt1** and **Pt2** are planar and rigid whereas **Pt3** and **Pt4** have flexible with dihedral angles of 32° and 22° respectively. For a comparison of the reactivity of monofunctional chloro complexes in Table 4.2, it can be seen that the substitution behaviour of the complexes is clearly dependant on the nature of the N^N^N chelating ligand. The k_2 values for planar rigid five-membered chelates with a C_{2v} symmetry; **Pt1** and **Pt2** are 3.70 M^{-1} s^{-1} and 0.452 M^{-1} s^{-1} with the entering

nucleophile as **Im**. Since these complexes undergo associative substitution mechanism, typical of d^8 square-planar Pt(II) complexes, the five coordinate *trans*ition state is stabilized by the *trans*fer of the electron density from the metal centre to the tridentate N-donor chelating ligand, leading to a more positively charged metal centre and enhanced substitution reactions.[40] The difference between these complexes are the *cis*-pyridine groups in **Pt1** and *cis*-pyrazolyl groups in **Pt2**, the presence of poor π-acceptor and good σ-donor pyrazole *cis* groups[41] in **Pt2** decreases the strength of π-backdonation of the metal electrons to the chelating ligand, resulting in the retardation of the incoming nucleophile, thus slow reactivity. This is supported by a significant decrease in the electrophilicity of the metal centre, as shown by the reduction of the NBO charge for **Pt2** compared to **Pt1** in Table 4.1.

The HOMO and LUMO frontier molecular orbitals with their respective energies were also determined in order to gain more insight on the reactivities of these complexes. Since the π-acceptor nature of the Pt(II) complex is essentially the *trans*fer of electron density from the nonbonding metal *d*-electrons (HOMO) to the ligand empty π^*-orbitals (LUMO), the HOMO-LUMO energy difference ($\Delta E_{LUMO-HOMO}$) can be used to explain the reactivity differences.[42-43] In comparing **Pt1** and **Pt2**, it can be noted that **Pt2** has a slightly increased $\Delta E_{LUMO-HOMO}$ than **Pt1,** consistent with the poor π-acceptor nature of pyrazolyl *cis* groups compared to pyridine.

The HOMO-LUMO energy gap also has a direct relationship with the chemical hardness of the complex, the greater the HOMO-LUMO energy gap, the harder the complex and the more stable and less reactive it is. [44] In comparing the five-membered chelates, Table 4.1 shows that **Pt2** is harder than **Pt1** and thus the observed reactivity. In order to measure the ability of the complex to accept electrons, the electrophilicity indices (ω)[45] for the complexes were calculated from their chemical hardness (η)[44] and electronic chemical potential (μ)[46] using Equation (2):

$$\omega = \frac{[(E_{HOMO+LUMO})/2]^2}{[(E_{HOMO-LUMO})/2] \times 2} = \frac{\mu^2}{2\eta} \qquad (2)$$

The data in Table 4.1 shows that **Pt1** (ω = 20.1) is more electrophilic than **Pt2** (ω = 19.2), indicating a higher capacity for the Pt(II) centre of **Pt1** to accept additional electrons from the N-donor nucleophiles compared to **Pt2**.

The effect of the *cis*-aromatic ring sizes on the reactivity of the complexes was also investigated. **Pt1** and **Pt3** consist of six-membered aromatic rings only, suggesting that the six electrons responsible for aromaticity are delocalized over six atoms.[38] The replacement of the C=C bonds in the *cis* groups of **Pt1** and **Pt3** complexes by a nitrogen heteroatom in **Pt2** and **Pt4** leads to the formation of the five membered, pyrrolic-N containing *cis* groups, suggesting that the 6 π-electrons are now delocalized over five atoms. This is responsible for the π-excessive nature of

the pyrazole and azaindole *cis*-groups in **Pt2** and **Pt4** respectively.[36-37, 39] The introduction of these electron rich *cis*-groups led to the retardation in reactivity of the complexes. This is consistent with the reduction in π-withdrawing character of the chelating ligands containing π-excessive *cis*-groups as depicted by a decrease in dipole character of these complexes (Table 4.1).[47] The cathodic shifts of ~1 V displayed by pyrazolyl and azaindole Pt(II) complexes compared to their respective analogues **Pt1** and **Pt3**, is also consistent with the poor π-acceptor nature of **Pt1** and **Pt3**.[41,48] The increased HOMO-LUMO energy gaps in **Pt2** and **Pt4** accompanied by a decrease in electrophilicities of the metal centres, results in the observed decrease in reactivity compared to **Pt1** and **Pt3** respectively.

The reactivities of the C_2 six-membered chelates with out of plane *cis* groups, quinoline in **Pt3** and azaindole in **Pt4** were also investigated. For comparison, steric effects due to out of plane twisting of the *cis* groups were considered in addition to the electronic effects of the fused rings. The k_2 values for the chloride substitution of **Pt3** and **Pt4** by **Im** are 0.525 M^{-1} s^{-1} and 0.238 M^{-1} s^{-1} respectively. This reactivity difference is expected since the azaindole unit is much more electron rich than the quinoline and thus cannot effectively accept the electron density from the Pt(II) centre.[48] This is corroborated by DFT calculations which reveal that the LUMO in **Pt4** is localized on the central pyridine with a minor contribution from the electron abundant *cis*-azaindole groups, whereas in **Pt3** there is delocalization of the LUMO in the quinolyl *cis*-groups. The HOMO-LUMO energy gaps, $\Delta E_{LUMO-HOMO}$ values show that the gap in **Pt4** is 0.47 eV greater than **Pt3**, which further explains the slow reactivity of **Pt4**. Chemical reactivity indices, chemical hardness (η) and the electrophilic indices (ω) of these complexes demonstrates that **Pt4** is more electrophilic and harder than **Pt3**, and therefore less susceptible to the incoming N-donor azole nucleophiles compared to its C_2 derivative **Pt3**. In **Pt4**, the presence of shorter Cl-H_α and smaller dihedral angles compared to **Pt3** hinders the approach of the N-donor nucleophiles also supporting the reactivity difference in C_2 complexes.

The low reactivities of the six-membered chelates (**Pt3** and **Pt4**) compared to five-membered chelates (**Pt1** and **Pt2**) were also studied. On analysing the reactivity of complexes with π-deficient *cis*-groups, **Pt1** and **Pt3**, it is found that **Pt3** reacts about 6 times slower than **Pt1**. A similar reactivity trend is observed when comparing the reactivities of **Pt2** and **Pt4**, both having π-excessive *cis* groups, as the data shows that **Pt4** reacts about two times slower than **Pt2** when **Im** is an incoming nucleophile. This relatively low reactivity of six-membered chelates (**Pt3** and **Pt4**) can be accounted for in terms electronic and steric effects due to the out of plane *cis* groups.

Electronic communication between the metal centre and the chelating ligand is usually responsible for the enhanced reactivity of the five-membered chelates such as terpy.[49] However the out of plane nature of fused heterocyclic *cis* groups in **Pt3** and **Pt4** tends to reduce the π-backdonation of the metal electrons because the 2*p*-orbitals on the *cis* nitrogens do not properly overlap with the *d*-orbitals of the Pt(II) centre.[49] This results in the widening of the HOMO-LUMO energy gaps (Figure 4.2) in six-membered chelates, resulting in electron rich Pt(II) centres as displayed by the NBO charges (Table 4.1) which demonstrates that **Pt1** and **Pt2** have slightly more electropositive metal centres than **Pt3** and **Pt4** respectively.

Steric hindrance due to the out of plane distortion of the *cis* groups in **Pt3** and **Pt4**, observed from the dihedral angles (θ) of 32° and 22° respectively, is another reason for the slow reactivity of six-membered chelates as the attack of the azole nucleophiles on the Pt(II) centre is hindered. Even the final coordination to the Pt(II) centre is hindered due to increased steric clash observed from the ground state shortening of the $Cl - H\alpha$ contact lengths in **Pt3** and **Pt4** (Table 4.1). These results are consistent with a study by van Eldik *et al*[50] on the role of π-acceptor effects in controlling the lability of monofunctional Pt(II) and Pd(II) complexes, which revealed that the out of plane twisting of the *cis* groups in six-membered chelates has a strong influence on the reactivity of the complex. Therefore, from this study, we conclude that the resulting change in the electronic properties of the *cis* groups and the chelate ring size of the complex upon the introduction of fused heterocyclic rings of extended π-conjugation plays a significant role on the substitution reactions of the investigated Pt(II) substitution reactions.

4.7. Conclusion

This investigation has demonstrated that relatively small structural modifications on the N^N^N chelating ligand has a strong influence on the rate of substitution of chloride in monofunctional Pt(II) complexes. In planar five-membered chelates, the presence of π-defficient *cis*-groups (Pyridine in **Pt1**) increase the rate of substitution, whereas by switching to electron rich *cis* groups (Pyrazole in **Pt2**), the rate of substitution decrease since the incoming azole nucleophile is repelled by the increased electron density around the metal centre. The use of bulky quinoline and azaindole fused rings in **Pt3** and **Pt4** respectively afforded C_2 symmetry with out of plane *cis* groups. The slow reacivities of the latter complexes compared to their C_{2v} analogues (**Pt1** and **Pt2**) is due to the poor electronic communication between the *d*-orbitals of the metal centre and the *p*-orbitals of the out of plane fused rings *cis* groups. Steric hindrance due to this out of plane twisting of the *cis* groups in C_2 complexes also decrease the rate of chloride substitution as the attack of the incoming nucleophile is hampered. The results obtained are clearly supported by DFT calculated NBO charges, trends in the HOMO-LUMO

energy gaps and the chemical reactivity indices. The rate of substitution also depends on the basicity and steric hindrance of the incoming azole nucleophile. The large negative values of the enthalpy of formation and the sensitivity of the second-order rate constant on the incoming nucleophile support the associative mechanism.

Supplementary Information

Electronic supplementary information (ESI) available: Mass and NMR spectra, A summary of wavelengths used for kinetic measurements, tables and kinetic traces summarising concentration and temperature dependence studies of selected complexes.

4.8. References

1. B. Lippert, *Cisplatin, Chemistry and Biochemistry of Leading antitumor Drugs*, Wiley-VHC, Weinheim, **1999**, p. 1 - 100
2. I. Kostova, *Recent Patents on Anti-Cancer Drug Discovery*, **2006,** 1, 1 - 22
3. J. Redijik, *Chem. Rev*, **1999**, *99*, 2499 - 2510
4. Ž. D. Burgarčić, J. Bogojeski, B. Petrović, S. Hochreuther, R. van Eldik, *Dalton. Trans.,* **2012**, *41*, 12329 - 12345
5. L. Ronconi, P. J. Sadler, *Coord. Chem. Rev*., **2007**, *251*, 1633 - 1648
6. N. J. Wheate, , S. Walker, G. E. Craig, R . Oun, *Dalton Trans.,* **2010**, *39*, 8113 – 8127.
7. M. J. Cleare, J. D. Hoeschele, *Bioinorg. Chem*. **1973**, *2*, 187 – 210.
8. V. Brabec, V. Boudny, *Met.-Based Drugs*, **1994***, 1*, 195 – 200.
9. L. S. Hollis, A. R. Amundsen, E. W. Stern, *J. Med. Chem*. **1989**, *32*, 128 – 136.
10. S. J. Lippard, P. J. Bond, K. C. Wu, W. R. Bauer, *Science*, **1976**, *194*, 726 - 728.
11. G. Lowe, A. S. Droz, G. W. Weaver, J. J. Park, J. M. Pratt, L. Tweedale, L. R. J. Kelland, *J. Med. Chem*., **1999**, *42*, 3167 - 3174
12. A. Shaira, D. Reddy, D. Jaganyi., *Dalton. Trans*., **2013**, *42*, 8426 - 8436
13. D. Jaganyi, D. Reddy, J. A. Gertenbach, A. Hofmann, R. van Eldik., *Dalton Trans*., **2004**, 299 - 304.
14. P. Ongoma, D. Jaganyi., *Dalton. Trans*., **2012**, *41*, 10724 - 10730
15. D. Reddy, K. J. Ackerman, M. P. Ackerman, D. Jaganyi., *Trans. Met. Chem*., **2011**, *36*, 593 - 602.
16. D. Jaganyi, K-L. De Boer, J. Gertenbach, J. Perils., *Int. J. Chem. Kinet*., **2008**, *40***,** 808 - 818.
17. D. Reddy, D. Jaganyi., *Dalton. Trans*., **2008**, 6724 - 6731
18. A. Hofmann, L. Dahlenburg, R. van Eldik., *Inorg. Chem.,* **2003**, *42*, 6528 - 6538

19. M. L. Tobe and J. Burgess, *Inorganic Reaction Mechanisms.*, Addision Wesley, London, **1999**, p. 30 - 39
20. F. Basolo and R. G. Pearson, *Mechanisms of Inorganic Reactions: A Study of Metal Compleces, 2nd* Ed., John Wilet & Sons, New York, **1967**, p. 351 - 406
21. R. Romeo, M. R. Plutino, J. M. Scolaro, S. Stoccoro, G. Minghetti., *Inorg. Chem.,* **2000**, *39*, 4749 - 4755.
22. B. Pitteri, G. Marangoni, L. Cattalini, T. Bobbo, J. *Chem. Soc. Dalton. Trans.,* **1995**, 3853 - 3859.
23. J. X. McDermott, J. F. White and G. M. Whitesides, *J. Am. Chem. Soc.*,**1976**, *98*, 6521.
24. D. L. Jameson, *J. Org. Chem.* **1990**,*55, 4992-4994*
25. T. E. Brader, S. D. Walker, J. R. Martinelli, S. L. Buchwald, *J. Am. Chem Soc*., **2005**, *127*, 4685.
26. K. L. Garner, L. F. Parkes, J. D. Piper, J. A. Gareth Williams, *Inorg. Chem.* **2010**, *49*, 476–487.
27. S. A. Willison, H. Jude, R. M. Antonelli, J. M. Rennekamp, N. A. Eckert, J. A. Krause Bauer, and W. B. Connick, *Inorg. Chem,* **2004**, *43*, 2548.
28. R. A. Freisner, Chem. Phys. Lett., **1985**, *116*, 39 - 43
29. (a) A. D. Becke, *J. Chem. Phys*., **1993**, 99, 3898 - 3905. (b) A. D. Becke, *J. Chem. Phys.,* **1993**, *98*, 5648 - 5652.
30. P. J. Hay, W. R. Wadt, *Chem. Phys.,***1985**, *82*, 270 - 282.
31. M. J. Frisch, G. W. Trucks, H. B. Schlegel, G. E. Scuseria, M. A. Robb, J. R. Cheeseman, G. Scalmani, V. Barone, B. Mennucci, G. A. Petersson, H. Nakatsuji, M. Caricato, X. Li, H. P. Hratchian, A. F. Izmaylov, J. Bloino, G. Zheng, J. L. Sonnenberg, M. Hada, M. Ehara, K. Toyota, R. Fukuda, J. Hasegawa, M. Ishida, T. Nakajima, Y. Honda, O. Kitao, H. Nakai, T. Vreven, J. A. Montgomery, Jr., J. E. Peralta, F. Ogliaro, M. Bearpark, J. J. Heyd, E. Brothers, K. N. Kudin, V. N. Staroverov, R. Kobayashi, J. Normand, K. Raghavachari, A. Rendell, J. C. Burant, S. S. Iyengar, J. Tomasi, M. Cossi, N. Rega, J. M. Millam, M. Klene, J. E. Knox, J. B. Cross, V. Bakken, C. Adamo, J. Jaramillo, R. Gomperts, R. E. Stratmann, O. Yazyev, A. J. Austin, R. Cammi, C. Pomelli, J. W. Ochterski, R. L. Martin, K. Morokuma, V. G. Zakrzewski, G. A. Voth, P. Salvador, J. J. Dannenberg, S. Dapprich, A. D. Daniels, O. Farkas, J. B. Foresman, J. V. Ortiz, J. Cioslowski, and D. J. Fox, *Gaussian 09, Revision **C.01**,* **2010**, Gaussian Inc., Wallingford CT.
32. Appleton, T. G. Hall, J. R. Ralph, S. F. and Thompson, C. S. M. *Inorg. Chem*. **1984**, *23*, 3521 - 3525.

33. J. D. Atwood, *Inorganic and Organic Reaction Mechanisms*, 2nd Ed., Wiley- VCH Inc., New York, **1997**, p. 32 - 61
34. A. Ymamoto, *Organotransition Metal Chemistry*: *Fundamentals Concepts and Applications*, John Willey and Sons, New York, **1986**, p. 181 - 203.
35. B. Pitteri, M. Bortoluzzi, *Polyhedron*., **2006**. *25*, 2698 - 2704.
36. A. R. Katritzky, *Physical Methods in Heterocyclic Chemistry: A Comprehensive Tretise in Two Volumes,* Volume 1.; Academic Press: New York, **1963**. 19 - 20, 45 - 49, 65.
37. A. R. Katritzky and J. M. Lagowski, *Principles of Heterocyclic Chemistry*, Methuen & CO LTD, London, **2000**, p. 146.
38. D. W. Young, *Heterocyclic Chemistry*, Longman Inc, New York, **1975**, p. 54 - 61.
39. T. Eicher, S. Hauptmann, *The Chemistry of Heterocycles: Structure, reactions, Syntheses and Application,* Stuttgart: New York, **1995**. p. 166, 181, 209.
40. R.H. Crabtree, *The Organometallic Chemistry of the Transition Metals*, John Willey and Sons, New York, **2001**, 96 - 109
41. S. Develay, O. Blackburn, A.L. Thompson and J.A. Gareth Williams, *Inorg. Chem*. **2008**, *47*, 11129 – 11142.
42. R. G. Pearson, *J. Chem. Educ.,* **1987**, *64*, 561 - 567.
43. R. G. Pearson, *Acc. Chem. Res.,* **1993**, *26*, 250.
44. R. G.Parr, R. A. Donnelly, M. Levy, W. E. Palke, *J. Chem. Phys*. **1978**, *68*, 3801 - 3807.
45. R. G.Parr, Szentpály, S. Liu, *J. Am. Chem. Soc*. **1999**, *121*, 1922 - 1924.
46. R. G.Parr and W. Yang, *Density Functional Theory of Atoms and Molecules*, Oxford University Press, **1989**, p. 95 - 96.
47. D. P. Rillema, A. J. Cruz, C. Moore, K. Saim, A. Jehan, D. Base, T. Nguyen, W. Huang., *Inorg. Chem.* **2013**, *52*, 596 – 607.
48. K. Garner, L. Parkes, J. D. Piper and J. A. G. Williams, *Inorg. Chem*., **2010**. *49*, 476 - 487.
49. P. Haake, P. A. Cronin*, Inorg. Chem,* **1963**, *2*, 879-880.
50. B. Petrović, Ž. D. Burgarčić, A. Dees, I. Ivanović-Burmazović, F. W. Heinemann, R. Puchta, S. N. Steinmann, C. Corminboeuf, R. van Eldik, *Inorg. Chem.,* **2012**, *51*, 1516 - 1521.

Chapter 4

Supporting Information (SI 4)

SI 4.2. Mass and ^{1}H NMR Spectra

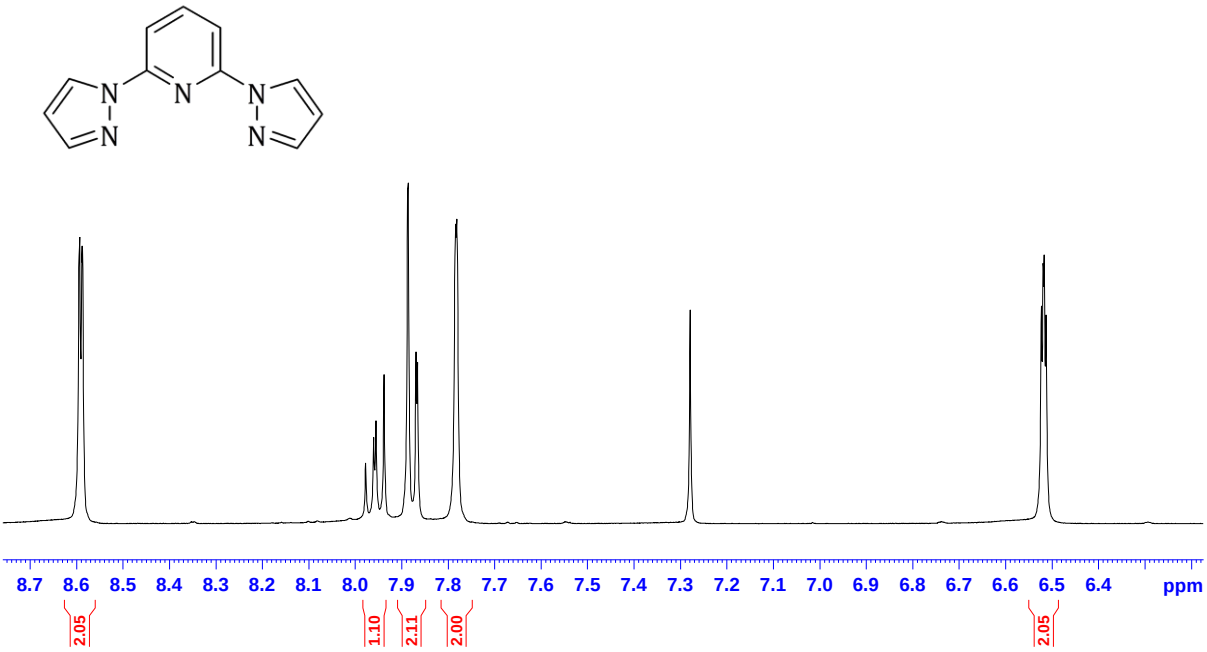

Figure SI 4.7. ^{1}H NMR spectrum of 2,6-Bis(N-pyrazolyl)pyridine, **L2**

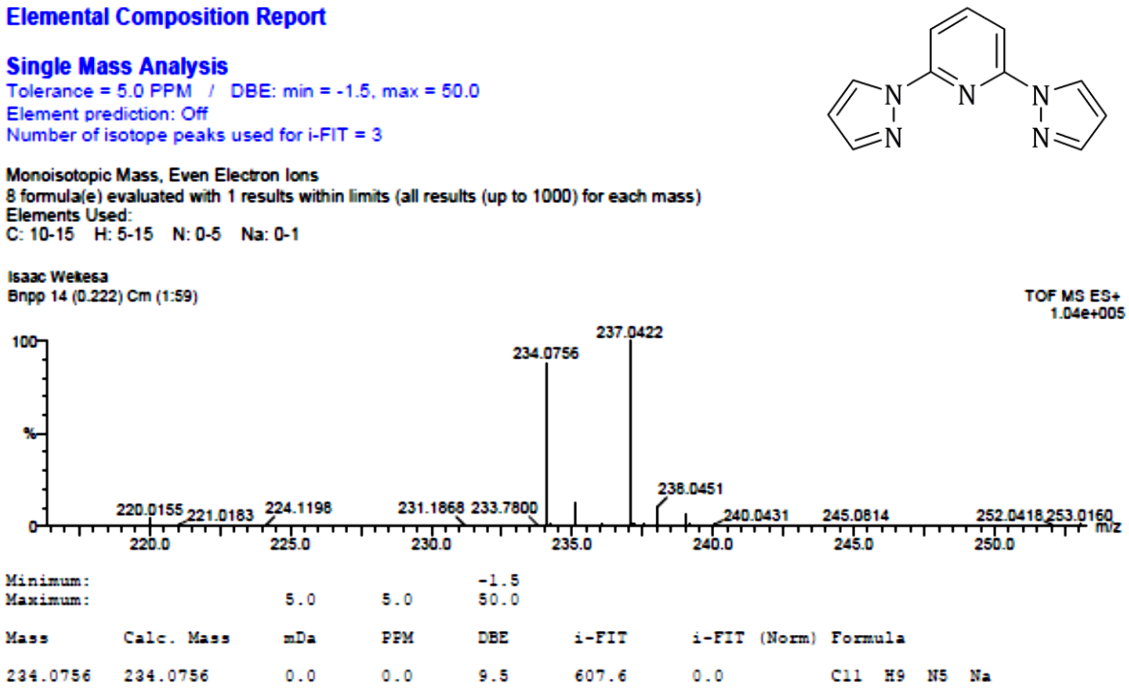

Figure SI 4.8. Mass spectrum of 2,6-Bis(N-pyrazolyl)pyridine, **L2**

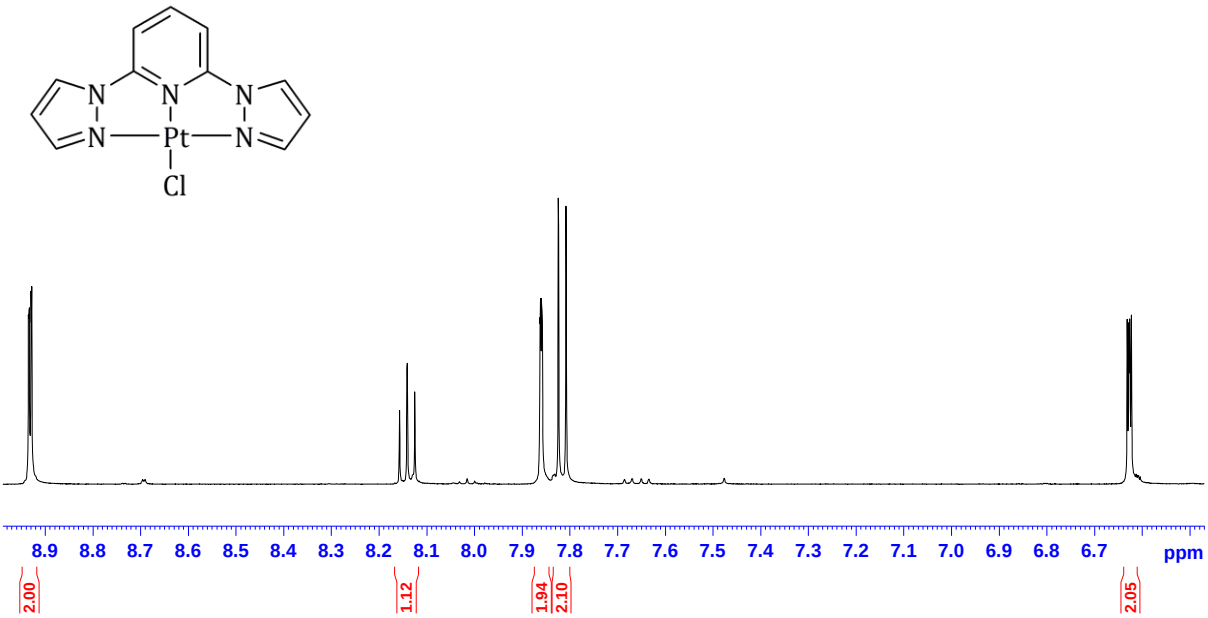

Figure SI 4.9. ^{1}H NMR spectrum of 2,6-Bis(N-pyrazolyl)pyridine platinum(II) chloride, **Pt2**

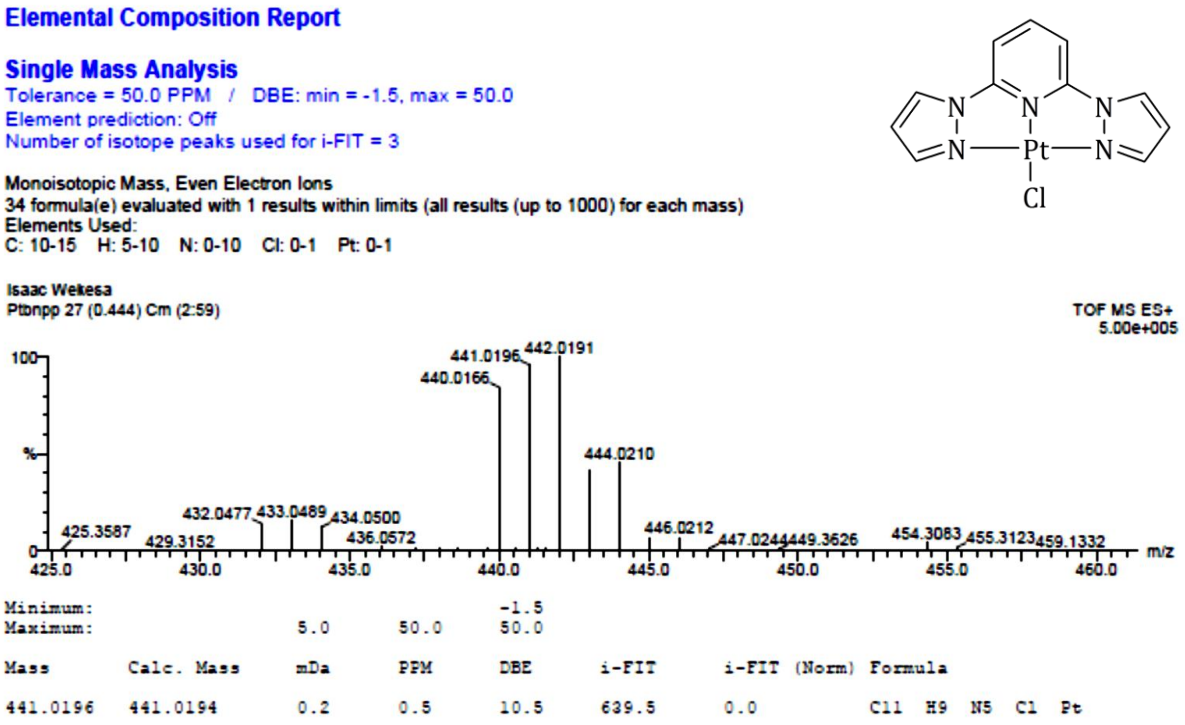

Figure SI 4.10. Mass spectrum of 2,6-Bis(N-pyrazolyl)pyridine platinum(II) chloride, **Pt2**

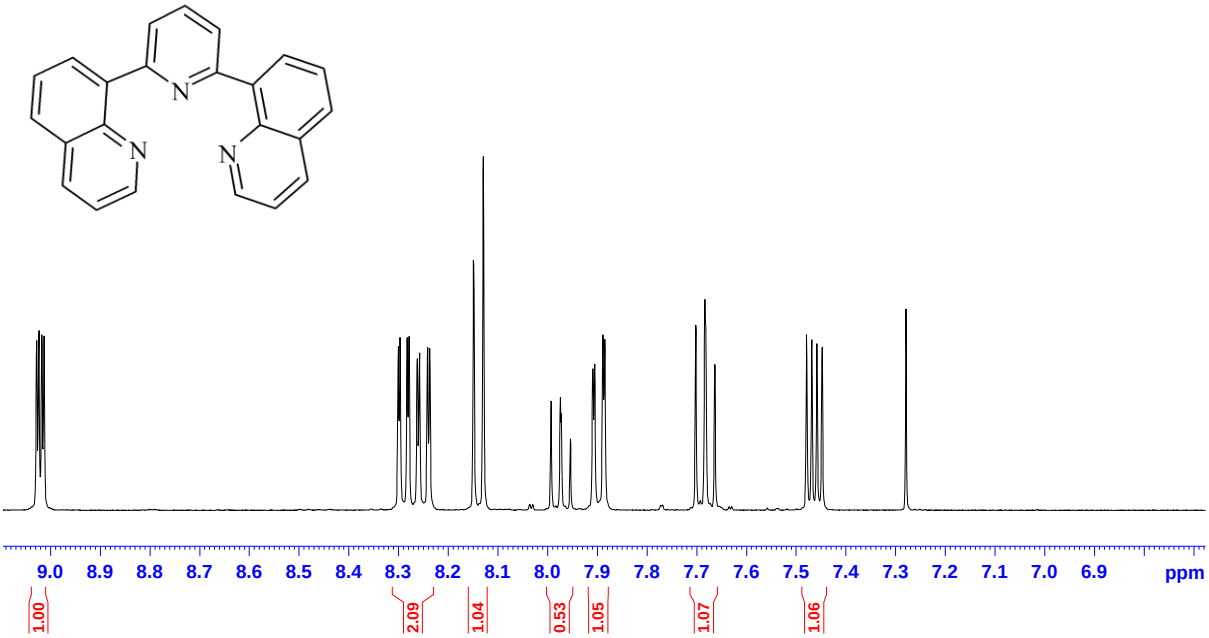

Figure SI 4.11. ^{1}H NMR spectrum of 2,6-Bis(quinolin-8-yl)pyridine, **L4**

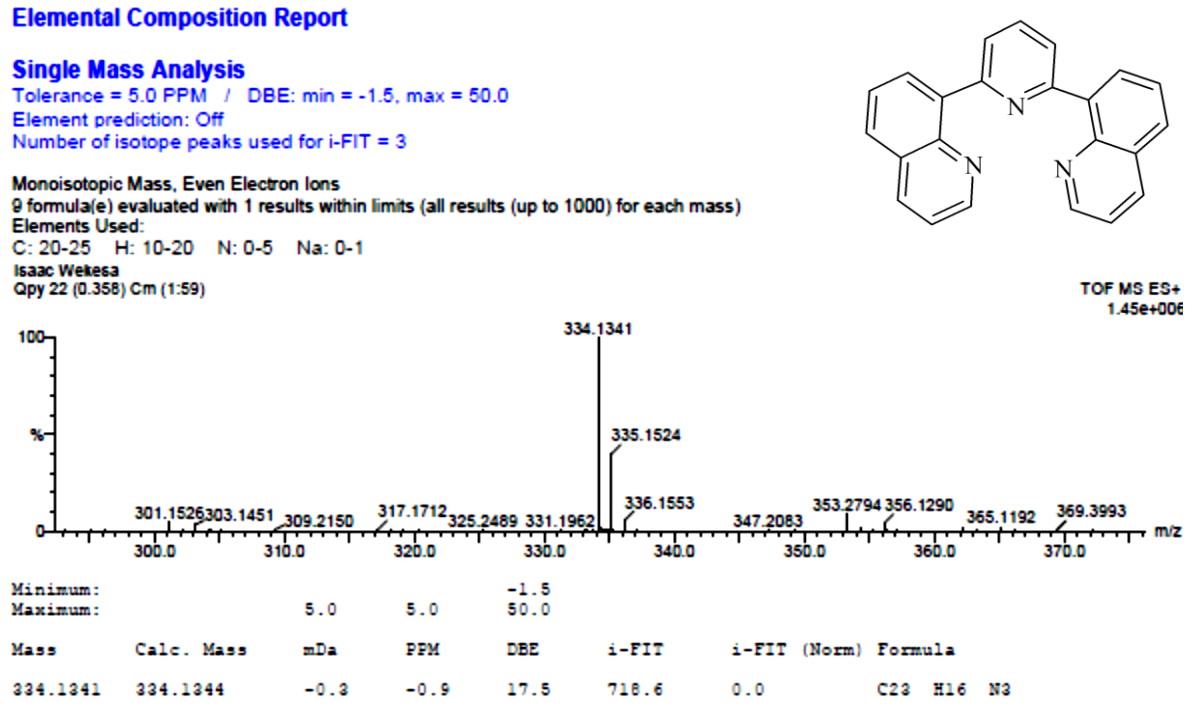

Figure SI 4.12. Mass spectrum of 2,6-Bis(quinolin-8-yl)pyridine, **L4**

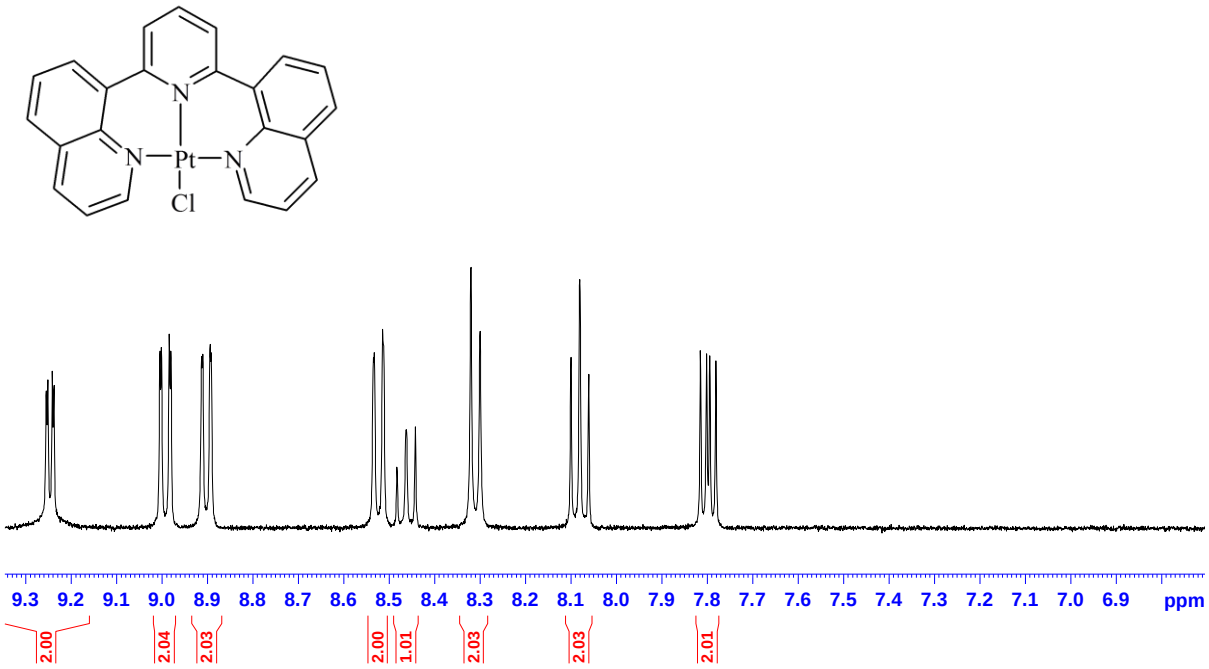

Figure SI 4.13 ^{1}H NMR spectrum of 2,6-Bis(quinolin-8-yl)pyridine platinum(II) chloride, **Pt4**

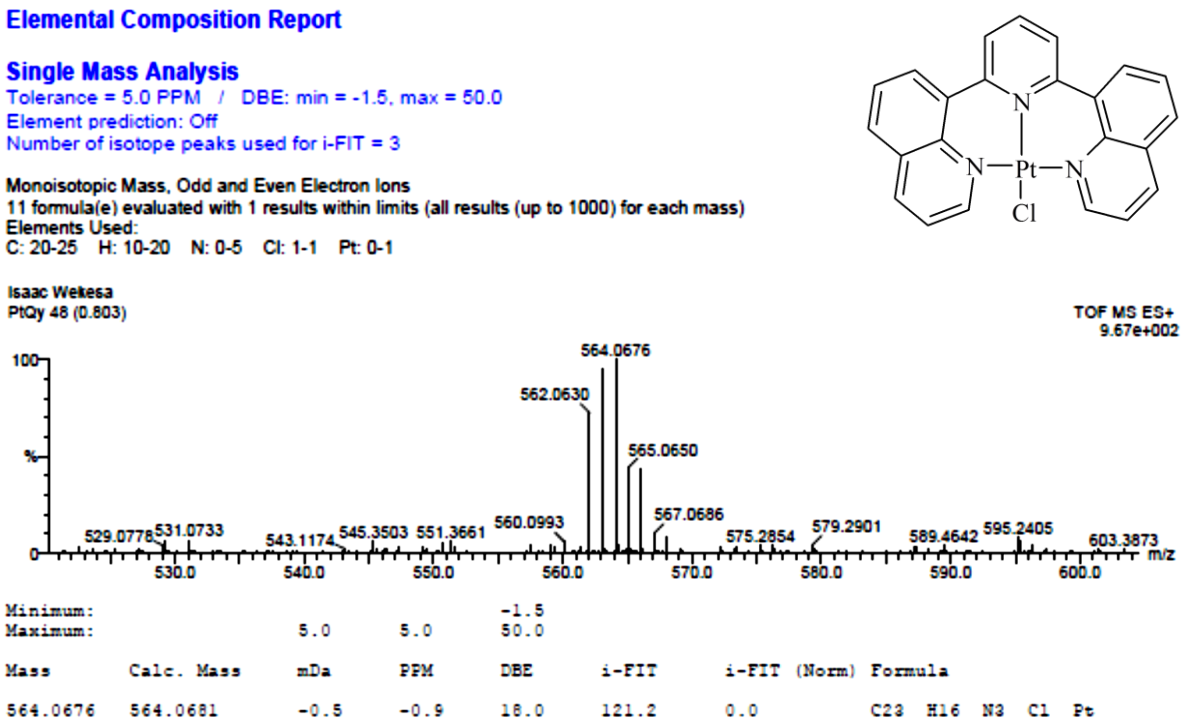

Figure SI 4.14 Mass spectrum of 2,6-Bis(quinolin-8-yl)pyridine platinum(II) chloride, **Pt4**

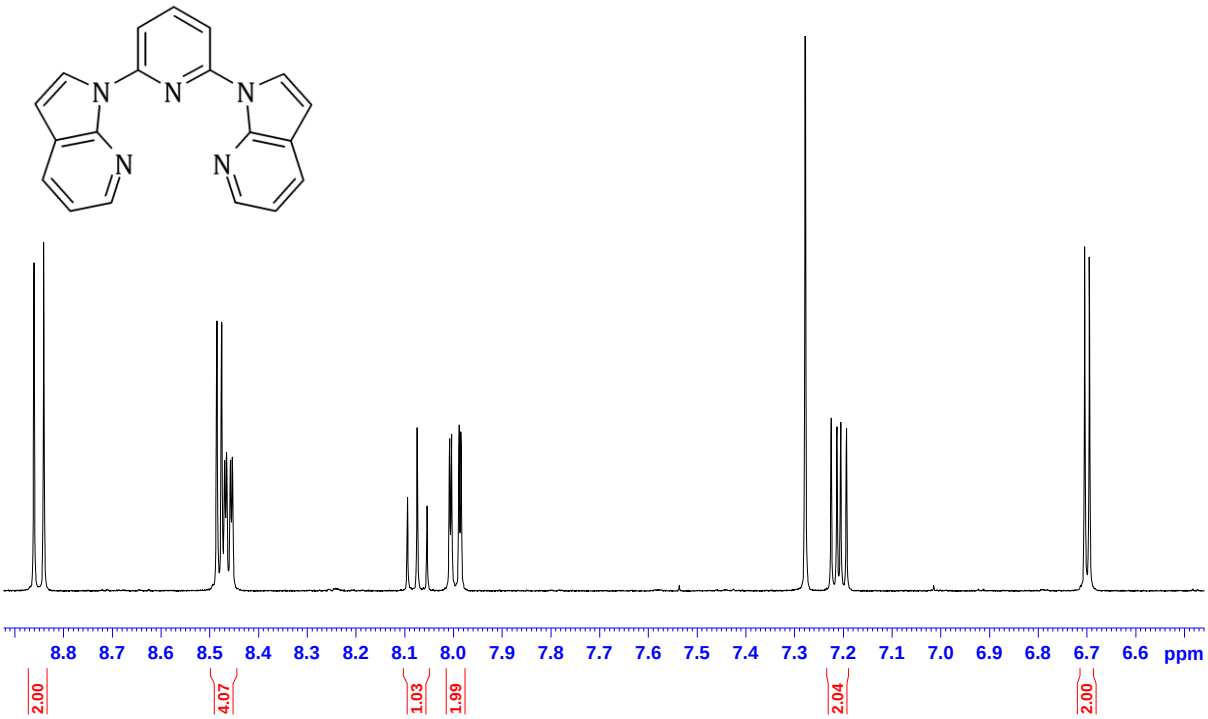

Figure SI 4.15 ^{1}H NMR spectrum of 2,6-Bis(7-Azaindolyl) pyridine, **L4**

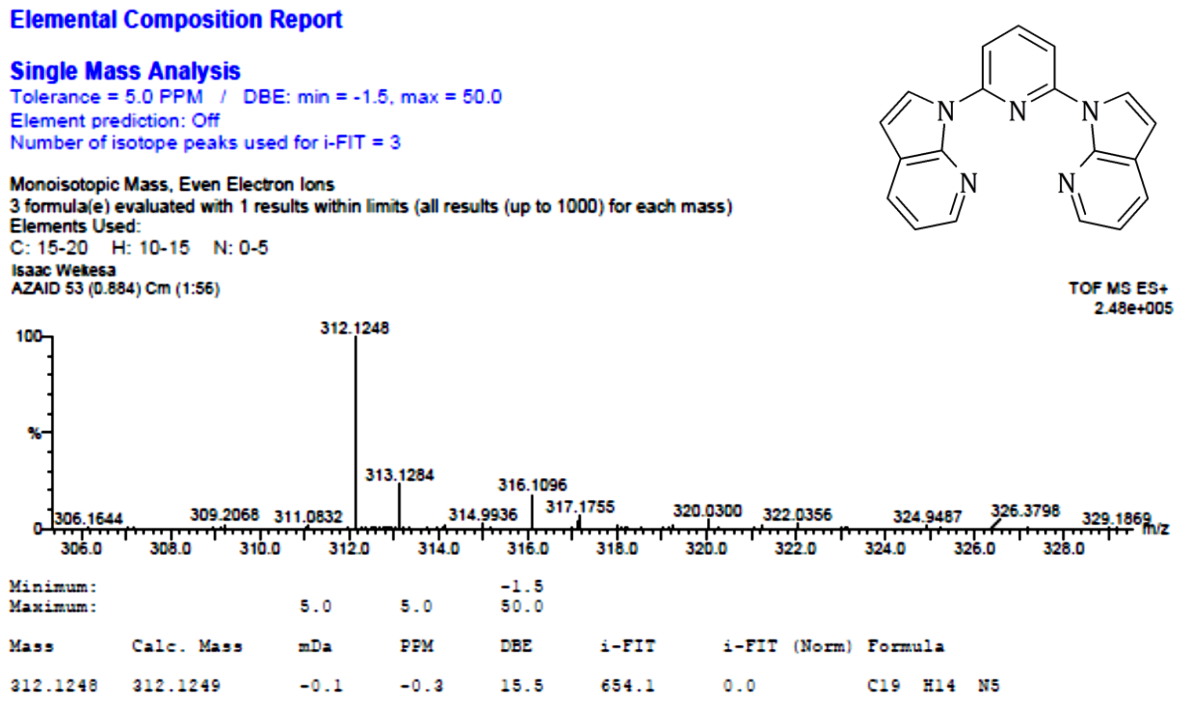

Figure SI 4.16 Mass spectrum of 2,6-Bis(7-Azaindolyl) pyridine, **L4**

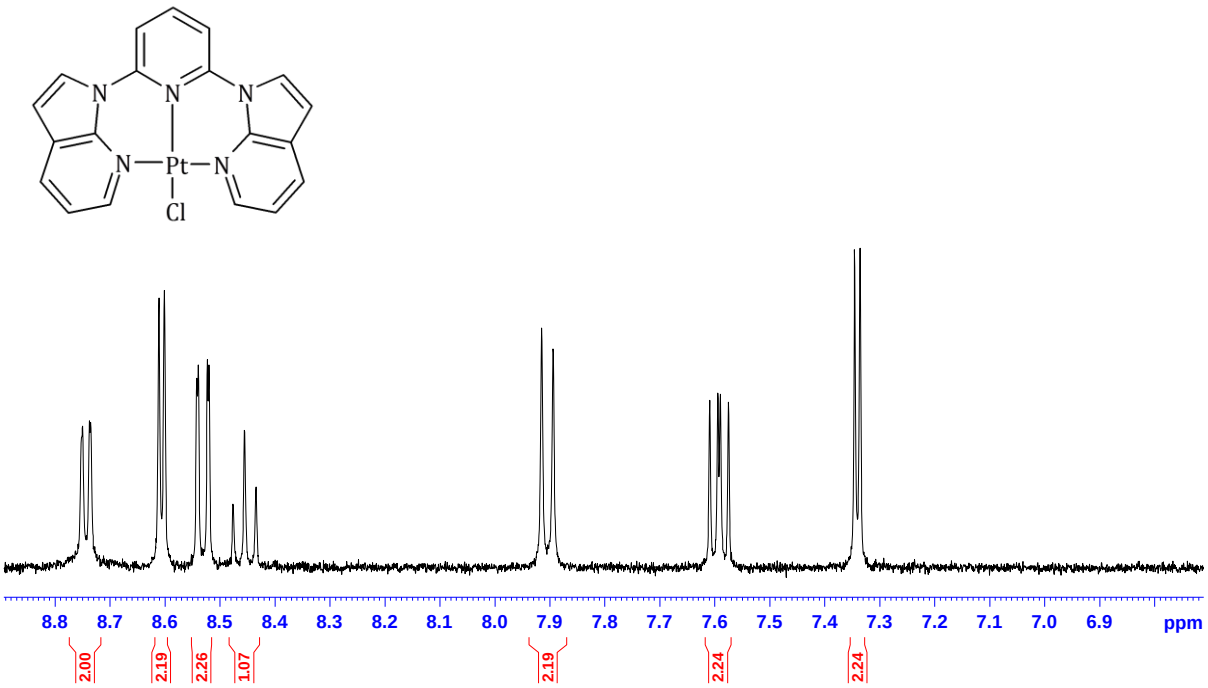

Figure SI 4.17 ^{1}H NMR spectrum of 2,6-Bis(7-Azaindolyl) pyridine platinum(II) chloride, **Pt4**

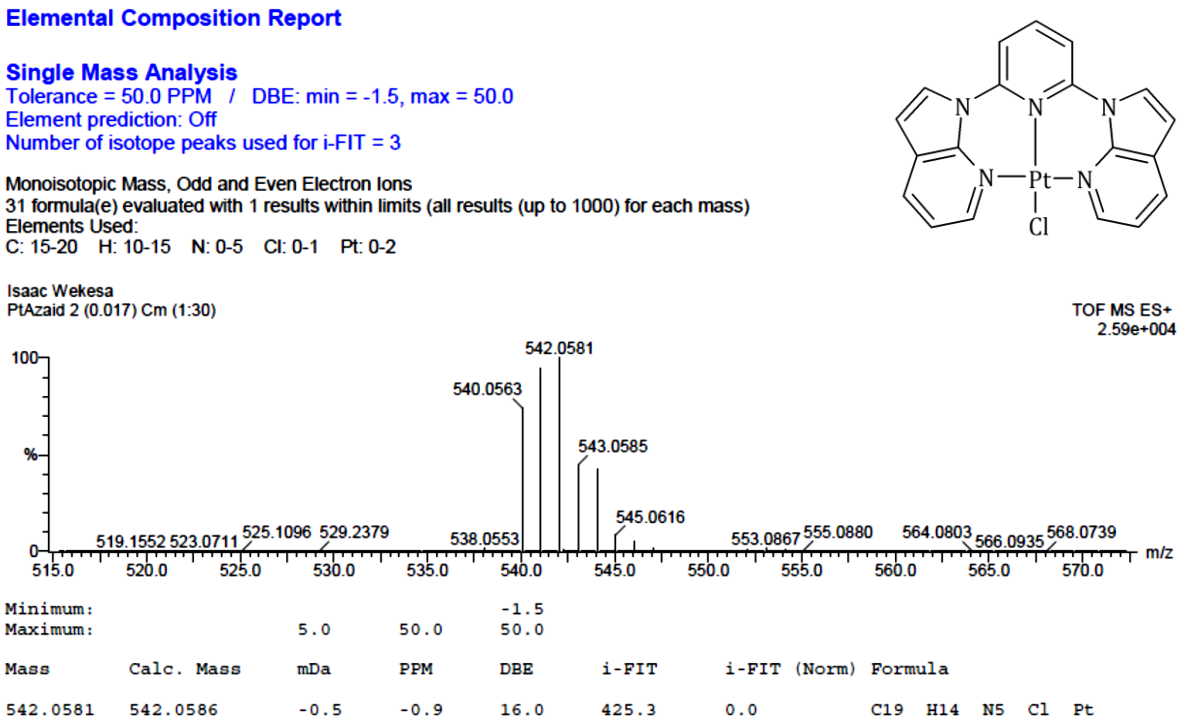

Figure SI 4.18 Mass spectrum of 2,6-Bis(7-Azaindolyl) pyridine platinum(II) chloride, **Pt4**

Chapter 5

Mechanistic Studies on the Reactions of N^C^N Platinum(II) Complexes With Nitrogen Bio-relevant Nucleophiles: Experimental and Computational Approach.

Mechanistic Studies on the Reactions of N^C^N Platinum(II) Complexes With Nitrogen Bio-relevant Nucleophiles: *Experimental and Computational Approach.*

Abstract

The nucleophilic substitution reactions of the complexes 1,3-bis(2-pyridinyl)benzene platinum(II) chloride (**PtL1**), 1,3-bis(*N*-pyrazolyl)benzeneplatinum(II) chloride (**PtL2**) , 1,3-bis(quinolin-8-yl)benzeneplatinum(II) chloride (**PtL3**) and 1,3-bis(7-azaindolyl)benzene platinum(II)chloride (**PtL4**) with a series of azole nucleophiles *viz.* Pyrazole (**Pz**), 1,2,4-Triazole (**Tz**), Imidazole (**Im**), 1-methylimidazole (**MIm**) and 1,2-dimethylimidazole (**DMIm**) were studied in ethanolic solution. Reactions of **PtL1**, **PtL3** and **PtL4** were investigated under *pseudo*-first order conditions as a function of nucleophile concentration and temperature using stopped flow spectrophotometry, whilst **PtL2** was studied using uv-visible spectrophotometry. The reactions follow a simple rate law $k_{\mathrm{obs}} = k_2[\mathbf{Nu}]$. The reactivity trend for the complexes follow the trend **PtL1** > **PtL3** > **PtL4** > **PtL2**. When coordinated ligands at the square planar platinum complexes are 1,3-bis(2-pyridinyl)benzene and 1,3-bis(N-pyrazolyl)benzene (**PtL1** and **PtL2**), the reactivity difference is purely electronic, π-backbonding by the good π-acceptor pyridinyl *cis*-groups increases the reactivity while the pyrazolyl *cis*-groups act as donors, thereby slowing down the rate of substitution. In the flexible six-membered chelate complexes, electronic and steric factors control the substitution reactions. The reactivity of the azole nucleophiles studied is dependent upon their basicity, while steric hindrance due to the methyl group in the α-position to the pyridinic nitrogen decreases the rate of the substitution reaction. DFT calculations support the kinetic results. The small but positive $\Delta H^{\ddagger}$ values and large negative values for $\Delta S^{\ddagger}$ support an associative substitution mechanism.

5.1. Introduction

Platinum-based anticancer drugs are now among the world's most used drugs in the treatment of various cancer lines.[1-3] Despite their wide use, their chemotherapeutic activity is limited to a narrow range of cell lines.[4] Some tumours have developed resistance against platinum-based drugs.[3] These drugs also have severe side effects, such as nephrotoxicity, myelotoxicity, ototoxicity, peripheral neuropathy, nausea and vomiting.[5] As a consequence, thousands of new

Pt(II) containing complexes are being developed and screened in search of a lead compound of improved efficacy.[6-7]

To augment this search, an understanding of the kinetics and mechanisms related to the interactions of the platinum(II) complexes with bio-relevant molecules has been the centre stage for preclinical research. Monofunctional $[Pt(N\text{-}N\text{-}N)Cl]^+$ such as $[Pt(terpy)Cl]^+$ (terpy = 2,2':6',2"-terpyridine) and related compounds are very useful models for understanding the substitution behaviour of square-planar platinum(II) complexes since only the fourth ligand is substituted during an associative substitution reaction.[8] These monofunctional Pt(II) complexes have also been found to be thermodynamically stable even under acidic conditions.[9] $[Pt(terpy)Cl]^+$ is a very labile cation, it is about 10^5-10^6 times more reactive than its monofunctional analogue $[Pt(dien)Cl]^+$ (dien = diethylenetriamine) when thiourea (**tu**) is an incoming nucleophile.[10-11] The origin of this rate enhancement is the π-acceptor capability of the terpy chelating ligand. [12-13] By relieving the excess electron density at the metal ion, the polypyridine ligand facilitates the addition of the incoming nucleophile and the stabilization of an 18-electron five-coordinate *trans*ition state.[14]

The lability of the leaving group in chelated mononuclear Pt(II) complexes has been found to be influenced by the nature of the tridentate chelating ligand. Planar complexes which form rigid five-membered chelate rings as in $[Pt(terpy)Cl]^+$ are usually more reactive than complexes with flexible six-membered chelates such as $[Pt(tpdm)Cl]^+$ (tpdm = tripyridinedimethane) due to decreased ring strain and increased steric hindrance in the six-membered chelated complexes. [15] Electronic effects (σ/π effects) are also responsible for the reactivity of Pt(II) complexes. The lability of the complex is enhanced more if stronger π-acceptors are in the *cis*-position than if they are in the *trans* position.[16-17] Introduction of strong σ-donor phenyl groups in the *cis*-position retards the rate of substitution due to reduced nucleophilic discrimination, whereas in the *trans*-position, the reactivity is enhanced due to the labilization of the Pt-Cl bond by the *trans* influence of phenyl ring. [18-20]

Platinum(II) complexes are soft acids,[21] as a result, they have a high affinity for soft bases such as sulfur and nitrogen biomolecules.[22] Binding of Pt(II) drug to sulfur biomolecules especially in proteins within the human body usually leads to toxicity effects, whereas binding to DNA causes the desired cytotoxicity.[22-23] In addition, the antitumor activity of Pt(II) drugs is now generally accepted to be due to interactions between these drugs and nuclear DNA, primarily through the pyridinic N7 of guanine bases.[24] The structural features of monofunctional Pt(II) complexes does not allow them to bind bifunctionally to DNA, therefore, these complexes do not display anti-tumour properties.[22] However, due to the simplicity of their substitution reactions, the

monofunctional Pt(II) complexes are ideal for the study of interactions of Pt(II) complexes with biorelevant sulphur and nitrogen containing ligands.

In this study, we investigated the kinetics and mechanisms of chelated N^C^N Pt(II) complexes (C = 1,3-substituted phenyl ring), with different *cis*-moieties. Two of the complexes have five-membered chelate rings while the other two form six-membered chelates. We used nitrogen donor azole nucleophiles to substitute the chloro ligand from the Pt(II) complexes. The monofunctional complexes are; 1,3-bis(2-pyridinyl)benzeneplatinum(II) chloride (**PtL1**), 1,3-bis(N-pyrazolyl)benzeneplatinum(II) chloride (**PtL2**), 1,3-bis(quinolin-8-yl)benzeneplatinum(II) chloride (**PtL3**) and 1,3-bis(7-azaindolyl)benzeneplatinum(II) chloride (**PtL4**).The nucleophiles used are; Pyrazole (**Pz**), 1,2,4-Triazole (**Tz**), Imidazole (**Im**), 1-methylimidazole (**MIm**) and 1,2-dimethylimidazole (**DMIm**). The azole nucleophiles used differ in the position and the number of N-atoms, basicity and steric hindrance due to methyl groups. For the investigated complexes, it is envisaged that, due to difference on chelate ring size, number of N-donor atoms within the chelate ring and planarity will result to different magnitudes of rate constants. The structures of the studied complexes and nucleophiles are summarised in Figure 5.1.

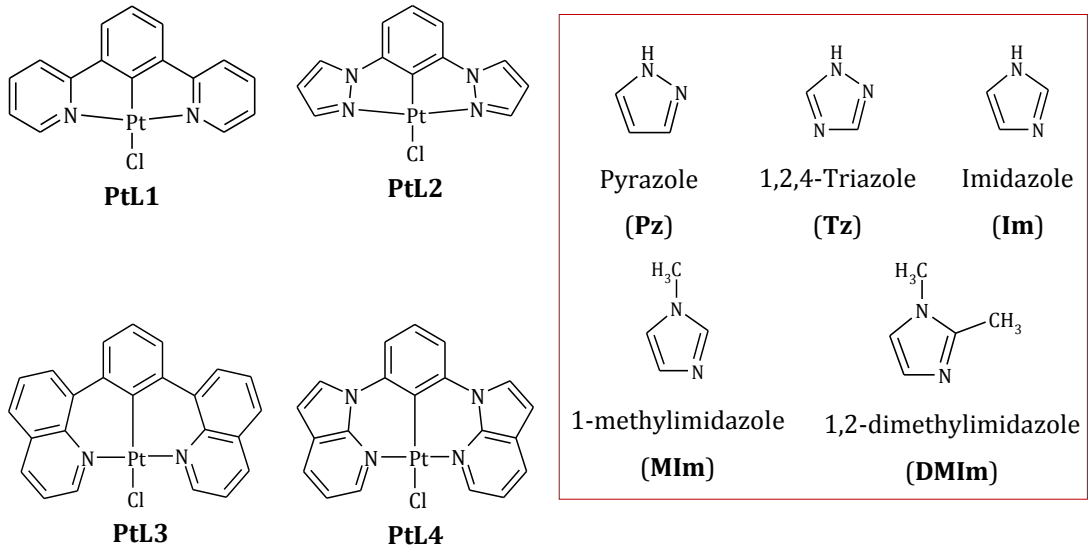

Figure 5.1 Structures of Pt(II) complexes and nucleophiles (**Nu**) used in the study.

5.2. Materials and Procedures

All solvents were dried and distilled prior to use. Copper(I) oxide, *syn*-2-pyridinealdoxime, pyrazole, 7-azaindole, 1,3-diodobenzene, potassium carbonate hydrate, copper(II) sulphate,

bis(dibenzylideneacetone)palladium(0), 2-dicyclohexylphosphoino-2,6–dimethoxybiphenyl, acetic acid, sodium perchlorate, lithium chloride and the azole nucleophiles were purchased from Aldrich and used as received. Cesium carbonate (Cs_2CO_3, 99.99%) and potassium tetrachlroplatinate (K_2PtCl_4, 99.99 %) were procured from STREM and used as received. The ligands; 1,3-bis(2-pyridinyl)benzene[25], 1,3-Bis(N-pyrazolyl)benzene.[26] 1,3-bis(quinolin-8-yl)benzene,[27] 1,3-bis(7azaindolyl) benzene[28] and the complexes **PtL1**,[25] **PtL2**,[26] **PtL3**[27] and **PtL4**[29] were prepared according to published procedures with slight modifications. All synthetic work were performed under inert nitrogen atmosphere using standard Schlenk techniques.

5.3. Synthesis of Ligands

1,3-Bis(2-pyridinyl)benzene. A mixture of 1,3-dibromobenzene (0.272 mL, 2.25 mmol), (2-pyridyl)tributylstanane (1.8 mL, 6.53 mmol), $Pd(PPh_3)Cl_2$ (5 mol %) and LiCl (810 mg, 22.6 mmol) in anhydrous toluene was heated under reflux for 3 days at 100 °C under a flow of nitroden gas. After cooling to 23 °C, a saturated KF solution was added and the mixture stirred for 35 minutes. The solid residue was then filterd off and CH_2Cl_2 (100 mL) and 5% w/v $NaHCO_3$ (100mL) were added to the filtrate. The organic layer was separated and dried over anhydrous sodium sulfate, and finally purified by column chromatography on silica gel eluting with 60% Hexane and 40 % Ethyl Acetate. The title compound was obtained as a bright yellow oil (155 mg, 25.5 %).^{1}H NMR (400 MHz, $CDCl_3$) ppm δ = 8.69 (d, 2H), 8.62 (t , 1H), 8.04 (dd, 2H), 7.81 (d, 2H), 7.73 (tm, 2H), 7.56 (t, 1H), 7.21 (ddm, 2H), TOF MS-ES$^+$, m/z: 255.0906 $(M + Na)^+$.

1,3-Bis(N-pyrazolyl)benzene. An oven dried reaction flask equipped with a magnetic stir bar was loaded with Cu_2O (0.4 mmol, 57 mg), *syn*-2-pyridinealdoxime (1.6 mmol, 195 mg), pyrazole (10 mmol, 680 mg), Cs_2CO_3 (20 mmol, 6516 mg), 1,3-diodobenzene (4 mmol,1320 mg), was evacuated and back-filled with nitrogen gas in four cycles after which anhydrous acetonitrile (20 mL) was added. The mixture was refluxed for 4 days. The reaction mixture was allowed to cool to room temperature, diluted with 50 mL dichloromethane and filtered through a plug of Celite. the celite bed was further washed with dichloromethane (30 mL) and the combined filtrate was reduced in volume under *vacuo* to yield a residue, which was purified by column chromatography using 60% Hexane and 40 % Ethyl Acetate. The title compound was obtained as a pale yellow oil (0.678 g, 80.2%). ^{1}H NMR (400MHz, $CDCl_3$) ppm δ = 8.09 (s,1H), 7.99 (d,2H), 7.73 (d, 2H), 7.59 (dd, 2H), 7.48 (t, 1H), 6.47 (d, 2H). ^{13}C NMR, 141.41, 141.15, 130.45, 126.88, 116.61, 109.94, 108.04. TOF MS ES$^+$, *m/z* : 211.0992 $(M + H)^+$.

1,3-Bis(quinolin-8-yl)benzene. A microwave tube was loaded with quinolin-8-yl boronic acid (243 mg, 1.40 mmol), 1,3-dibromobenzene (163.5 mg, 0.695 mmol), $Pd(dba)_2$ (14 mg, 0.025 mmol), 2-dicyclohexylphosphoino-2,6-dimethoxybiphenyl (0.0225 g, 0.055 mmol), and potassium carbonate (640 mg, 4.65 mmol). After addition of MeCN (3.75 mL) and H_2O (4.00

mL), the tube was sealed, then evacuated and flushed with nitrogen gas three times. Finally, the mixture was heated at 80 ℃ (50 W) for 2 hrs in a CEM Focused Microwave oven. The crude product was poured into H_2O/CH_2Cl_2 mixture, the organic layer separated and dried over sodium sulphate, and finally purified by column chromatography on silica gel eluting with mixtures of ethyl acetate/hexanes (30 to 100%). Title compound was obtained as off-white solid (63 mg, 22.5%). *Anal. Calc. for* $C_{24}H_{16}N_2$; C: 86.72, H: 4.85, N: 8.43 *Found*; C: 86.53, H: 4.96, N: 8.11. ^{1}H NMR (400 MHz, $CDCl_3$): δ = 8.98 (dd, 2H), 8.20 (dd, 2H), 7.98 (t, 1H), 7.86 (dd, 2H), 7.84-7.77(m, 4H), 7.62 (m, 3H), 7.41 (quartet, 2H). ^{13}C NMR (400 MHz, $CDCl_3$) δ = 149.78, 145.67, 140.68, 138.69, 135.91, 132.37, 130.21, 129.62, 128.37, 127.09, 127.01, 125.98, 120.54. TOF MS-ES$^+$, m/z: 355.1215 $(M + Na)^+$.

1,3-Bis(7-azaindolyl)benzene. 7-Azaindole (14 mmol, 1654 mg), 1,3-dibromobenzene (5 mmol, 1180 mg), potassium carbonate (12 mmol, 1658 mg), and copper(II) sulphate (0.1 mmol, 25 mg) were mixed in a flask. The mixture was heated at 473 K for 6 h under nitrogen gas. After cooling to ambient temperature, the reaction mixture was dissolved in 300 mL of CH_2Cl_2 and washed by water. The organic layer was separated, dried by sodium sulphate, and concentrated in vacuo. The residue was passed through a column on silica using a 3:1 hexanes/ethyl acetate solution as the eluent. The solution collected was evaporated by vacuum and dissolved in 5 mL of CH_2Cl_2, and then 2 mL of hexanes was added to the solution to crystallize the product. After one night of standing, colourless crystals of the title compound was obtained (170 mg, 11%).*Anal. Calc. for*$C_{20}H_{14}N_4$; C: 77.42, H: 4.52, N: 18.06 *Found*; C: 77.53, H: 4.66, N: 18.11. ^{1}H NMR400 MHz ($CDCl_3$, ppm, 303K)δ = 8.37 (dd, 2H), 8.3 (t, 1H), 7.97 (dd, 2H), 7.77 (dd, 2H), 7.66 (t, 1H), 7.61 (d, 2H), 7.14 (q, 2H), 6.66 (d, 2H). ^{13}C NMR 400 MHz ($CDCl_3$, ppm, 303K): δ = 147.59, 143.70, 139.43, 130.12, 129.15, 127.80, 121.79, 121.45, 119.42, 116.88, 102.03. (TOF MS-ES$^+$, m/z: 333.1112 $(M + Na)^+$.

5.4. Synthesis of Pt(II) complexes

1,3-Bis(2-pyridinyl)benzeneplatinum(II) chloride, PtL1. A mixture of 1,3-di(2-pyridinyl)benzene (82.3 mg, 0.355 mmol) in 9 mL acetic acid and K_2PtCl_4 (147.2 mg, 0.355 mmol) in 1 mL H_2O was placed into a reaction flask. This mixture was degassed and purged with nitrogen gas and refluxed at 110 – 115 ℃. After 3 days the reaction mixture was cooled to 23 ℃ and the resulting yellow suspension was filtered off and washed sequentially with methanol, ethanol, water and diethyl ether. Finally dried under vacuo to yield a bright yellow solid. (124 mg, 65%). *Anal. Calc. for* $C_{16}H_{11}N_2PtCl$; C: 41.60, H: 2.40, N: 6.07. *Found;* C: 41.98, H: 2.41, N: 5.88. TOF MS-ES$^+$, m/z: 463.0415 $(M + 2H)^+$

1,3-Bis(N-pyrazolyl)benzene platinum(II) chloride, **PtL2**. (200 mg, 0.94 mmol) of 1,3-bis(N-pyrazolyl)benzene in acetic acid and (393 mg, 0.94 mmol) of K_2PtCl_4 were poured to the reaction flask. The mixture was degassed and purged with nitrogen gas, then refluxed at 90 °C for 3 days. Upon cooling to room temperature, the precipitate was filtered, washed sequentially with water, methanol, chloroform, ethanol and diethyl ether. And finally dried under vacuo to yield a pale yellow solid. (196 mg, 47.5%). *Anal. Calc. for* $C_{12}H_9N_4PtCl$; C: 32.76, H: 2.04, N: 12.74. *Found*; C: 33.23, H: 1.89, N: 13.19. TOF MS-ES$^+$, m/z: 404.0033 $(M - Cl)^+$.

1, 3 Bis(quinolin-8-yl)benzeneplatinum(II) chloride, **PtL3.** Solutions of 1,3-di(quinolin-8-yl)benzene (**L7**) (50 mg, 0.15 mmol) in acetonitrile (3 mL) and K_2PtCl_4 (63 mg, 0.15 mmol) in water (1 mL) were added to a reaction flask and the mixture degassed by three freeze-pump-thaw cycles. The latter was added to the former via a cannula under nitrogen atmosphere, and the mixture heated at reflux for 64 h. After cooling, the precipitate which formed was separated by centrifugation, washed successively with water, methanol, ethanol, and diethyl ether and dried under vacuum leading to a yellow-green powder (47 mg, 55.9%). *Anal Calc. for* $C_{24}H_{15}N_2PtCl$; C: 51.29, H: 2.67 N: 4.98 *Found*; C: 50.91 H: 2.86 N: 4.74. ^{1}H NMR (500 MHz, CDCl3) δ = 9.75 (d, 2H), 8.41 – 8.37 (t, 4H), 7.84 (d, 2H), 7.70 (t, 2H), 7.56 (d, 2H), 7.37- 7.29 (m, 3H). TOF MS-ES$^+$, m/z: 526.0895 $(M - Cl)^+$.

1,3-Bis(7-azaindolyl)benzeneplatinum(II) chloride, PtL4. To a solution of K_2PtCl_4 (0.2 mmol, 83 mg), in minimal amount of ultrapure water was added a solution of 1,3-bis(7-azaindolyl)benzene (0.2 mmol, 62 mg) in 20 mL of CH_3CN. The mixture was refluxed overnight under nitrogen. After the reaction mixture was cooled to ambient temperature, the solid was collected by filtration and washed successfully with water, ethanol, methanol, diethyl ether to obtain a pale yellow solid (32mg, 30%). *Anal Calc. for* $C_{20}H_{13}N_4PtCl.\ 1.5CH_2Cl_2$; C: 40.41 H: 2.40 N: 8.98. *Found*; C: 39.95 H: 2.77 N: 9.24. ^{1}H NMR 500 MHz (CD_2Cl_2, ppm, 303 K): δ = 9.38 (dd, 2H), 8.15 (dd, 2H), 8.01(d, 2H), 7.28 (t, 1H), 7.19 – 7.13 (m, 4H), 6.86 (d, 2H). (TOF MS-ES$^+$, m/z: 504.0796 $(M - Cl)^+$.

5.5. Computational Studies

Density functional theory (DFT) calculations for the ground state electronic structures of the studied complexes were carried out to gain more insight on the observed reactivity. The calculations were carried out in the gas phase using the B3LYP functional[30], a three parameter non-local hybrid functional procedure, utilising LANL2DZ (Los Alamos National Laboratory 2 Double (ζ) basis set. The computational software package Gaussian09 was employed for all computations.[31] The structural and key calculated data are summarized in Table 5.1 and Table 5.2 respectively.

Table 5.1 DFT optimized minimum energy structures, HOMO and LUMO frontier molecular orbitals and the side view showing the planarities for platinum complexes at B3LYP/ LANL2DZ level of theory (Isovalue = 0.02).

COMPLEX	STRUCTURE	HOMO map	LUMO map	PLANARITY Side view
	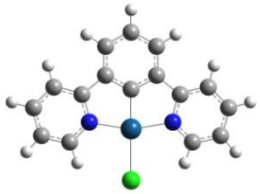	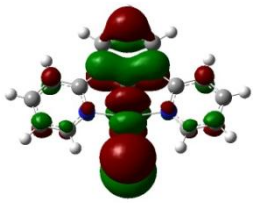	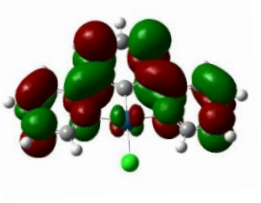	
PtL1				
	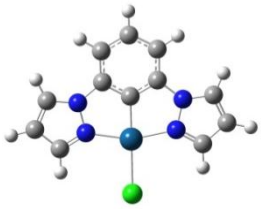	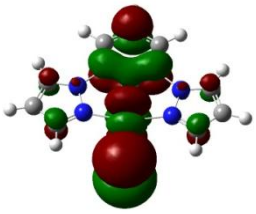	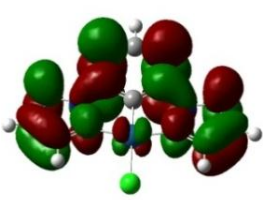	
PtL2				
	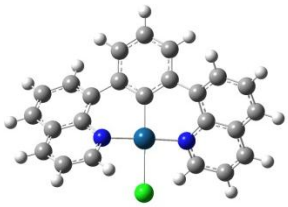	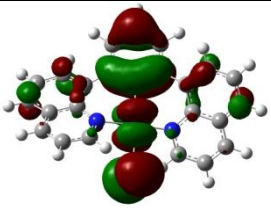	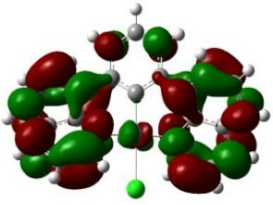	
PtL3				
	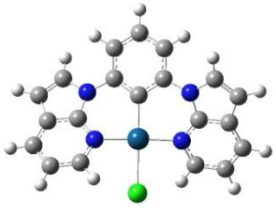	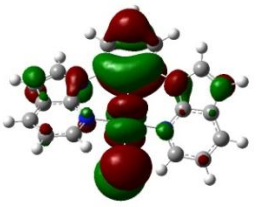	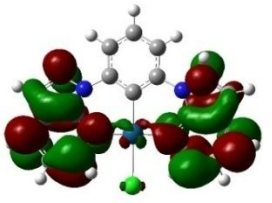	
PtL4				

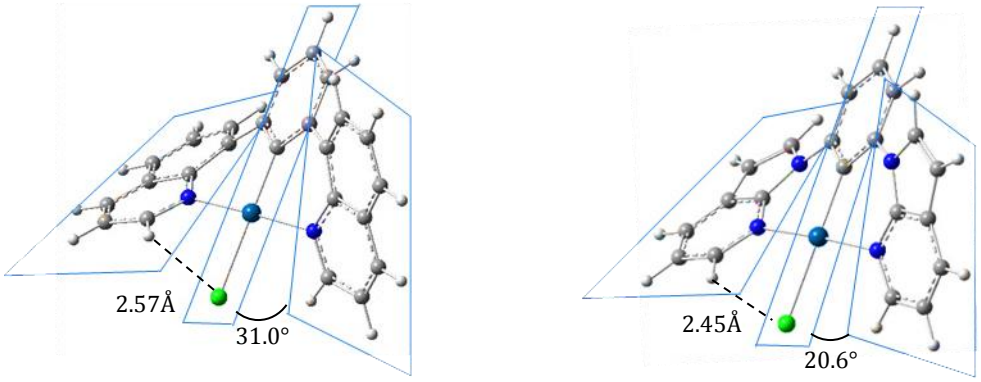

Figure 5.2 Dihedral angles and Cl – H_α contact lengths for **PtL3** (left) and **PtL4** (right).

Table 5.2 Summary of DFT data for the investigated platinum complexes.

Property	**PtL1**	**PtL2**	**PtL3**	**PtL4**
				
Bond angle / °				
Bite	161.51	159.97	177.97	177.01
Dihedral	0.041	0.015	31.00	20.60
Bond Length /Å				
Trans C – Pt bond	1.932	1.941	1.991	2.034
Cl – Pt bond	2.505	2.480	2.546	2.523
Cl – H_α contact	2.738	3.330	2.570	2.458
Energy (E) /eV				
LUMO energy	-2.1726	-1.8430	-2.2869	-1.8082
HOMO energy	-5.5743	-5.5637	-5.4404	-5.6162
$\Delta E_{LUMO-HOMO}$	3.4017	3.7243	3.1535	3.8080
NBO charges				
Pt	0.426	0.411	0.400	0.369
Trans C	-0.101	-0.190	-0.144	-0.232
Cis N	-0.492	-0.300	-0.480	-0.502
Dipole moment (*D*)	6.652	8.604	3.676	5.327
Symmetry	C_{2v}	C_{2v}	C_2	C_2
Electrophilicity /*ω*	4.410	3.686	4.734	3.619

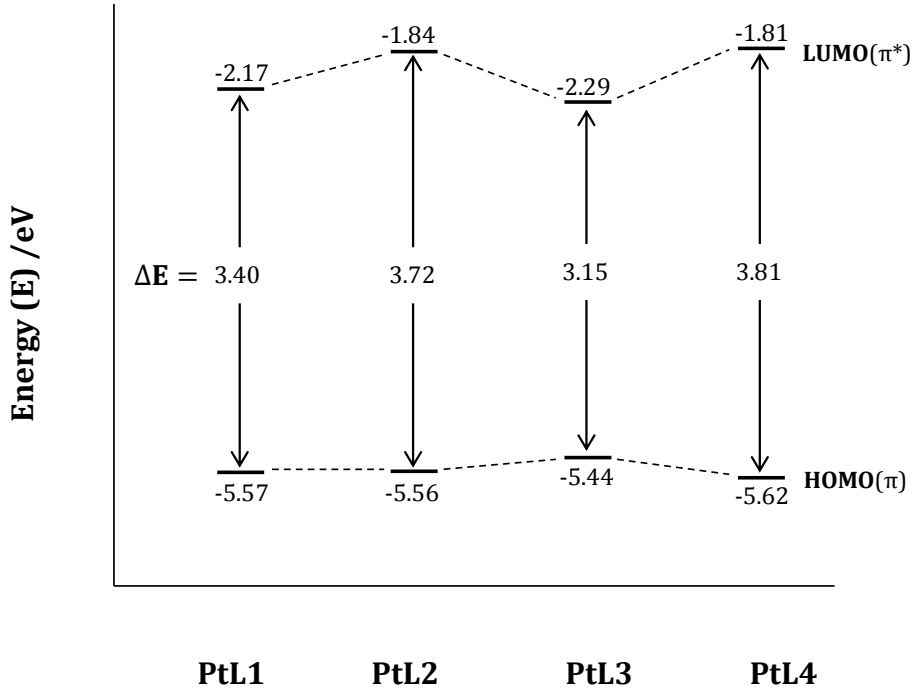

Figure 5.3 HOMO and LUMO energy levels of the studied complexes.

Because of the different chelate ring sizes; five-membered chelate for **PtL1** and **PtL2** and six-membered chelate rings for **PtL3** and **PtL4**, the ring strain affects the *trans* C–Pt bond length, leading to $\geq$ 0.05 Å longer bonds in complexes with six-membered chelate rings, **PtL3** and **PtL4** (see Table 5.2). The influence of the chelate ring size can also be observed in the bite angles of the studied complexes. For five-membered chelates, the bite angles (N-Pt-N) are 161.51° and 159.97 ° for **PtL1** and **PtL2** respectively. However, for six-membered chelates the bite angles are 178 ° and 177 ° for **PtL3** and **PtL4** respectively. The coordination geometry of the latter complexes is almost that of an ideal square planar with slight distortions from ideal values.[15] However, major deviations from ideal square planar observed in **PtL1** and **PtL2** are not surprising since various research groups studying Pt(II) complexes with five-membered chelate rings obtained similar values.[15,32]

5.6. Kinetic Measurements

Kinetic measurements were performed under *pseudo* first-order conditions by following the changes in absorbance as a function of time at suitable wavelengths using a Varian Cary 100 UV/ Visible spectrophotometer with an online kinetics application and an attached Varian Peltier temperature control unit. The wavelengths at which the greatest absorbance change was

observed were used for the kinetic analyses and are reported in Table SI 1. More rapid reactions were followed using an Applied Photophysics SX.20MV (v2.2.5.6) stopped–flow system with an online Pro – Data ™ instrument software for Windows®. Kinetics of **PtL1**, **PtL3** and **PtL4** were followed using the stopped–flow spectrophotometer whereas **PtL2** was studied using UV/Visible spectrophotometer. For the UV/Visible kinetic studies, an average of at least two kinetic reactions was used and six to eight independent runs were averaged for the stopped-flow spectrophotometer kinetic reactions. The temperatures were controlled to within 0.1 °C.

The solvent system used for preparing the complexes and nucleophiles for kinetic measurements was prepared by dissolving required amounts of $LiCF_3SO_3$ and LiCl in absolute ethanol to afford a solution with the ionic strength of 0.10 M (0.09 M $LiCF_3SO_3$ + 0.01 M LiCl). The triflate ion ($CF_3SO_3^-$) is a good choice for maintaining the ionic strength since it does not coordinate to the Pt(II) centre.[33] Furthermore, LiCl was used to prevent spontaneous solvolysis reaction. Metal complex solutions were prepared by dissolving a required amount of metal complex to 250 mL ethanol solution (I = 0.10 M (0.09 M $LiCF_3SO_3$ + 0.01 M LiCl). Stock solutions of **Pz**, **Tz**, **Im**, **MIm** and **DMIm** were prepared by dissolving a known amount of nucleophile in 25 mL of the ionic strength solution and subsequent dilutions of each stock solution were performed to obtain a series of standards of lower concentrations.

5.7. Results

Kinetics of substitution of coordinated chloride (Scheme 1) from four Pt(II) complexes namely **PtL1**, **PtL2**, **PtL3** and **PtL4** by five different nucleophiles (**Nu**), namely; Pyrazole (**Pz**), 1,2,4-Triazole (**Tz**), Imidazole (**Im**), *n*-Methylimidazole (**MIm**) and 1,2-Dimethylimidazole (**DMIm**), were investigated under *pseudo*-first order conditions as a function of concentration and temperature.

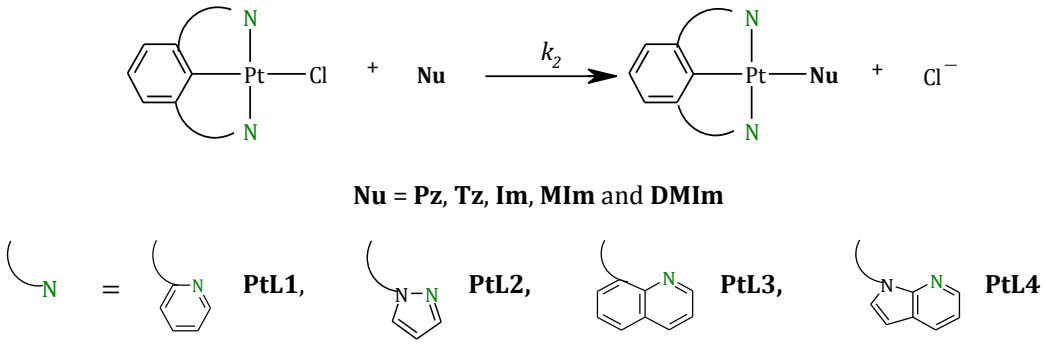

Scheme 1 Proposed mechanism of chloride substitution.

The kinetic traces obtained using the stopped–flow spectrophotometer and the UV/Visible spectrophotometer gave good single exponential fits. A typical kinetic trace obtained from the UV/ Visible spectrophotometer is given in Figure 5.4 (also Figures SI 5.1 to SI 5.19)

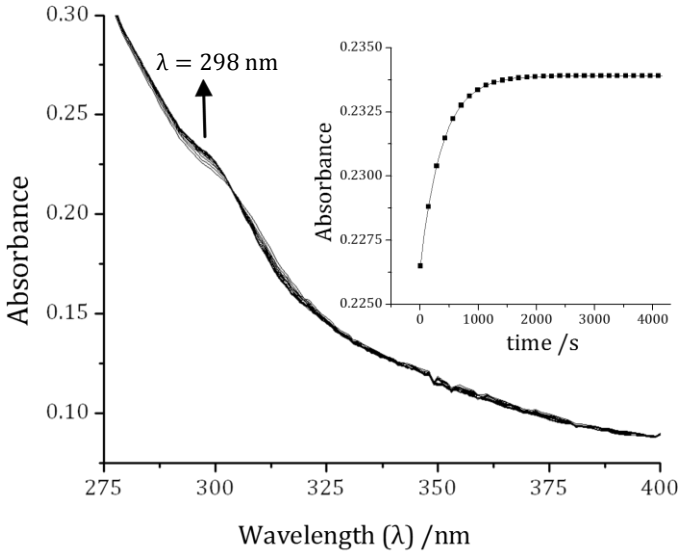

Figure 5.4 First-order exponential fit for the reaction of **PtL6** with **1,2,4-triazole** (2.77 mM) at 298 nm, T=298.15 K.

The *pseudo* first-order rate constants, k_{obs} were plotted against the concentration of the entering nucleophile (Figure 5.5) to obtain the second-order rate constant, k_2 for the forward reaction from the slope. All kinetic plots obtained were linear with zero intercepts (

Figure 5.5) which indicate that solvolysis pathways were absent or insignificant. In addition, there was no observable dechelation (ring opening) reaction observed within the studied time frame. The summary of the second-order rate constants for the reactions between complexes and nucleophiles is given in Table 5.3. The rate of substitution is described by Equation (1).

$$k_{\text{obs}} = k_2[\mathbf{Nu}] \quad (1)$$

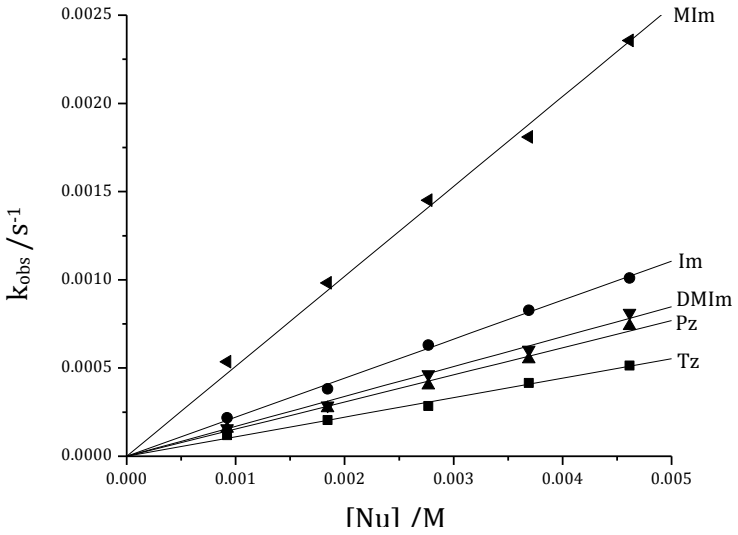

Figure 5.5 Dependence of the *pseudo* first-order rate constants (k_{obs}) on the concentrations of the nucleophiles for the chloride substitution from **PtL2** in ethanol solution (I = 0.10 M (0.09 M $LiCF_3SO_3$ + 0.01 M LiCl)) at 298.15 K.

Temperature dependence studies were also conducted to determine the activation parameters by measuring the rate constant (k_2) as a function of temperature over a temperature range of 15 - 40 °C at 5 °C intervals. Eyring plots (Figure 5.6) were used to calculate the thermodynamic parameters, enthalpy ($\Delta H^{\neq}$) and entropy ($\Delta S^{\neq}$) of activation from the slopes and intercepts respectively, using the Eyring equation (2).[34] Results are summarised in Table 2.

$$\ln\left(\frac{k_2}{T}\right) = -\frac{\Delta H^{\neq}}{RT} + \left(23.8 + \frac{\Delta S^{\neq}}{R}\right) \quad (2)$$

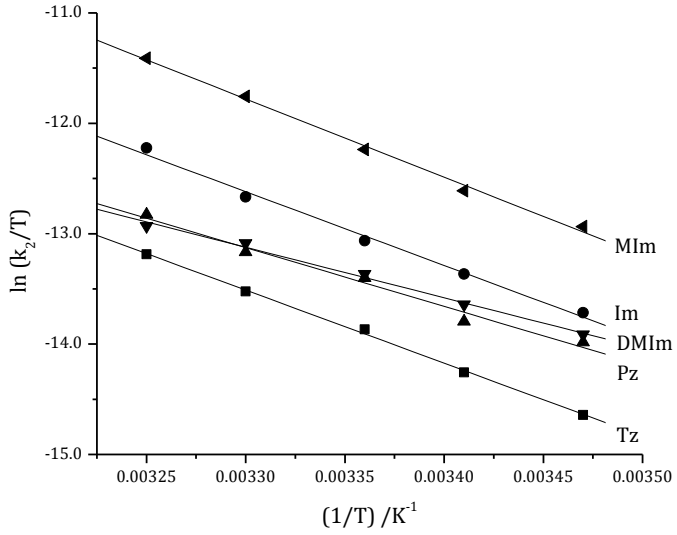

Figure 5.6 Typical Eyring plot to obtain the activation parameters for the direct nucleophilic substitution reaction for **PtL4** and five azole nucleophiles.

Table 5.3 Summary of the first – order rate constants (k_2) and their standard deviations for the substitution of the chloride from the platinum complexes by **Pz**, **Tz**, **Im**, **MIm** and **DMIm** in ethanol, (I = 0.10 M (0.09 M $LiCF_3SO_3$ + 0.01 M LiCl)) at 298.15 K.

Nucleophile		**PtL1** 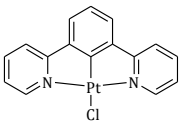	**PtL2** 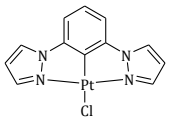	**PtL3** 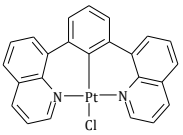	**PtL4** 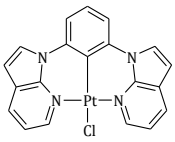
		k_2 in $M^{-1} s^{-1}$ for the nucleophilic substitution reactions studied			
	**Pz**	620 ± 24	0.316 ± 0.01	20 ± 0.9	21 ± 0.5
	**Tz**	580 ± 30	0.109 ± 0.01	18 ± 0.9	10 ±0.3
	**Im**	637 ± 9	0.410 ± 0.01	45 ± 0.7	27 ± 0.5
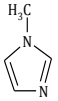	**MIm**	1068 ± 75	0.510 ± 0.01	62 ± 1	41 ± 0.8
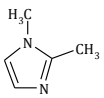	**DMIm**	269 ± 3	0.220 ± 0.003	46 ± 1	14 ± 0.2

Table 5.4 Summary of the activation parameters for the substitution of the chloride from the platinum complexes by **Pz**, **Tz**, **Im**, **MIm** and **DMIm** in ethanol,(I = 0.10 M (0.09 M $LiCF_3SO_3$ + 0.01 M LiCl)) at 298.15 K.

Nucleophile	Activation Parameter $\Delta H^{\neq}$/k J mol^{-1} $\Delta S^{\neq}$/J K^{-1} mol^{-1}	Complexes			
		PtL1	**PtL2**	**PtL3**	**PtL4**
Pz	$\Delta H^{\neq}$	43 ± 3	42 ± 3	58 ± 0.5	18 ± 1
	$\Delta S^{\neq}$	-104 ± 10	-167 ± 10	-68 ± 1.4	-108 ± 3
Tz	$\Delta H^{\neq}$	36 ± 1	53 ± 3	42 ± 3	34 ± 3
	$\Delta S^{\neq}$	-125 ± 3	-135 ± 8	-124 ± 10	-156 ± 9
Im	$\Delta H^{\neq}$	58 ± 2	55 ± 4	48 ± 3	19 ± 2
	$\Delta S^{\neq}$	-39 ± 5	-118 ± 12	-91 ± 11	-183 ± 6
MIm	$\Delta H^{\neq}$	58 ± 2	57 ± 1	32 ± 2	22 ± 1
	$\Delta S^{\neq}$	-139 ± 5	-106 ± 3	-144 ± 6	-170 ± 3
DMIm	$\Delta H^{\neq}$	62 ± 2	37 ± 2	41 ± 2	43 ± 1
	$\Delta S^{\neq}$	-30 ± 6	-182 ± 6	-115 ± 7	-183 ± 4

5.8. Discussion

Table 5.1 and Table 5.2, shows that DFT data for optimised complexes are significantly different in terms of planarity, geometry, metrices and chelate ring sizes. The studied complexes have a common phenyl group *trans* to the chloride ligand, implying that the σ-donor and π-acceptor properties of the *trans* phenyl ligands are kept constant. For the purpose of discussing the results, the reactivity of the complexes are grouped according to chelate ring sizes, presence and absence of pyrrolic nitrogen. In addition, the azole nucleophiles used differ in the position and the number of N-atoms and also various number of attached methyl substituents.

The comparative study of the rates of substitution of the chloride leaving group from the studied complexes shows a general reactivity trend for the forward reaction to be: **PtL1** > **PtL3** > **PtL4** > **PtL2**.

It is worth noting that the difference in the structures of **PtL1** and **PtL2** is the presence of a five-membered pyrazolyl *cis* ring in **PtL2** in place of the pyridine in **PtL1**. The second order rate constants ($\boldsymbol{k_2}$) of **PtL2** (Table 5.3) decrease by three orders of magnitude or higher depending

on the incoming nucleophile. Since the reactions of d^8 square planar Pt(II) complexes are associative in nature, the *trans*ition state is stabilised by the π-backdonation from the nonbonding metal *d*-electrons to the empty π^*-orbitals of the chelating ligand.[35] Therefore, this profound reactivity difference is not surprising since it is already known that the *cis* π-effect is greater than the *trans* π-effect.[36] Since the structural differences in these compounds are *cis*-groups, it is expected that the reactivity is enhanced more if stronger π-acceptors are in the *cis*-position.[16] The poor π-acceptor nature of the pyrazolyl rings compared to pyridinyl rings is consistent with this decreased reactivity of **PtL2** due to the accumulation of the electron density at the metal centre leading to the metal centre electrophilicity being decreased and thus retardation of the incoming nucleophile. This clearly shows that the π-excessive *cis*-pyrazole rings in **PtL2** are weak π-acceptors and probably act merely as π-donors which is also expected to slow down the substitution of the leaving group by lowering the electrophilicity of the platinum centre in **PtL2**. This is also supported by the **NBO** charges (Table 5.2) which shows that the metal centre in **PtL1** has a slightly more positive charge (0.426) compared to that of **PtL2** (0.411). This is also supported by the Electrophilicity values ($\boldsymbol{\omega}$) of the whole complex which shows that **PtL1** has overall $\boldsymbol{\pi}$-bonding effect compared to **PtL2**.

A study by Develay *et al.*[26] on the contrasting influence of pyrazolyl and pyridyl rings on luminescence of cyclometalated Pt(II) complexes, provides useful information supporting the fact that pyrazole is a weaker π-acceptor than pyridine. Electrochemical data showed that **PtL1** has a reduction potential occurring around -0.2 V while the pyrazolyl coordinated Pt(II) complexes each displayed an irreversible reduction wave in the range of -2.5 and -2.8 V.[26] The cathodic shift for Pt(II) pyrazolyl complexes confirms their poor π- acceptor character. Since the π-acceptor property of the complex is basically the *trans*fer of the electron density from the calculated HOMO centred at the metal orbital to the LUMO centred at the ligand, Table 5.3 shows that the HOMO–LUMO energy gap is wider in **PtL2** compared to **PtL1**. This suggests an increase in the energy barrier consistent with slower substitution reactions in **PtL2**.[37-38]

The introduction of fused rings in the *cis*-positions of chelating ligands; quinoline in **PtL3** and 7–azaindole in **PtL4** afforded six-membered chelated Pt(II)complexes. The 7–azaindole fused ring system comprises of an electron rich pyrrole ring and an electron deficient pyridine ring. Additionally, it has been found to be a potential π-donor to the indolyl moiety through the indole nitrogen atom.[26] As depicted in Table 5.3, the obtained data for k_2 for the substitution reactions of the six-membered chelate Pt(II) complexes with five different azole nucleophiles, the data shows that **PtL3** is more reactive than **PtL4**. This is consistent with the simplistic picture of the azaindole unit being more electron rich than a quinoline.[27] Also supported by the electrophilicity values (ω) of 4.734 eV and 3.619 eV for **PtL3** and **PtL4** respectively. The increased HOMO-LUMO energy gap accompanied by a decrease in Pt atom **NBO** charge in **PtL4**

results in the observed decrease in reactivity compared to **PtL3**. This implies that the quinoline in **PtL3** accepts the electron density from the metal centre better than the azaindole moiety, making a more electrophilic metal centre, leading to a more stabilized *trans*ition state which aids the approach of the entering nucleophile, enhancing the formation of a new Pt–azole bond.[27] The approach of the entering nucleophile in **PtL4** is also severely hindered by the electronic repulsion due to shortening of the Cl–H_α contact length (Figure 5.2)[39] leading to slower substitution reactions in **PtL4** compared to **PtL3**.

Another important difference which may be significant in controlling the reactivity of the complexes is structural. The geometry of **PtL1** and **PtL2** is $\mathbf{C_{2v}}$ while that of **PtL3** and **PtL4** is $\mathbf{C_2}$ (Table 5.2) The difference in geometry between the two groups is due to the significant twisting of the azaindole/ quinoline rings relative to the principal axes, C–Pt–Cl plane, whereas **PtL1** and **PtL2** are almost planar. Figure 5.2 indicates that each quinolone ring in **PtL3** has a dihedral angle of 31.0° while the azaindole rings in **PtL4** are twisted by 20.6° each relative to the central phenyl ring. This distortion is expected since the bis(7-azaindolyl) and bis(8-quinolyl) groups are sterically demanding of the square planar geometry around the platinum ion.[27] Therefore, by twisting the plane of the heterocyclic rings (azindole/ quinolone), stable Pt(II) ions are formed with the preferred square-planar coordination. A similar reorganisation of a flexible ligand is exemplified in a recently reported crystal structure of [Pt(tpdm)Cl]Cl.[15] When comparing the reactivity of the C_{2v} complexes to that of the C_2 complexes, it is expected that the distortion on the C_2 complexes lowers the reactivity in at least two ways. Firstly, the aromaticity of the chelate ring is disturbed as the overlap between the nitrogen *p*-orbitals and the d_z orbitals on the platinum centre is reduced.[40] Secondly, the attack of the nucleophile on the Pt(II) center is sterically hindered.[15] Surprisingly, **PtL2** reacts slower than its analogue **PtL4**. Therefore, in this study, the inability of the electron rich in-plane 5-membered pyrazolyl rings of **PtL2** to effectively accept the π-electrons from the metal centre in the ground state is more effective than the effects caused by the out of plane twisting of the *cis*-groups in **PtL3** and **PtL4**.

The effect of the pyrrolic nitrogen and ring sizes of the *cis*-groups was also investigated in the series of complexes studied. The reactivity was found to decrease in both five and six-membered chelated Pt(II) complexes (**PtL2** and **PtL4**) having 5-membered, pyrrolic nitrogen containing *cis*-groups. The pyrazolyl groups in (**PtL2**) and the 7-azaindolyl fused ring in (**PtL4**) are considered as π-excessive due to the presence of these 5-atom, 6-electron heterocycles.[41] Such π-excessive nature of these heterocycles reduces the π-acceptor ability of the chelating ligand compared to 6-membered heterocycles.[26] This is supported by **DFT** data showing a significant increase in the LUMO energies of **PtL2** and **PtL4** compared to **PtL1** and **PtL3**

respectively (Figure 5.3) and lower electrophilicity values for **PtL2** and **PtL4** compared to that of PtL1 and **PtL3** respectively. Therefore, fusing an additional benzene ring to a monocyclic π-deficient pyridine group (**PtL3**) affords a π-deficient fused ring system, whereas if a pyrrole ring is used instead of benzene, the ring system becomes π-excessive (7-azaindole), supporting the notion that N-containing 5-membered heterocycles consists of more electron rich carbon atoms than benzene.[41]

When comparing the nucleophiles used, it is important to group them according to their structural similarities. The first group consists of **Pz**, **Im** and **Tz**, all having nitrogens at different positions and no substituents attached. The second investigated group consists of **MIm** and **DMIm** both having at least one methyl substituent on their imidazole rings. These nucleophiles were included in order to quantify the inductive effect and/or steric hindrance in the rate of substitution. The reactivity of the entering unhindered five-membered N-donor heterocyclic nucleophile has been found to depend linearly on their basicities according to a linear free energy relationship (LFER) of the type $k_2 = \alpha(pK_a) + b$, where the parameters α and b take into account the electronic and steric effects.[42] Similar results were reported by Jaganyi *et al.*[43] while investigating the substitution reactions of [Pt(terpy)Cl]$^+$ and analogues by a series of azole nucleophiles. In studies involving DNA and related nucleobases, it is known that substitution of Pt(II) complexes occurs *via* coordination of mainly purine bases which contain a fused imidazole ahead of pyrimidine bases due to the favourable basicity of the former type of a base.[44]

Looking at the first group of nucleophiles, it is clear that the general reactivity trend of the nucleophiles is **Im** > **Pz** > **Tz**. This reactivity trend is consistent with the basicities of the nucleophiles reflected in the relative magnitudes of their *p*Ka values of 7.00, 2.52 and 2.19 for **Im**, **Pz** and **Tz** respectively.[45] For the second set of nucleophiles the reactivity trend observed is **MIm** > **DMIm** with the *p*Ka values of 7.30 and 7.85 respectively.[45-46] In this case, **DMIm** has a higher *p*Ka while it is the least reactive nucleophile. The 2-methly substituent of DMIm sterically hinders the nucleophilic pyridinyl nitrogen which slows down the substitution reaction as previously reported in literature.[10, 43, 47] Therefore, the presence of only one methyl substituent in MIm leads to the inductive effect being more dominant than steric hindrance, which explains the higher reactivity of **MIm** compared to **DMIm**.[47]

The obtained activation parameters, the enthalpy of formation, $\Delta H^{\ddagger}$ are all small and positive while those of the activation entropy, $\Delta S^{\ddagger}$ are large and negative for all the studied complexes. This is indicative of an associative substitution mechanism and a net increase in the bond order in the *trans*ition state, typical of d^8 platinum(II) complexes.[48]

5.9. Conclusion

The reactivity trend for the complexes is **PtL1** > **PtL3** > **PtL4** > **PtL2**. The reactivity of the studied complexes depends on the electronic and steric effects of the tridentate chelate ligands. These results indicate that, a switch of the coordinated ligands from 1,3-bis(2-pyridinyl)benzene to 1,3-bis(*N*-pyrazolyl)benzene in monofunctional Pt(II) complexes is accompanied by a reduction of the rate of substitution by three orders of magnitude. This confirms the profound effect on reactivity due to the *cis* π- effect. Introduction of 8-quinolyl and 7-azaindolyl *cis*-groups leads to out of plane twisting of these groups also preventing effective π-back donation of the metal electrons, leading to slower reactivity compared to **PtL1** with in plane *cis*-pyridinyl groups. The reactivity of **PtL3** and **PtL4** relative to their analogues **PtL1** and **PtL2** respectively, is also decreased by steric hindrance due to out of plane twisting of the *cis* groups. The reactivity trend of the complexes is further supported by DFT calculations (B3LYP/LANL2DZ). The nucleophile reactivity is dependent upon the basicity of the reactive pyridinic nitrogen, as well as steric hindrance due to the methyl group in the *α*-position in **DMIm** which significantly decreases the reactivity of this nucleophile. Temperature dependence studies afforded large negative activation entropy values ($\Delta S^{\neq}$) and amall positive enthalpy of activation ($\Delta H^{\neq}$), supporting an associative mechanism of substitution.

Supplementary Information

Electronic supplementary information (ESI) available: Mass and NMR spectra, a summary of wavelengths used for kinetic measurements, tables and kinetic traces summarising concentration and temperature dependence studies of selected complexes.

5.10. References

1. Hambley, T.W., J. Chem. Soc., *Dalton Trans*. **2001**, 2711-2718.
2. Milacic, V., Ping Dou, Q., *Coord. Chem. Rev*. **2009**, *253*, 1649-1660.
3. Kalinowska-Lis, U., Ochocki, J., Matlawska-Wasowska, K. *Coord. Chem. Rev*. **2008**, *252*, 1328-1345.
4. Lippert, B. *Cisplatin: Chemistry and Biochemistry of a Leading Anticancer Drug.* Wiley-VHC, Weinheim, **1999**, 55-57.

5. Ho, Y-P., Au-Yeung, S. C. F., To, K. K. W., *Medicinal Research Reviews*., **2003**. *23*, 633-655.
6. Weiss, R. B., Christian, M.C. *Drugs*, **1993**, *46*, 360-377
7. Kostova, I. *Recent Patents on Anti-Cancer Drug Discovery*. **2006**, 1, 1-22
8. Selimović, E., Petrović, B., Čanovič, D., Bugarčić, Ž. D., Bogojeski, J. *Aust. J. Chem.* **2013** , http://dx.doi.org/10.1071/CH12218
9. Jaganyi, D.; Tiba, F.; Munro, O. Q.; Petrović, B.; Bugarčić, Ž. D. *J. Chem. Soc., Dalton Trans,* **2006**, 2943-2949.
10. Pitteri, B., Marangoni, G., Cattalini, L., Bobbo, T. J. *Chem. Soc. Dalton. Trans.* **1995**, 3853-3859.
11. Romeo, R., Plutino, M. R., Scolaro, J. M., Stoccoro, S.,Minghetti, G. *Inorg. Chem.* **2000**, *39*, 4749-4755.
12. Burgarčić, Ž. D., Petrovic, B., Zangrando, E. *Inorg. Chim. Acta,* **2004**, 357, 2650.
13. Burgarčić, Ž. D., Nandibewoor, S. T., Hamza, M. S. A., Heinemann, F., van Eldik, R. *Dalton Trans.*, **2006**, 2984–2990
14. Moeller, T., *Inorganic Chemistry: A Modern Introduction*, **1982**, 714-719.
15. Petrović, B., Burgarčić, Ž. D., Dees, A., Ivanović-Burmazović, I., Heinemann, F. W., Puchta, R., Steinmann, S. N., Corminboeuf, C., van Eldik, R., *Inorg. Chem.,* **2012**, *51*, 1516-1521.
16. Hofman, A., Jaganyi, D., Munro, O. Q., Liehr, G., van Eldik, R. *Inorg. Chem*., **2003**, *42*, 1688-1700.
17. Jaganyi, D.; Reddy, D.; Gertenbach, J. A.; Hofmann, A.; van Eldik, R., *Dalton Trans.*, **2004**, 299-304.
18. Basolo, F. Chatt, J. Gray, H.B. Pearson R. G. Shaw. B. L. *J. Chem. Soc*., **1961**, 2207-2215.
19. Alibrandi, G. Minniti, D. Scolaro L. M and Romeo, R. *Inorg. Chem.,* **1988**, *27*, 318-324.
20. Atwood, J. D. *Inorganic and Organometallic Reaction Mechanisms*, Wiley-VCH Inc., New York, 2nd edition, **1997**, 43-60.
21. Pearson, R. G.; *Inorg. Chem.* **1988**, *27*, 734-740.
22. Burgarčić, Ž. D.; Bogojeski, J.; Petrovic, B. Hochreuther, S.; van Eldik, R.; *Dalton Trans.*, **2012**, *41*, 12329-12345.
23. Burgarčić, Ž. D.; Liehr, G.; van Eldik, R. *J. Chem. Soc., Dalton Trans.* **2002**, 2825-2830.
24. (a) Weiss, R. B., Christian, M.C. *Drugs.*, **1993**, 46, 360-377 (b) Kozelka, J. *Inorganica. Chimica. Acta.* **2009**, *362*, 651-668.

25. Cárdenas, D.J. and Echavaren, A.M. *Organometalics*., **1999**, *18*, 3337-3341
26. Develay, S., Blackburn, O., Thompson, A.L. and Gareth Williams, J.A. *Inorg. Chem*. **2008**, *47*, 11129 – 11142.
27. Garner,K.,Parkes, L., Piper J, D. and Williams, J. A. G., *Inorg.Chem*., **2010**. *49*, 476-487.
28. Wu, Q., Lavigne.A.J., Tao, Y., D'Ioro, M., Wang, S. *Chem. Mater*., **2001**, *13*, 71.
29. Song, D., Wu, Q., Hook, A., Kozin, I., Wang, S. *Organometallics.*, **2001**, *20*, 4683.
30. Becke, A. D. *Chem. Phys.* **1993**, *99*, 3898-3905.
31. M. J. Frisch, G. W. Trucks, H. B. Schlegel, G. E. Scuseria, M. A. Robb, J. R. Cheeseman, G. Scalmani, V. Barone, B. Mennucci, G. A. Petersson, H. Nakatsuji, M. Caricato, X. Li, H. P. Hratchian, A. F. Izmaylov, J. Bloino, G. Zheng, J. L. Sonnenberg, M. Hada, M. Ehara, K. Toyota, R. Fukuda, J. Hasegawa, M. Ishida, T. Nakajima, Y. Honda, O. Kitao, H. Nakai, T. Vreven, J. A. Montgomery, Jr., J. E. Peralta, F. Ogliaro, M. Bearpark, J. J. Heyd, E. Brothers, K. N. Kudin, V. N. Staroverov, R. Kobayashi, J. Normand, K. Raghavachari, A. Rendell, J. C. Burant, S. S. Iyengar, J. Tomasi, M. Cossi, N. Rega, J. M. Millam, M. Klene, J. E. Knox, J. B. Cross, V. Bakken, C. Adamo, J. Jaramillo, R. Gomperts, R. E. Stratmann, O. Yazyev, A. J. Austin, R. Cammi, C. Pomelli, J. W. Ochterski, R. L. Martin, K. Morokuma, V. G. Zakrzewski, G. A. Voth, P. Salvador, J. J. Dannenberg, S. Dapprich, A. D. Daniels, O. Farkas, J. B. Foresman, J. V. Ortiz, J. Cioslowski, and D. J. Fox, *Gaussian 09, Revision **C.01**,* **2010**,Gaussian Inc., Wallingford CT.
32. Jaganyi, D., De Boer, K-L., Gertenbach, J., Perils, J. *International Journal of Chemical Kinetics*., **2008**, *40***,** 808 - 818.
33. Appleton, T. G. Hall, J. R. Ralph, S. F. and Thompson, C. S. M., *Inorg. Chem*., **1984**, *23*, 3521-3525.
34. Eyring, H. *J. Chem. Phys.,* **1935**. *3*, 107-115
35. Crabtree, R.H. The Organometallic Chemistry of the Transition Metals, John Willey and Sons, New York, **2001**, 96-109
36. Hofmann, A.; Jaganyi, D., Munro, O. Q., Liehr, G., van Eldik, R., *Inorg. Chem*. *42*, **2003**, 1688-1700.
37. Pearson R. G. *J. Chem. Educ.,* **1987**, *64*, 561-567.
38. Pearson R. G. *Acc. Chem. Res.,* **1993**, *26*, 250.

39. (a) Appleton, T. G.; Hall, J. R. *Inorg. Chem.,* **1970**, *9*, 1717-1725. (b) Appleton, T. G.; Hall, J. R. *Inorg. Chem.,* **1970**, *9*, 1800-1806. (C) Appleton, T. G.; Hall, J. R. *Inorg. Chem.,* **1970**, *9*, 1807-1814.
40. Bodwell, G. J.; Bridson, J. N.; Cyranski, M. K.; Kennedy, J. W.; Krygowski, T. M.; Mannion, M. R., Miller, D. O. *J. Org. Chem.,* **2003**, *68*, 2089-2098.
41. Gilchrist, T. L. *Heterocyclic Chemistry*, Addison Wesley Longman Ltd, 2nd edition, **1997**, 8-13
42. Pitteri, B., Bortoluzzi, M. *Polyhedron*., **2006**. *25*, 2698-2704.
43. Reddy, D., Ackerman, K. J., Ackerman, M. P., Jaganyi, D., *Transition. Met. Chem*., **2011**, 36, 593-602.
44. Sigel, H., Massoud, S. S., Corfu, N. A. *J. Am. Chem., Soc*. **1994**, 116, 2958
45. Katritzky, A. R. *Physical Methods in Heterocyclic Chemistry: A Comprehensive Tretise in Two Volumes,* Volume 1.; Academic Press: New York, **1963**. 19-20, 45-49, 65.
46. Eicher, T.; Hauptmann, S. *The Chemistry of Heterocycles: Structure, reactions, Syntheses and Application,* Stuttgart: New York, 1995. *166*, 181, 209.
47. Shaira, A.; Reddy, D.; Jaganyi, D. *Dalton. Trans.* **2013**, Manuscript in Progress.
48. Ymamoto, A. *Organotransition Metal Chemistry*: *Fundamentals Concepts and Applications*, John Willey and Sons, New York, **1986**, 181-203.

Chapter 5

Supporting Information (SI 5)

SI 5.2. Mass and ^{1}H NMR Spectra

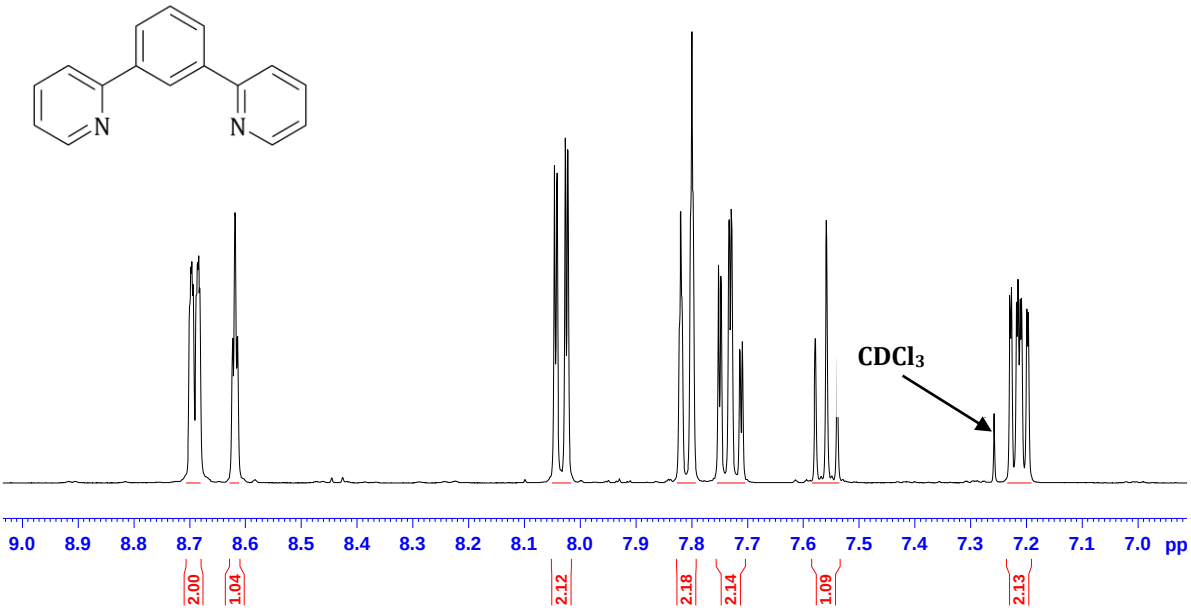

Figure SI 5.29 ^{1}H NMR Spectrum of 1,3-Di(2-pyridinyl)benzene in $CDCl_3$.

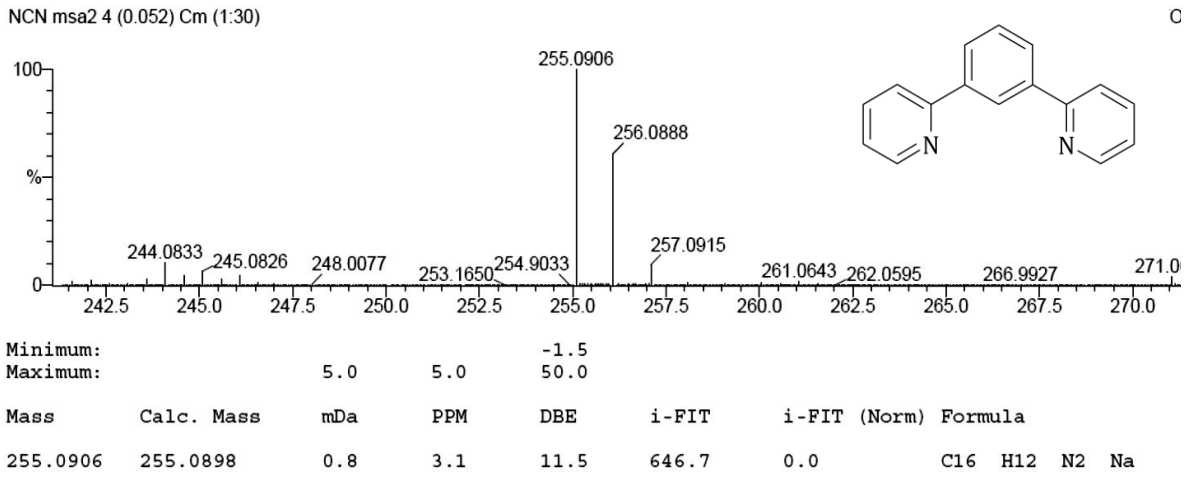

Minimum:				-1.5			
Maximum:		5.0	5.0	50.0			
Mass	Calc. Mass	mDa	PPM	DBE	i-FIT	i-FIT (Norm)	Formula
255.0906	255.0898	0.8	3.1	11.5	646.7	0.0	C16 H12 N2 Na

Figure SI 5.30 Mass Spectrum of 1,3-Di(2-pyridinyl)benzene.

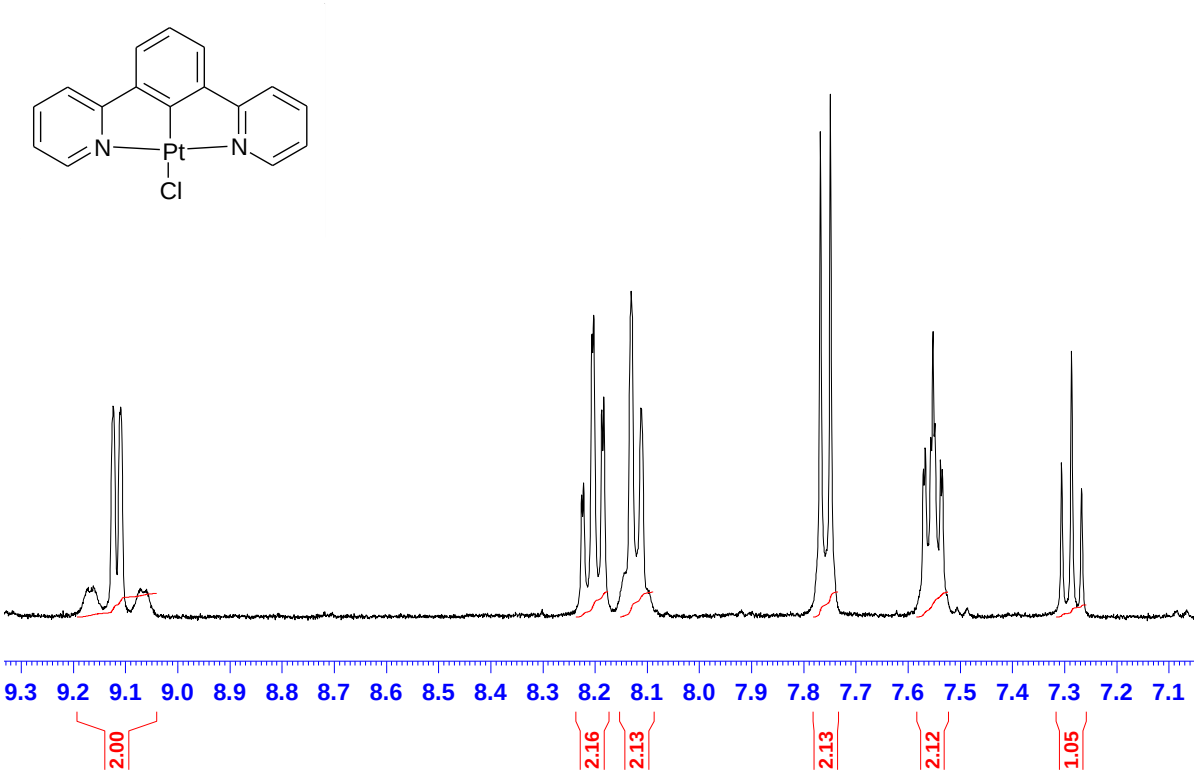

Figure SI 5.31 ^{1}H NMR of 1,3-Di(2-pyridinyl)benzene platinum(II)complex, **PtL5**.

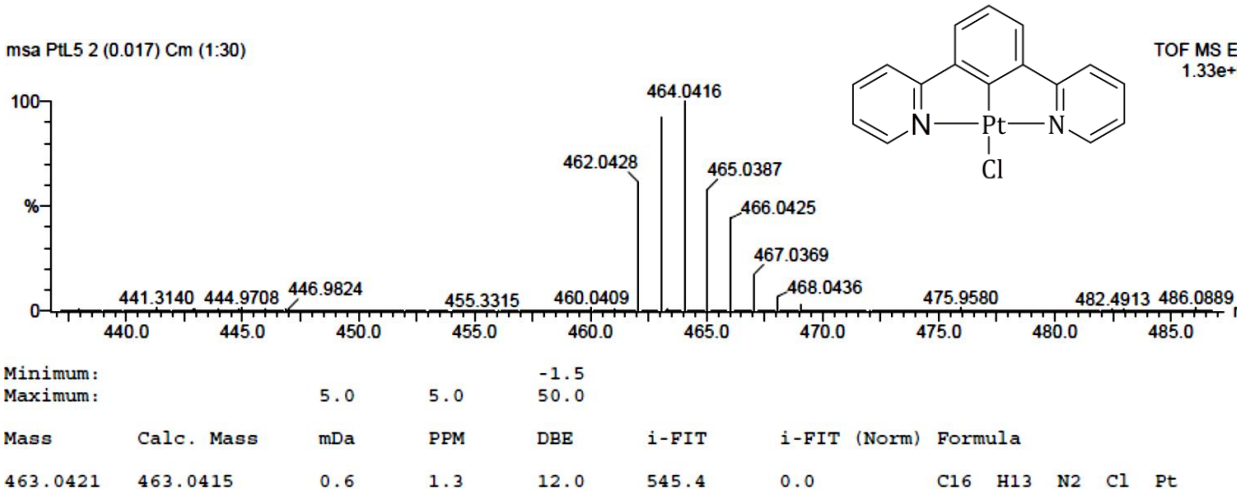

Minimum:				-1.5			
Maximum:		5.0	5.0	50.0			
Mass	Calc. Mass	mDa	PPM	DBE	i-FIT	i-FIT (Norm)	Formula
463.0421	463.0415	0.6	1.3	12.0	545.4	0.0	C16 H13 N2 Cl Pt

Figure SI 5.32 Mass spectrum of 1,3-Di(2-pyridinyl)benzene platinum(II)complex, **PtL5**.

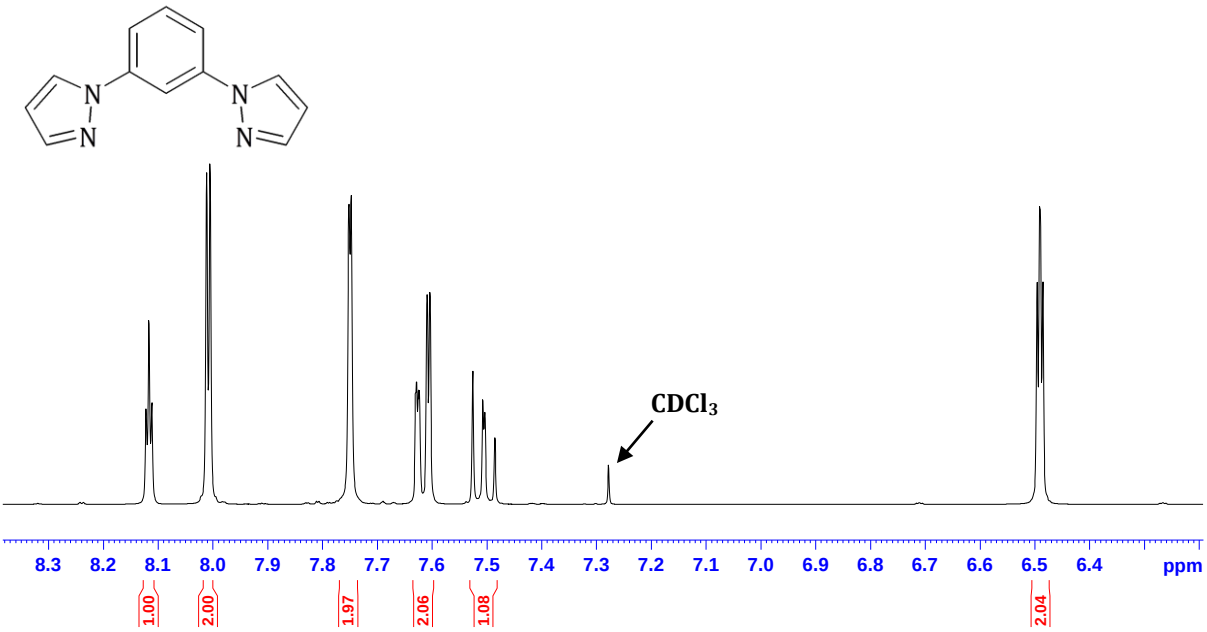

Figure SI 5.33 ^{1}H NMR spectrum of 1,3-Bis(N-pyrazolyl)benzene.

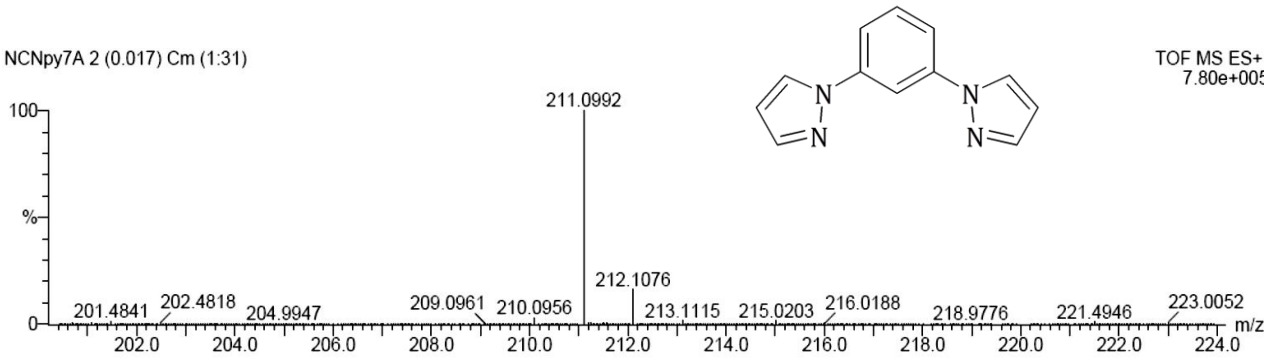

Minimum:				-1.5			
Maximum:		5.0	5000.0	50.0			
Mass	Calc. Mass	mDa	PPM	DBE	i-FIT	i-FIT (Norm)	Formula
211.0992	211.0984	0.8	3.8	9.5	761.7	0.0	C12 H11 N4

Figure SI 5.34 Mass Spectrum of 1,3-Bis(N-pyrazolyl)benzene.

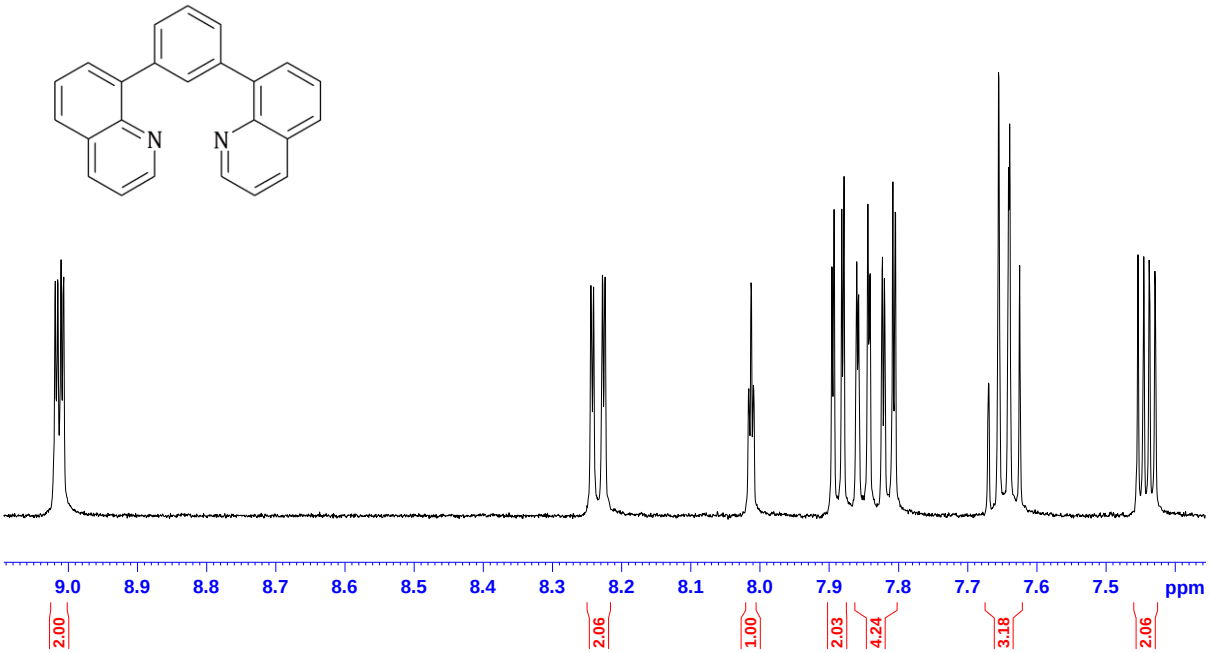

Figure SI 5.35 ^{1}H NMR Spectrum of 1,3-Bis(quinolin-8-yl)benzene.

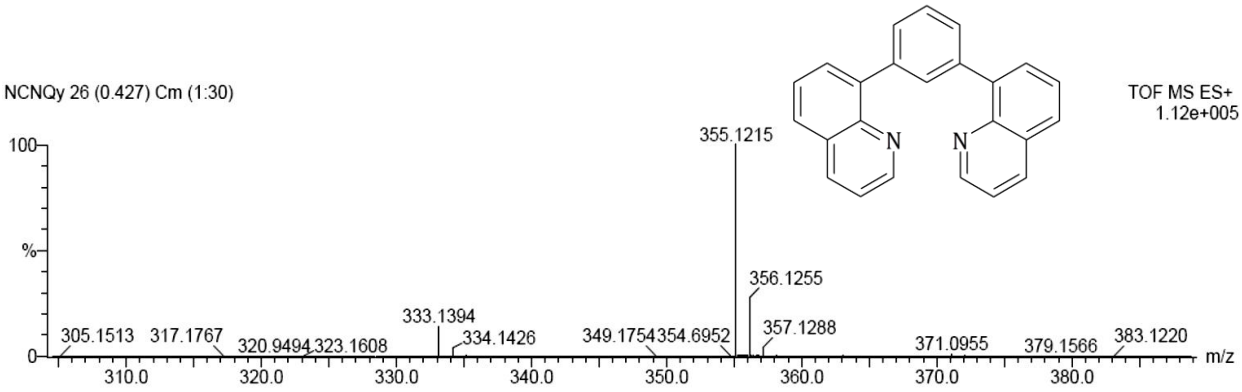

Minimum:				-1.5			
Maximum:		5.0	5.0	50.0			
Mass	Calc. Mass	mDa	PPM	DBE	i-FIT	i-FIT (Norm)	Formula
355.1215	355.1211	0.4	1.1	17.5	517.3	0.0	C24 H16 N2 Na

Figure SI 5.36 Mass Spectrum of 1,3-Bis(quinolin-8-yl)benzene.

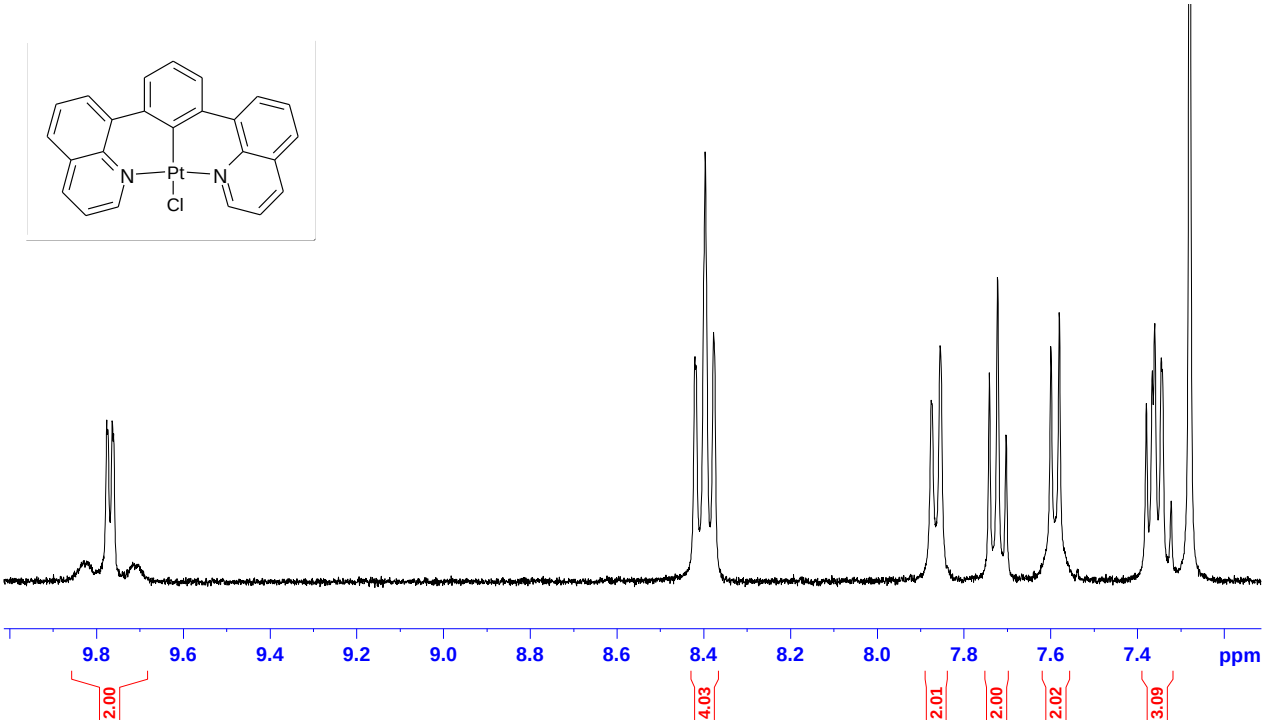

Figure SI 5.37 ^{1}H NMR of 1, 3 Bis(quinolin-8-yl)benzene platinum(II) complex, **PtL7**.

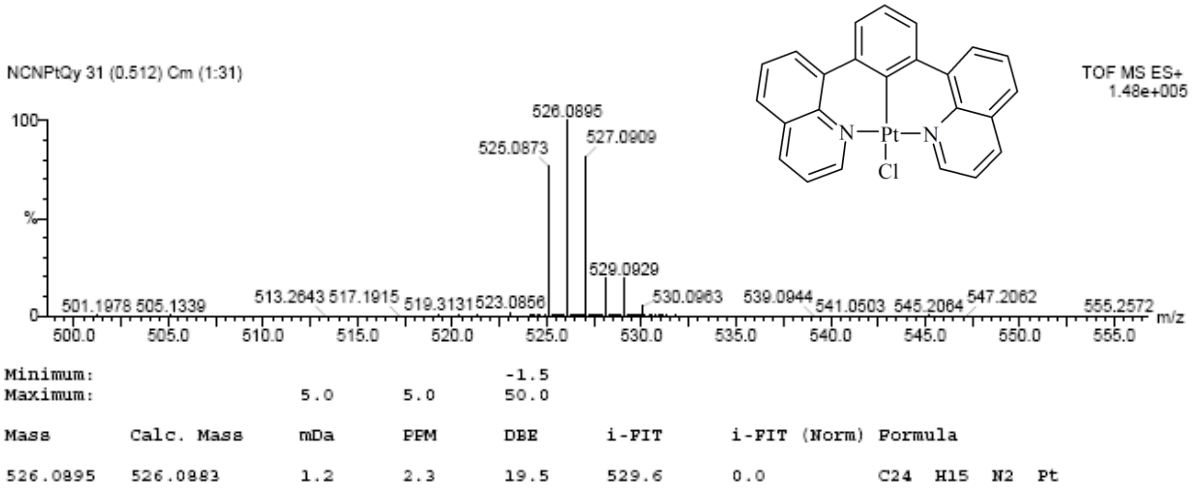

Minimum:				-1.5			
Maximum:		5.0	5.0	50.0			
Mass	**Calc. Mass**	**mDa**	**PPM**	**DBE**	**i-FIT**	**i-FIT (Norm)**	**Formula**
526.0895	526.0883	1.2	2.3	19.5	529.6	0.0	C24 H15 N2 Pt

Figure SI 5.37 Mass spectrum of 1,3 Bis(quinolin-8-yl)benzene platinum(II) complex, **PtL7**.

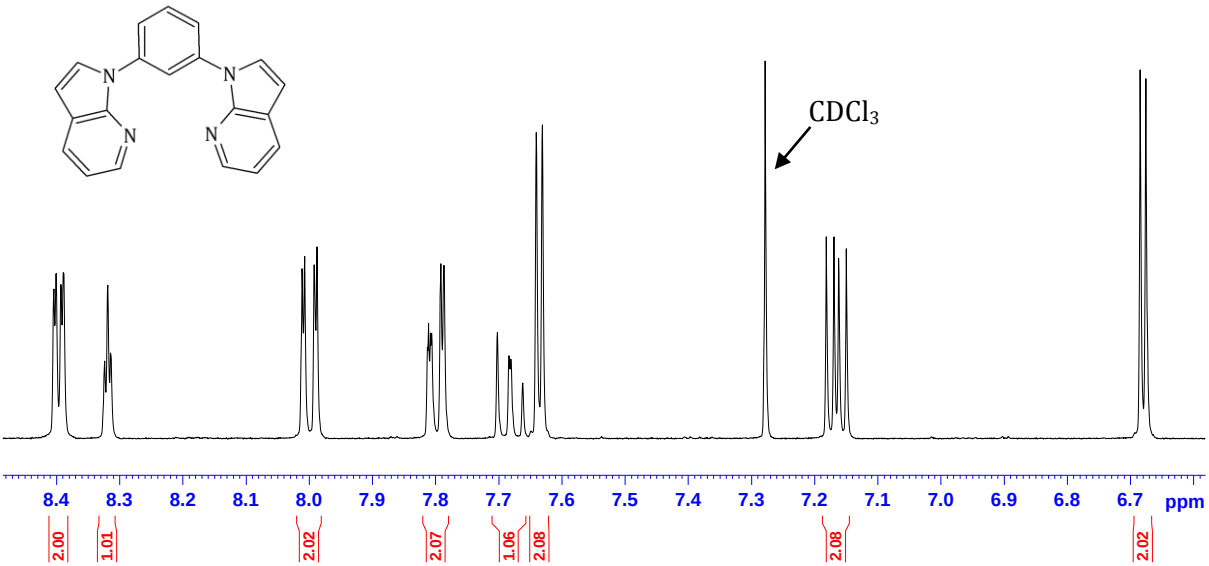

Figure SI 5.38 ^{1}H NMR of 1,3-Bis(7-azaindolyl)benzene in $CDCl_3$.

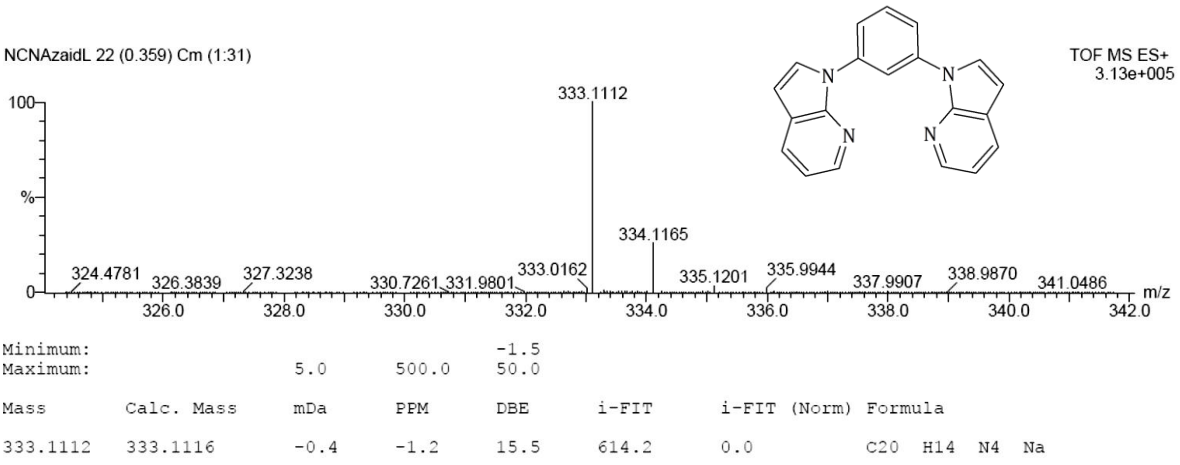

Minimum:				-1.5			
Maximum:		5.0	500.0	50.0			
Mass	Calc. Mass	mDa	PPM	DBE	i-FIT	i-FIT (Norm)	Formula
333.1112	333.1116	-0.4	-1.2	15.5	614.2	0.0	C20 H14 N4 Na

Figure SI 5.39 Mass spectrum of 1,3-Bis(7-azaindolyl)benzene.

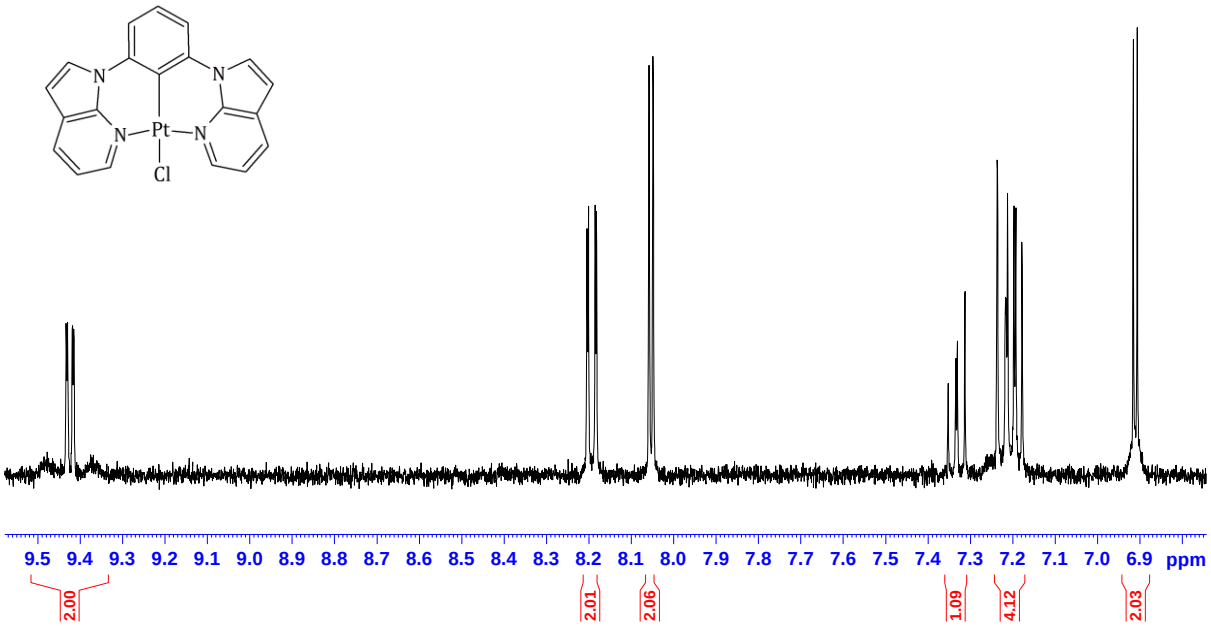

Figure SI 5.40 ^{1}H NMR of PtL8 1,3-Bis(7-azaindolyl)benzene platinum(II) complex, **PtL8**.

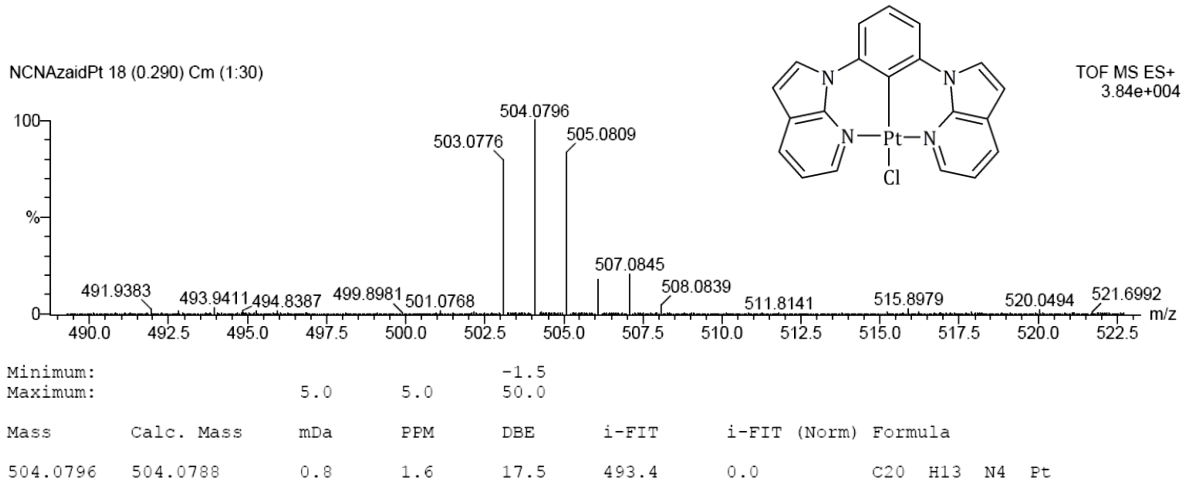

Minimum:				-1.5			
Maximum:		5.0	5.0	50.0			
Mass	Calc. Mass	mDa	PPM	DBE	i-FIT	i-FIT (Norm)	Formula
504.0796	504.0788	0.8	1.6	17.5	493.4	0.0	C20 H13 N4 Pt

Figure SI 5.41 Mass spectrum of 1,3-Bis(7-azaindolyl)benzene platinum(II) complex, **PtL8**.

Chapter 6

Conclusion and Future Work

6. Conclusion and Future Work

6.1. Concluding Remarks

From the experimental data obtained, it has been found that the rate of chloride substitution by selected azole nucleophiles is highly influenced by relatively small structural modifications on the N^N^N and N^C^N chelating ligands. When comparing the two schemes studied, we found that the presence of a Pt − C bond *trans* to the chloride leaving group in N^C^N chelates, leads to enhanced reaction rates of up to two orders of magnitude compared to their N^N^N analogues which contain a Pt − N bond in the similar position. Such acceleration of the substitution process is due to ground state destabilization of the Pt − Cl bond due to the strong σ-electron donation by the phenyl group along the C − Pt − Cl plane as shown by longer DFT calculated Pt − Cl bonds.[1-2] In planar five membered chelates, the presence of π-defficient pyridine *cis*-groups increase the rate of substitution, whereas a switch to electron rich pyrazole *cis* groups, decrease the rate of substitution since the incoming azole nucleophile is repelled by the increased electron density around the metal centre.[3] Introduction of 8-quinolyl and 7-azaindolyl *cis*-groups leads to out of plane twisting of these groups which also prevents effective π-back donation of the metal electrons, leading to slower reactivity of these complexes. [4] Steric hindrance due to this out of plane twisting of the *cis* groups in C_2 complexes also decrease the rate of chloride substitution as the attack of the incoming nucleophile is hampered. The results obtained are supported by DFT calculated NBO charges, HOMO-LUMO energy gaps and the chemical reactivity indices.

The observed general reactivity trend for the studied nucleophiles is **MIm>Im>DMIm>Pz>Tz**. The reactivity difference in methyl substituted, **MIm** and **DMIm** azoles was explained in terms of the inductive effect and/or steric hindrance. The enhanced reactivity of **MIm** is due to the inductive σ-donation of electrons by the methyl substituent in the β-position to the reactive nitrogen, making the nucleophilic nitrogen more reactive.[5-6] However, in **DMIm**, steric hindrance due to the additional methyl group in the α-position to the reactive nitrogen dominates over the inductive effect leading to steric clash in the transition state and retarded reactivity of the nucleophile. The reactivity difference in the entering unhindered five membered N-donor heterocyclic nucleophiles (**Im**, **Pz** and **Tz**) was found to depend linearly on their basicities according to a linear free energy relationship of the type $k_2 = \alpha(pK_a) + b$ where α and b account for the electronic and steric effects.

The significantly positive $\Delta H^{\ddagger}$ values and significantly negative values for $\Delta S^{\ddagger}$ support an associative substitution mechanism, typical of d^8 Pt(II) complexes. It is projected that the

thermodynamic and kinetic data obtained in this comparative study will contribute to a better understanding of the modes of interaction of monofunctional Pt(II) complexes with *in vivo* targets in the on-going search for improved metal based anticancer drugs.

6.2. Future Work

Tuning the electronic and structural properties of conjugated 5 and 6-membered Pt(II) chelates has been found to influence their reactivity with selected azoles. However, this understanding can be further extended by studying kinetic and thermodynamic behaviour of the more reactive aquated forms of these complexes with sulphur and nitrogen bio-relevant nucleophiles. We also aim to perform DNA titrations of these complexes and obtain single X-ray crystal structures of these DNA bound complexes in order to elucidate the mode of action of these complexes with DNA which will aid in the development of improved Pt(II) anticancer drugs.

6.3. References

1. A. Hofmann, L. Dahlenburg, R. van Eldik., *Inorg. Chem*., **2003**, *42*, 6528-6538
2. A. Pidcock, R. E. Richards and L. M. Venanzi. *J. Chem. Soc.* **1966**, 1707-1710.
3. S. Develay, O. Blackburn, A.L. Thompson and J.A. Gareth Williams, *Inorg. Chem*. **2008**, *47*, 11129 – 11142.
4. P. Haake, P. A. Cronin, Inorg. Chem, **1963**, *2*, 879-880.
5. A. Shaira, D. Reddy, D. Jaganyi., *Dalton. Trans*. **2013**, *42*, 8426 - 8436
6. D. Reddy, K. J. Ackerman, M. P. Ackerman, D. Jaganyi, D., *Transition. Met. Chem*. **2011**, *36*, 593-602.